UNIVERSITY OF IOANNINA
CHEMISTRY DEPARTMENT

Supervised by:
Assist. Prof. Dr. Mavroudis Demertzis

29

Cristina Ioana Vijdeluc
CHEMIST

SPECTROFLUORIMETRIC DETERMINATION OF ALUMINUM IN BIOLOGICAL, ENVIRONMENTAL AND PHARMACEUTICAL FORMULATION SAMPLES

PhD Thesis

IOANNINA 2007

ΠΑΝΕΠΙΣΤΗΜΙΟ ΙΩΑΝΝΙΝΩΝ
ΤΜΗΜΑ ΧΗΜΕΙΑΣ
ΤΟΜΕΑΣ ΑΝΟΡΓΑΝΗΣ ΚΑΙ ΑΝΑΛΥΤΙΚΗΣ ΧΗΜΕΙΑΣ
451 10 ΙΩΑΝΝΙΝΑ Τηλ.: ++30-26510- Fax: ++30-26510-44831

23-11-2007
Ιωάννινα,

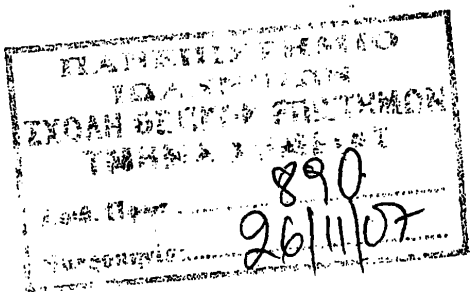

Π ρ ο ς
το Τμήμα Χημείας
του Παν/μίου Ιωαννίνων

Θέμα: «Απόφαση επταμελούς εξεταστικής επιτροπής ενώπιον της οποίας η κ. **Vijdeluc Cristina-Ioana** υποστήριξε τη διδακτορική της διατριβή»

Σήμερα 23/11/2007 και ώρα 13:00 μ.μ. έγινε δημόσια παρουσίαση της διδακτορικής διατριβής με θέμα: «*Φθορισμομετρικός προσδιορισμός αργιλλίου σε βιολογικά, περιβαλλοντικά και φαρμακευτικά δείγματα*», από την υποψήφια διδάκτορα κ. Vijdeluc Cristina-Ioana. Η παρουσίαση έλαβε χώρα στην αίθουσα Φ2-145 του Τμήματος Χημείας, Πανεπιστημίου Ιωαννίνων, ενώπιον της κατά τον νόμο επταμελούς εξεταστικής επιτροπής.

Η κ. Vijdeluc Cristina-Ioana. ανέπτυξε επί μία ώρα τα κυριότερα αποτελέσματα της διατριβής της και στη συνέχεια απάντησε σε σειρά ερωτημάτων της εξεταστικής επιτροπής και του ακροατηρίου. Κατόπιν αποχώρησε η υποψήφια και το ακροατήριο και ακολούθησε σύσκεψη μεταξύ των μελών της επταμελούς επιτροπής. Η επιτροπή έκρινε ότι η Διατριβή είναι πρωτότυπη και συμβάλλει στην πρόοδο της επιστήμης. Προχώρησε δε στην έγκριση αυτής με βαθμό **«Αριστα»** και αποφάσισε την απονομή του Τίτλου του Διδάκτορα στην κ. Vijdeluc Cristina-Ioana. από το Τμήμα Χημείας του Πανεπιστημίου Ιωαννίνων.

Τα μέλη της εξεταστικής επιτροπής

1) Μαυρουδής Δεμερτζής, Επίκ.Καθηγητής (Επιβλέπων)
2) Δήμητρα Κόβαλα-Δεμερτζή, Καθηγήτρια, (Μέλος Τριμελούς Συμβουλ. Επιτροπής)
3) Χρήστος Παπαδημητρίου, Επίκ. Καθηγητής (Μέλος Τριμελούς Συμβουλ. Επιτροπής)
4) Τριαντάφυλλος Αλμπάνης, Καθηγητής
5) Ιωάννης Ε. Κουντουρέλλης, Καθηγητής, Τμήμα Φαρμακευτικής, 54124 Θεσσαλονίκη
6) Κων/νος Σταλίκας, Επίκ.Καθηγητής
7) Χρήστος Νάνος, Λέκτορας

Αφιερωμένο στο σύζυγο και στην οικογένεια μου

ΠΡΟΛΟΓΟΣ

Η παρούσα διατριβή εκπονήθηκε στο Εργαστήριο Αναλυτικής Χημείας του Πανεπιστημίου Ιωαννίνων.

Οφείλω να ευχαριστήσω το Ίδρυμα Κρατικών Υποτροφιών (Ι.Κ.Υ.) για την υποτροφία που μου χορήγησε για τέσσερα συνεχή έτη και κατέστη δυνατό να περατωθεί η παρούσα διατριβή με επιτυχία.

Η ανάθεση του θέματος και η γενική επίβλεψη της διατριβής έγινε από τον Επίκουρο Καθηγητή του Τομέα Ανόργανης και Αναλυτικής Χημείας του Πανεπιστημίου Ιωαννίνων κ. Μαυρουδή Δεμερτζή, τον οποίο και ευχαριστώ, αρχικά για την αποδοχή της αίτησής μου για έρευνα στην Ελλάδα και για την συνεχή επίβλεψη, καθοδήγηση και σημαντική βοήθεια κατά την εκτέλεση των πειραμάτων και τη συγγραφή της εργασίας αυτής.

Ευχαριστώ επίσης τα μέλη της τριμελούς συμβουλευτικής επιτροπής, την Καθηγήτρια κα. Δήμητρα Κόβαλα-Δεμερτζή, για την καθοδήγηση και βοήθεια κατά την εκτέλεση των πειραμάτων, καθώς και τον Επίκουρο Καθηγητή κ. Χρήστο Παπαδημητρίου για το ενδιαφέρον που επέδειξαν καθ' όλη τη διάρκεια εκτέλεσης της διατριβής.

Ευχαριστίες οφείλω στο Πανεπιστήμιο Ιωαννίνων και στο Τμήμα Χημείας του Πανεπιστημίου Ιωαννίνων για την εξασφάλιση της στέγης διαμονής. Θα ήθελα για το ενδιαφέρον και την συμπαράστασή τους τον Πρύτανη κ. Ι. Γεροθανάση και τον Πρόεδρο του Τμήματος Χημείας Καθηγητή κ. Τ.Αλμπάνη.

Εκφράζω τις ευχαριστίες μου στον Καθηγητή κ. Πομώνη Φίλλιπο, στη Λέκτορα κα. Λουκατζίκου Λουκία, στο Δρ. κ. Ιωάννη Φιαμέγκο και Δρ. κα. Αγγελική Φλώρου για την βοήθεια τους.

Τον Καθηγητή κ. Δράϊνα Κων/νο για την βοήθεια και συμπαράστασή του.

Για τη σημαντική βοήθεια και την άψογη συνεργασία ευχαριστώ τους κ. Alexandru Vasile Calin, Δρ. κ. Χρήστο Κρίνα και κ. Αναστάσιο Παληό για το αίσθημα εμπιστοσύνης, φιλίας και συνεργασίας που μου προσέφεραν.

Επίσης οφείλω ευχαριστίες στη Γραμματεία του Τμήματος Χημείας, στην κα. Σοφία Βαμβέτσου, στον κ. Νικόλαο Βράκα, στον κ. Κωνσταντίνο Λιανό, στην κα. Μαίρη Λιόντου και στην κα. Φρειδερίκη Μασαλά.

Ευχαριστώ επίσης όλα τα μέλη της επταμελούς εξεταστικής επιτροπής, τον Επιβλέποντα Καθηγητή κ. Μ. Δεμερτζή, την Καθηγήτρια κ. Δ. Κόβαλα-Δεμερτζή, τον Επίκουρο Καθηγητή κ. Χρήστο Παπαδημητρίου, τον Καθηγητή κ. Τριαντάφυλλο Αλμπάνη, τον Καθηγητή κ. Ιωάννη Ε. Κουντουρέλλη, τον Επίκουρο Καθηγητή κ. Κων/νο Σταλίκα, και τον Λέκτορα κ. Χρήστο Νάνο για το χρόνο που διέθεσαν, για την εκτίμηση της αξιολόγησης της διατριβής μου.

Επίσης τις ευχαριστίες μου στους Πατέρες Δημοσθένη, Ιωήλ, Αθανάσιο και Γεώργιο για την πνευματική και ηθική τους συμπαράσταση.

Ιδιαιτέρες θερμές ευχαριστίες θέλω να εκφράσω στους γονείς μου, τον αδερφό μου και τους παππούδες μου για την ηθική υποστήριξη, την ποικιλόμορφη βοήθεια και τη συμπαράστασή τους. Επίσης, οφείλω να ευχαριστήσω πολύ την οικογένεια του συζύγου μου για την υποστήριξη και τη συμπαράστασή τους.

Τέλος οφείλω ένα μεγάλο ευχαριστώ στο σύζυγό μου Γεώργιο, για την υπομονή, την αμέριστη κατανόηση και την συμπαράσταση που έδειξε σε όλη τη διάρκεια της διατριβής.

Vijdeluc Cristina Ioana,

Ιωάννινα, Σεπτέμβριο 2007

Contents

1. Aluminum

1.1 General information

Aluminum is the third most abundant element (8%) in the Earth's crust, exceeded by oxygen (47%) and silicon (28%).

Because of its strong affinity to oxygen, aluminium never occurs as a metal in nature but is found only in the form of its compounds, such as alumina. This strong affinity to oxygen also explains why it withstood all attempts to prepare it in its elemental form until well into the 19th century. The metal's name is derived from alumen, the Latin name for alum. In 1761 the French chemist Guyton de Morveau proposed the name alumine for the base in alum, and in 1787 Antoine Lavoisier identified alumine as the oxide of a still undiscovered metal. In 1807 Sir Humphry Davy assigned the name aluminum to the metal and later agreed to change it to aluminum. Shortly thereafter, the name aluminium was adopted to conform with the -ium ending of most elements, and this spelling is now in general use throughout the world, except in the United States (where the second i was dropped in 1925) and Italy (where alluminio is used) [1].

1.2 Properties of aluminum

Aluminum has the chemical symbol Al, atomic number 13, and atomic weight 26.98. The isotope with mass number 27 is the only stable isotope. It is a soft, light, grey metal that resists corrosion when pure in spite of its chemical activity because of a thin surface layer of oxide. It is nonmagnetic and nonsparking. Its density is 2.6989 g/cm^3, melting point 669.7°C and boiling point 1800°C. Its electrical resistivity is 2.824 μΩ-cm at 20°C, with temperature coefficient 0.0039°C^{-1}, the same as copper's. Its thermal conductivity is 2.37 W/cm-K at 300K, and the linear coefficient of expansion is 23.86×10^{-6}°C^{-1}. The specific heat is 0.2259 cal/g-K, and the heat of fusion is 93 cal/g. The first ionization potential is 5.96V, second 18.74V and third 28.31V. Its electrode potential is 1.67V positive with respect to hydrogen. When near its melting point, it becomes 'hot short' and crumbles easily. As a pure metal, it is quite soft, and must be strengthened by alloying with Cu, Mg, Si or Mn before it can be used structurally. Aluminum bronze is 90 Cu, 10 Al, a strong, golden-yellow alloy with excellent physical properties. The Young's modulus of pure aluminum is 10×10^6 psi, the shear modulus

3.8×10^6 psi, Poisson's ratio 0.33, and the ultimate tensile strength 10,000 psi, with 60% elongation. Pure aluminum is very ductile and malleable, and unsuitable as a structural material. Its hardness is 15 Brinell (500 kg, 10 mm). The useful wrought alloys contain 1-7% magnesium and 1% manganese. Its crystal form is face-centred cubic, with lattice constant a = 0.404 nm, and nearest-neighbour spacing of 0.286 nm.

The familiar strong aluminum alloy Duralumin is an alloy 96 Al, 3.5 Cu, 0.5 Mg. The hard intermetallic $CuAl_2$ is forming slowly, making hard bits that would hinder the propagation of slip dislocations.

Liquid aluminum easily absorbs gases from the air, and these gases are expelled on solidification, causing flaws in castings. Casting alloys include silicon, and perhaps a little copper or nickel to help to avoid this. Also, large crystals may be a problem if the aluminum is poured while too hot [2].

1.3 Chemistry of aluminum

The electron configuration of aluminum is $1s^22s^22p^63s^23p$. The outer three electrons occupy three s^2p hybrid orbitals that point in orthogonal directions.

Aluminum shows a strong tendency to covalency, although the Al^{3+} cation is present in AlF_3, Al_2O_3, Al_4C_3 and as the hydrated ion $[Al(H_2O)_6]^{3+}$ in some of its salts.

1.*Air*. Aluminum is stable in air at ordinary temperatures, because of the formation of a highly protective film of oxide which can be removed by rubbing with mercury or mercury (II) chloride solution. This forms an amalgam which reacts readily with moist air, and the surface of the metal soon becomes covered with a furry growth of oxide and hydroxide. Aluminum burns when heated in air, forming a mixture of oxide and nitride (Al_2O_3, AlN).

2.*Water*. Water has no action on aluminum, because the oxide film protects it. Sea water corrodes Al readily. Aluminum does not react with steam even at high temperature because of the protective film of oxide.

3.*Acids*.

HCl. Aluminum reacts slowly with cold dilute HCl, rapidly with hot concentrated because of the solubility of Al_2O_3 in HCl.

$$Al + 3H^+ \rightarrow Al^{3+} + \frac{3}{2} H_2\uparrow$$

H_2SO_4. The dilute acid has little or no action on Al. The oxide film on the aluminum is not soluble in dilute sulphuric acid.

Hot concentration sulphuric acid reacts vigorously as an oxidizing agent with Al, forming aluminum sulphate, and being itself reduced to SO_2.

$$2Al + 6H_2SO_4 \rightarrow Al_2(SO_4)_3 + 6H_2O + 3SO_2\uparrow$$

HNO_3. Aluminum is unaffected by dilute nitric acid, cold or hot, and by cold concentrated nitric acid. The metal is rendered passive because of an unreactive oxide layer. The concentrated acid when heated to about 90°C reacts quite vigorously with aluminum, oxides of nitrogen being evolved.

1 *Alkalis.* Aluminum dissolves in aqueous caustic soda or potash giving aluminate ion and hydrogen.

$$Al + OH^- + 3H_2O \rightarrow [Al(OH)_4]^- + \frac{3}{2}H_2\uparrow$$

The protective Al_2O_3 film has been removed by OH^- ions, because aluminum oxide is amphoteric.

5.*Combination with non-metals.* Aluminum combines directly with halogens, oxygen, sulphur, nitrogen, and carbon forming binary compounds; the more electronegative the other elements are, the more readily does combination take place. The compounds formed with aluminum are thus: AlF_3, Al_2O_3, Al_2S_3, AlN, Al_4C_3.

6.*Reducing action.* Because of its great affinity for oxygen and other electronegative elements, Al is powerful reducing agents [3].

1.4 Aluminum occurrence in soil

1.4.1 Mineralogy

Aluminum is a highly electropositive element and a strong lithophile, being found exclusively as aluminum(III) in combinations with oxygen. Some of important minerals are shown in Table 1.1:

Table 1.1. *Some important Al-containing minerals*[4].

Mineral	*Typical composition*
Feldspars:	
plagioclase	$(K,Ca)[(Al,Si)_4O_8]$
alkali	$(Na,K)[AlSi_3O_8]$
Clay minerals:	
kaolinite	$Al_4[Si_4O_{10}](OH)_8$
montmorillonite	$(Ca,Na)_{0.7}(Al,Mg,Fe)_4[(Si,Al)_8O_{20}](OH)_4 \cdot nH_2O$
Constituents of bauxite:	
gibbsite	$Al(OH)_3$
boehmite and diaspore	$AlO(OH)$

The *aluminosilicate feldspars* are the most abundant minerals of the crust, being major components of igneous rocks such as granite.

Feldspar, $KAlSi_3O_8$ (potash feldspar), hydrates on weathering to form clay, such as *kaolin*, $Al_4[Si_4O_{10}](OH)_8$. Lapis lazuli, the *mineral lazurite*, is $Na_{4\text{-}5}Al_3(SiO_4)_3S$. This beautiful dark blue stone was greatly prized in antiquity, and is one aluminum compound that is not white. The best comes from northeastern Afghanistan. Finely ground, it made the pigment *ultramarine*. Ultramarine is now artificially made by fusing clay, carbon and sodium sulphate. Also not white is *turquoise*, $Al_2(OH)_3PO_4 \cdot H_2O$. These two stones are beautiful enough to compensate for all the white powders. *Garnet* and *jade* (*jadeite*, not *nephrite*) also contain some aluminum [2].

At the Earth's surface the aluminosilicates are broken down by weathering reaction through the action of water and carbon dioxide, to form *clay minerals*. These are important constituents of most soils, and play an essential role in retaining water and nutrient elements such as potassium and calcium [4]. The commonest clay minerals are kaolinite, montmorillonite.

Further weathering under tropical conditions leads to the removal of the most elements and the formation of oxide and hydroxide minerals, which make up bauxite, the major mineral source of aluminum [4].

The variable rock *bauxite*, named after the deposit at Les Baux-de-Provence, in southern France near Arles, is a mixture of the mineral *gibbsite*, α-$Al(OH)_3$, with lesser amounts of the denser and harder *boemite*, γ-$AlO(OH)$ and *diaspore*, α-$AlO(OH)$. It is produced by lateric supergene weathering of clays in most cases, and is *pisolitic* in form. This is a gaudy way of saying that it is weathered by water from above, and consists of pea-like granules. A notable

deposit is in Trinidad, but Australia, Brazil and Guinea have most of the resources. A famous deposit in the United States was in Arkansas, and other deposits were in Alabama and Georgia.

Alumina, Al_2O_3, is the refractory oxide of aluminum, which does not melt below 2000°C. *Corundum* is the natural form of alumina α-Al_2O_3, a very hard (9 on the Mohs scale, just below diamond) and heavy (4.02 g/cm^3) that is a valuable gem when transparent. A chromium impurity makes *ruby*, while iron, cobalt or titanium makes *sapphire*. *Emery* is a natural corundum substance with magnetite or hematite as an impurity, which turns it black. At 1700°C, alumina crystal becomes plastic and can be bent into any desired shape, for things like thread guides and phonograph needles.

Aluminum sulphate is found in nature as the rare mineral Kalinite, which is soluble in water, so it is found only near volcanoes and such places where it is made by the action of sulphuric acid on clays, such as on Lipari, near Vesuvius, and a few places in Germany and South America. *Alum*, $KAl(SO_4)_2 \cdot 12H_2O$ (or twice this) is not as scarce, but is still rare, found in Europe and Utah. This mineral is partly hydrated, crystallizes in the hexagonal system, and is insoluble. It dissolves in sulphuric acid, however.

Cryolite is sodium fluoroaluminate, Na_3AlF_6. The density of cryolite is 2.90, and its melting point is 1000°C. It is a soft rock, with hardness only 2.5, but its curious distinction is an index of refraction of 1.364, very close to that of water. Because of this, particles of it in water seem to disappear. Its name, based on Greek, means 'ice-rock', because of its appearance as a cloudy warm ice [2].

1.4.2 Soil and soil solution

Transformation of primary minerals by chemical weathering reactions results in new solid phases (i.e., secondary minerals). Aluminum-bearing secondary minerals such as smectite, vermiculite and chlorite are often found soils in developed on glacial till.

Inputs of aluminum into soil solutions usually occur by mobilization of aluminum derived from the chemical weathering of soil minerals. The most important reaction in the chemical weathering of the common silicate minerals is hydrolysis. However, aluminum is not very soluble over the normal soil pH range; thus, it generally remains near its site of release to form clay minerals or precipitate as amorphous or crystalline oxides, hydroxides or hydrous oxides [6]. In some parts of the world, the extent of chemical transformation by chelation is believed to exceed that by hydrolysis alone. In forest soils of cold and humid

regions, such as those of eastern Canada, aluminum is believed to be transported from upper to lower mineral soil horizons by organic acids leached from foliage and the slow decomposition of organic matter in the forest floor [7]. The movement of aluminum–organic complexes stops when the soil solution becomes saturated (or when the aluminum-to-organic-carbon ratio reaches a critical value), thereby reducing their solubility. A third important reaction involving aluminum is the transformation of one mineral into another through the exchange of interlayer cations [8].

Although the dissolution and precipitation reactions of aluminum-bearing minerals are often good indicators of the solubility of aluminum in soils, they are by no means the only pedogenic processes controlling the concentrations of aluminum in soil solutions. Many other processes may partly control the bioavailability of aluminum to plant and soil organisms. Aluminum may be

1 adsorbed on cation exchange sites,
2 incorporated into soil organic matter,
3 absorbed by vegetation,
4 leached out of the soil system [9].

In eastern Canada, the atmospheric deposition of strong acids, such as nitric acid and sulphuric acid, has accelerated the soil's natural acidification. The increased H^+ activity (lower pH) in the soil solution creates a new equilibrium where more aluminum(III) is dissolved in the soil solution, cation nutrients (Ca^{2+}, Mg^{2+} and K^+) are replaced on the soil exchange complex by aluminum(III)and the base cations are eventually leached out of the soil.

The fluoride and hydroxide complexes are the two strongest groups of inorganic ion associations with aluminum in soil solutions [10]. In very acidic soils, aluminum in the soil solution is present mainly as free Al^{3+}; as pH increases, free Al^{3+} hydrolyses to form complexes with OH^- ions (e.g., $AlOH^{2+}$, $Al(OH)_2^+$, $Al(OH)_3^0$). Near pH 6.5, aluminum solubility is at a minimum, but it increases at neutral to alkaline conditions because of the formation of $Al(OH)_4^-$ [8]. According to Lindsay et al. (1989) [11], fluorine, the most electronegative and one of the most reactive elements, is released through the dissolution of fluoride-bearing minerals. In acidic soils (pH <5.5), low-ligand-number complexes such as AlF^{2+} are normally formed. In neutral to alkaline conditions, it is more difficult for F^- to compete with OH^- for aluminum in the soil solution because of the increased level of OH^-.

Consequently, aluminum–hydroxide complexes predominate over aluminum–fluoride complexes in alkaline conditions.

The complexation of aluminum with sulphate is weaker than that with fluoride. However, in acidic soils where the sulphate concentration is high, aluminum may also form aluminum–sulphate complexes [8]. At low sulphate concentrations, $AlSO_4^+$ is the dominant aqueous form, whereas $Al(S0_4)_2^-$ is predominant in soil solutions with higher sulphate concentrations. Brown and Driscoll (1992) [12] showed that several aluminosilicate complexes, including $AlSiO(OH)_3^{2-}$.

The use of alum sludge as a soil amendment is the primary pathway by which aluminum enters the terrestrial environment. However, the amount of aluminum added to soil through this practice is small in comparison with aluminum naturally present in soil. Moreover, since spreading on agricultural land is permitted only when the pH is greater than 6.0 or when liming and fertilization (if necessary) are done, the solubility (and hence bioavailability) of this aluminum is expected to be very limited [5].

1.4.3 Sediment

Sediments, where the metal is generally considered as biologically unavailable, are an important compartment for aluminum [13,14]. Aluminum occurs naturally in aluminosilicates, mainly as silt and clay particles, and it can be bound to organic matter (fulvic/humic acids) in sediments [13]. At pH >5.0, dissolved organic matter (DOM) can co-precipitate with aluminum, thereby controlling its concentrations in lakes with elevated concentrations of DOM [15].

Experimental acidification of lakes and limnocorrals has shown that aqueous aluminum concentrations rapidly increase in response to inputs of acid [16]. Mass-balance studies have demonstrated that retention of aluminum by sediments decreases as pH decreases [17,18]. Under such conditions, sediments in acidified watersheds can provide a source of aluminum to the water column [19].

1.5 Process for aluminum occurrence in water

The aluminum ion bonds through oxygen to form a wide variety of functional groups. In igneous rocks, aluminum is largely bonded to oxygen ions in tetrahedral coordination. As the rocks weather, aluminum progressively acquires more octahedral bonding. The weathering release of aluminum from 2:1 layer silicates in soils is enhanced by inputs of acids from the

natural decomposition of organic matter and minerals and from pollution [20]. Acids as weak as dilute H_2CO_3 have been shown to decompose the silicates and montmorillonite (hydrous aluminum silicate) layers facilitating the release of aluminum [21].

1.5.1 Aluminum speciation in water

The aqueous chemistry of aluminum has been extensively reviewed by Driscoll and Schecher, 1989 [22]. Three major categories define the various aluminum fractions in water [23]:

(1) Total aluminum, which is the sum of suspended, colloidal, and monomeric forms of aluminum. (2) Particulate aluminum, which is the sum of suspended and colloidal aluminum. (3) Monomeric aluminum, which is further divided into two forms, those of non-labile (aluminum associated with dissolved organic carbon) and labile (aquo, and hydroxide, fluoride, and sulphate complexes of aluminum). See Figure 1.1.

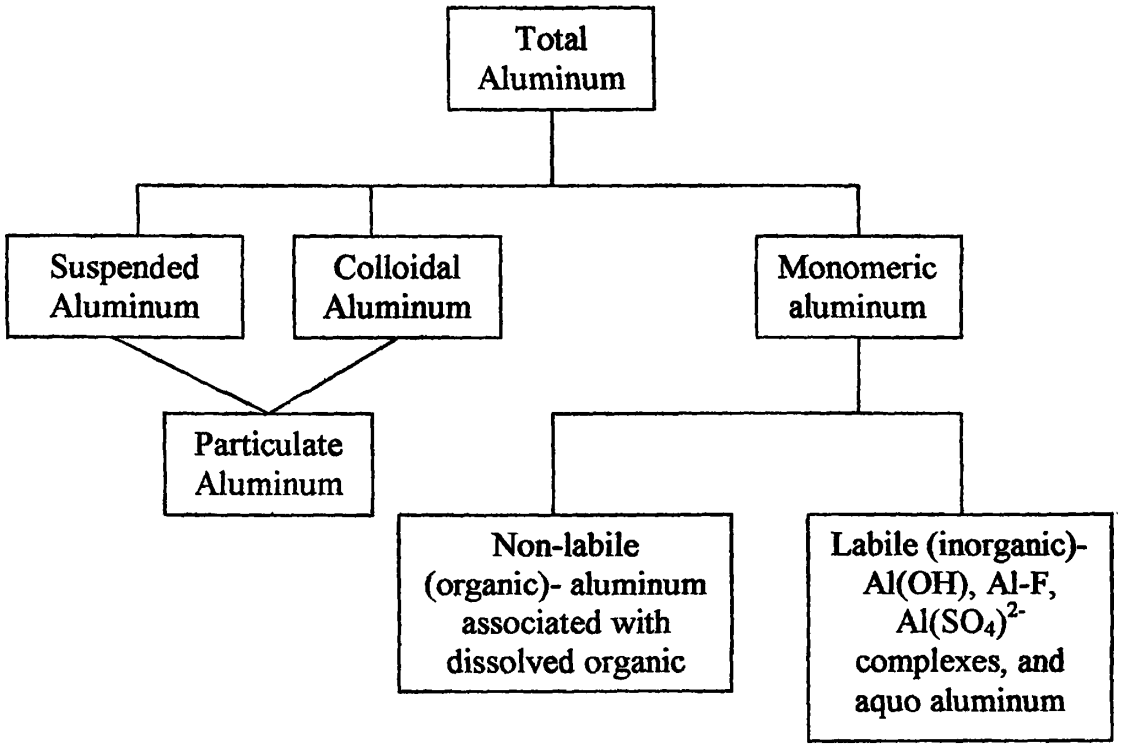

Figure 1.1. *The Various Fractions of Aluminum in Water* Source: Srinivasan et al. (1999) [23].

1.5.1.1 Raw water

The solubility of aluminum in equilibrium with solid phase $Al(OH)_3$ depends on the surrounding pH [24]. The aquo complex $Al(H_2O)_6^{3+}$ predominates at pH<4.0. As the pH (and/or temperature increases), the hydrated trivalent aluminum ion undergoes hydrolysis, (see Scheme 1.1) initially forming the $Al(OH)(H_2O)_5^{2+}$ ion and then hydroxyaluminum species such as $Al(OH)_2^+$, $Al(OH)_3$ (insoluble), $Al(OH)_4^-$, $Al_2(OH)_2^{4+}$, and $Al(OH)_5^{2-}$, and eventually hydroxypolymers such as $Al_{13}(OH)_{32}^{7+}$ and others (See Table 1.2), which had been proposed by various researchers. [24,25]. [Fluoride ions can substitute in these complexes; however, in neutral and alkaline solutions, aluminum has greater affinity for the hydroxide ion [26]]. Between pH 5.0 and 6.0, the predominant hydrolysis products are $Al(OH)^{2+}$ and $Al(OH)_2^+$; between pH 5.2 and 8.8, the solid $Al(OH)_3$ is most prevalent; and above pH 9.0, the soluble species $Al(OH)_4^-$ is the predominant species and the only species present above pH 10.0. Throughout the pH gradient (pH 4.7 and 10.5), polymeric aluminum hydroxides can be found. As polymers come together, aluminum hydroxide becomes large enough to precipitate from solution. Additionally, at pH>7.0 the aluminum hydroxide complexes dominate when the content of dissolved organic matter and silicate is low. At lower pH, aluminum sulphate complexes exist, as well as aluminum-humic acid and aluminum-fulvic acid complexes. [27].

Scheme 1.1. [28] *The steps in the dissociation of protons from the hydrated aluminum ion in dilute solution*

$$[Al(H_2O)_6]^{3+} \leftrightarrow [Al(OH)(H_2O)_5]^{2+} + H^+$$

$$[Al(OH)(H_2O)_5]^{2+} \leftrightarrow [Al(OH)_2(H_2O)_4]^+ + H^+$$

$$[Al(OH)_2(H_2O)_4]^+ \leftrightarrow [Al(OH)_3(H_2O)_3] + H^+$$

$$[Al(OH)_3(H_2O)_3] \leftrightarrow [Al(OH)_4(H_2O)_2]^- + H^+$$

$$[Al(OH)_4(H_2O)_2]^- \leftrightarrow [Al(OH)_5(H_2O)]^{2-} + H^+$$

$$[Al(OH)_5(H_2O)]^{2-} \leftrightarrow [Al(OH)_6]^{3-} + H^+$$

$$\xrightarrow{\text{heat}}$$

$$[Al(OH)_6]^{3-} \rightarrow AlO^{2-} + 2H_2O + 2OH^-$$

1.5.1.2 Treated Water

The use of aluminum-based coagulants for the removal of particulate, colloidal, and dissolved substances in water usually results in an increase in the amount of aluminum in the finished water, with a portion of the coagulant remaining as residual aluminum, which

consists of dissolved and particulate species [23]. However, treatment can also decrease the total aluminum content. Generally, a concentration between 1 and 5 mg/L is desired with addition of an aluminum salt during water treatment [26].

The speciation of aluminum in the treated water depends on pH, temperature of the water during treatment, the type of organic and inorganic ligands in the raw water, and treatment conditions (e.g., the amount of coagulant employed) [23].

The form in which aluminium is presented in drinking water is also dependent on whether the water is fluoridated, as fluoride has a strong affinity for aluminum, particularly under acidic conditions. In unfluoridated water at pH values above 6.5 and with an aluminum concentration of 100 μg/L, the predominant species is $Al(OH)_4^-$. In fluoridated water (typically 53 μmol/L), AlF_2^+ and AlF_3 species are among those that can be found below pH 6.5; above pH 6.5, mixed OH^-/F^- complexes or $Al(OH)_4^-$ may occur [29].

Table 1.2. *Polymeric aluminum hydrolysis species* [27]

Polymer	***Reference***
$Al_2(OH)_2^{4+}$	Kubota (1956)
$Al_6(OH)_{12}^{6+}$	Hsu and Bates (1964)
$Al_6(OH)_{15}^{3+}$	Brosset (1981)
$Al_7(OH)_{17}^{4+}$ and $Al_{13}(OH)_{34}^{5+}$	Snoeyink and Jenkins (1980)
$Al_8(OH)_{22}^{2+}$	Matijevic et al. (1961)
	Hayden and Rubin (1974)
$Al_{10}(OH)_{22}^{8+}$	Hsu and Bates (1964)
$Al_{10}(OH)_{22}^{8+}$ and $Al_{13}(OH)_{30}^{9+}$	Hsu (1977)
$Al_{13}O_4(OH)_{24}^{7+}$	Johanason (1960)
	Bottero et al. (1980)
$Al_{13}(OH)_{32}^{7+}$	Aveston (1965)

1.5.2 Water treatment processes

Drinking water production begins with coagulation, followed by flocculation, clarification, filtration, and finally disinfection [26]. Aluminum removal depends on the transformation of the aluminum ions into $Al(OH)_3$ species [23].

Treatment therefore involves chemical precipitation by pH adjustment (pH range 6.5-8.0). The addition of sulphate expands this range of coagulation (lowers the limit of pH to 6.0) while serving as a catalyst in the formation of solid $Al(OH)_3$ particles. Treatment by cation-exchange resin, reverse osmosis, and electrodialysis is the most effective process for the removal of aluminum in water (90-100% efficiency), whereas processes involving

aeration and stripping, anion-exchange resin, and chemical oxidation/disinfection are poor (0-20% efficiency) [23]. Lime softening and coagulation coupled with sedimentation and filtration are moderately effective methods (0-70% efficiency). The treatment of the water supply is not without problems [23,30]. The increased aluminum concentration in treated water can enhance turbidity through the post-precipitation of a hydrous aluminum precipitate in the distribution system, limit the disinfection process by enmeshing and protecting microorganisms, and reduce the carrying capacity of pipes with the accumulation of aluminum hydrolysis products on their walls. Reduction of residual aluminum, which consists primarily of particulate and dissolved forms of aluminum, as much as possible is, therefore, essential. Since particulate aluminum is mostly derived from turbidity-causing substances, the elimination of turbidity from raw water will reduce its presence in treated waters. Particulate aluminum can be readily removed by solid- liquid separation facilities such as clarifiers (93-96% efficiency observed) and filters (75-87% efficiency observed using sand filtration). Experimental data indicate that the soluble aluminum fraction can be removed by granular activated carbon (65% efficiency).

1.6 Aluminum occurrence in air

The largest source of airborne aluminium-containing particulates is dust from soil, the weathering of rocks, volcanic activity, and human activities, such as mining and agriculture [25]. Aluminum is found as silicates, oxides, and hydroxides in the particles, which are deposited onto land and water by wet and dry deposition. Aluminosilicates from aluminium dust comprise up to 14% of the Earth's surface [31].

Levels of aluminum vary in the atmosphere, depending on the location of the sampling site, meteorological conditions (e.g., summer versus winter), and the level of industrial activity or traffic in the area [25]. They are expected to be low in areas near the ocean and high in areas with wind-blown soil. Background levels of aluminum in the atmosphere generally range from 0.005 to 0.18 ng/m^3, but are significantly higher in cities and industrial areas, which range from about 0.4 to 10 ng/m^3. In the late 1960s to mid-1970s, concentrations up to 8678 ng/m^3 were measured [24]. Anthropogenic releases are primarily to the atmosphere and account for about 13 % of atmospheric aluminum [25]. The major anthropogenic sources of aluminum-containing particulate matter include coal combustion, aluminum production, and other industrial activities processing crustal minerals. Aluminum levels ranging from (3.7-37) $\times 10^{-3}$ M have been found in air particulate emissions from iron

and steel foundries and brass and bronze refineries. Additionally, motor vehicle emissions add 0.9 to 9 % of the observed elemental concentration of aluminum in the air. Aluminosilicates, which can be manmade, are found in products such as talcum powder, asbestos, cat-box litter, table salt, and cigarette smoke [31]. Because aluminum in compounds cannot be oxidized, atmospheric transformations are not expected to occur during transport [25].

However, if aluminum metal particles are released during anthropogenic activities such as metal processing, they would be rapidly oxidized.

1.7 Health impacts of aluminum

1.7.1 Human exposure

The large quantity of aluminum in nature and its many uses make exposure to aluminum unavoidable. Table 1.3 shows the determined or estimated daily intakes of aluminum. Exposure for the generally population is mainly through oral intake, and the major sources are drinking water (from the use of aluminum in municipal water treatment), residues in foods, cooking utensils, food and beverage packaging, and aluminum-containing medications (e.g., antacids and buffered aspirins).

Table 1.3. *Daily intake of aluminum by human [32].*

Sample	*Aluminum concentration*
Tea (1% extract)	14-90.6 μM
Herbal tea	5.18-39.5 μM
Drinking water	0.08-0.224 mg/day
Food	24 mg/day (median)
beverages	0.74-159.4 μM
animal products	2.22-522.6 μM
fruits	1.85-114.9 μM
grains	1.48-14825.8 μM
vegetables and legumes	3.7-934 μM
dried herbs	$(3.04\text{-}114.2)\times10^3$ μM
baking powder	85.3×10^3 μM
Canned drink stored	3.7-2742.8 μM
Medications	
antacid	35-208 mg/dose
buffered aspirins	9-52 mg/dose
antidiarrheal drugs	36-1450 mg/dose
anti-ulcerative	207 mg/dose
Atmospheric dust	3.6ng/day

Additionally, children may ingest aluminum from dirt from unwashed hands or when playing in contaminated soils, vitamin/mineral supplements, treatment for hyperphosphatemia, and from consumer products not normally ingested by adults (e.g., toothpaste) [25]. The daily ingestion of aluminum is 30 to 50 mg for almost every individual [31]. Other sources for potential exposure to aluminum for children are vaccinations containing aluminum adjuvants, parenteral feeding of premature infants, and dialysis fluids. Other routes of potential exposure to aluminum are via inhalation of atmospheric dust and through the skin (e.g., via use of antiperspirants) [24, 25].

Occupational exposure to aluminum occurs in the refining of the primary metal and in secondary industries that use aluminum products, such as aircrafts, automotives, and metal products.

Greater exposure to aluminum is possible for persons living in the vicinity of industrial emission sources and hazardous waste sites, undergoing long-term hemodialysis treatment, drinking water from residential well, and those consuming large quantities of antacid formulations, anti-ulcerative medications, buffered analgesics, or kaolin-based anti-diarrhoea medications [25].

1.7.2 Aluminum as neurotoxicant

Historically, aluminum has been considered relatively non-toxic; healthy individuals can tolerate oral doses as high as 7 grams per day without experiencing harmful effects. However, abundant evidence now shows that aluminum may adversely affect the nervous system in humans and animals.

1.7.2.1 Dialysis encephalopathy

Patients with kidney disease who undergo dialysis regularly and who consequently may be exposed to high levels of aluminum in dialysis fluids and medications can develop dialysis encephalopathy, a progressive form of dementia characterized by tremors, convulsions, psychosis and other changes in speech and behavior [33, 34]. Most experts agree that high levels of aluminum in dialysis fluids and medications are responsible for the dementia, and that controlling the levels of aluminum significantly reduces the incidence of this disease.

1.7.2.2 Alzheimer's disease

Alzheimer's disease is the most common primary degenerative brain disease in Canada and is a leading cause of death. The first recognizable symptoms of Alzheimer's disease, which mark the start of progressive mental deterioration, include memory lapses, disorientation, confusion, and depression.

Scientists are investigating possible theories to determine the causes of Alzheimer's disease. These theories take into account the roles of genetic factors, abnormal proteins, infectious agents, environmental agents including aluminum, other metals or solvents, and metabolic changes. Growing evidence suggests that complex interactions exist between genetic predisposition and aging, for example, and the series of events leading to the onset of the disease.

Aluminum exposure was suggested as a possible cause of Alzheimer's disease because the average aluminum content of control human brains (1.9±0.7 mg/kg dry weight) was found to be less than that of AD-affected brains (3.8 mg/kg dry weight) [35]. However, it is not clear whether the accumulation of aluminum is a cause or a result of the disease.

Several studies on humans have shown a slightly increased risk of Alzheimer's disease or related dementia in communities where the drinking water contains high concentrations of aluminum [36, 37]. On the other hand, a number of other studies have shown no relationship between aluminum in drinking water and the onset of dementia [38, 39]. In addition, scientists have been unable to induce Alzheimer's disease-type changes in the brains of laboratory animals exposed to aluminum, or to explain the absence of Alzheimer's disease-type changes in brains of patients suffering from dialysis encephalopathy [40,41,42,43]. Some studies have also shown little or no accumulation of aluminum in the brain tissues of Alzheimer's patients [44].

After weighing all the evidence, experts have concluded that even though a true association between dementia (including Alzheimer's disease) and high concentrations of aluminum in drinking water has not yet been proven, the possibility cannot be ruled out, especially for the most elderly.

1.7.2.3 Lou Gehrig's and Parkinson's diseases

Aluminum has also been associated with other severe diseases of the nervous system, such as Lou Gehrig's disease (often referred to as amyotrophic lateral sclerosis, which is a progressive neurodegenerative disease that affects nerve cells in the brain and the spinal cord)

and Parkinson's disease (which belongs to a group of conditions called movement disorders and characterized by muscle rigidity, tremor, a slowing of physical movement (bradykinesia) and, in extreme cases, a loss of physical movement (akinesia).). As with Alzheimer's disease, the significance, if any, of the association is unknown.

An unusually high incidence of Lou Gehrig's and Parkinson's diseases in indigenous populations in Guam and New Guinea suggests a possible correlation between the diseases and local environmental conditions, including high levels of aluminum and low levels of calcium and magnesium in soil and food [45]. As with Alzheimer's, humans with these disorders tend to have high levels of aluminum in some areas of their brains, although it has not been demonstrated that the presence of aluminum in the brain initiates the onset of the diseases [46]. Other possible contributing factors that need to be examined more closely include the diet of the Guam population - in particular, the seeds of the false sago palm [47, 48], which contain a toxic amino acid that causes a condition similar to Lou Gehrig's disease in monkeys - as well as the possibility that the dementia is caused by genetic rather than environmental factors [49].

1.7.2.4 Other health effects

The intake of large amounts of aluminum can also cause anemia [50,51], osteomalacia [52, 53] (brittle or soft bones), glucose intolerance of uranemia [54], and cardiac arrest in humans [53].

1.7.3 Absorption, Distribution, Metabolism, and Excretion

The human body burden originating from largely insoluble environmental sources of aluminum is very low (about 0.1 %). In Table 1.4 are reported concentration of aluminum in various human tissues and body fluids.

Table 1.4 *Mean concentrations of aluminium in a body tissue* [4]:

Tissue	*Aluminum concentration, μM*
Whole blood	5.2-231.3
Plasma	4.8-5.93
Serum	<0.37
Urine	0.1-0.3
Bone (dry weight)	37-111.2
Brain (mostly grey matter)	37-111.2

Most aluminum compounds are poorly absorbed through the lungs, skin, and gastrointestinal tract. Uptake from the gastrointestinal tract may be regulated by water solubility of the aluminum species and by mucosally associated luminal metal-binding ligands. Aluminum is also poorly distributed in most tissues except the lung. Aluminum transport in the blood is about 89 % bound to iron transferrin and about 11 % as aluminum citrate. Elimination of absorbed aluminum is mainly through the kidney. Chelation with compounds such as desferrioxamine (deferoxamine [DFO]) may increase urinary aluminum excretion.

Of particular concern is the possible enhancement of intestinal absorption in the presence of dietary constituents such as citrate and fluoride. Added or natural fluoride in drinking water may form strong, water-soluble aluminum complexes (one to five fluoride ions per aluminum atom). Slightly acidic pH favours formation of aluminum fluoride and citrate complexes.

The standard American diet contains about 4 g citrate per day. Citrate is known to increase intestinal absorption as well as tissue accumulation of aluminum. However, in one study with human volunteers administered aluminum and citrate in the drinking water, no difference was observed between the plasma concentrations of aluminum in subjects receiving citrate with the drinking water and those that did not. While increasing aluminum absorption, citrate may also enhance urinary excretion, resulting in no significant increase in aluminum plasma concentration in individuals with normal kidney function. The greatest risk of aluminum absorption and distribution after citrate exposure would be for those individuals with renal insufficiency or failure.

Aluminum may form complexes with other dietary acids, for example, malic, oxalic, tartaric, succinic, aspartic, and glutamic acids, which may increase its gastrointestinal absorption.

Formation of aluminum maltolate from the dietary constituent maltol (a common food additive) may also occur. The aluminum maltolate complex is also associated with increased aluminum uptake.

Administration of fluoride with aluminum has resulted in decreased fluoride absorption from the intestinal tract, indicating that aluminum-fluoride complexes are not absorbed as readily as fluoride alone. It has been suggested, however, that administration of fluoride alone can cause the co-accumulation of aluminum in bone [32].

References:

1. http://www.trufax.org/general/aluminum.html
2. http://www.du.edu/~jcalvert/phys/alumin.htm
3. Wilson J.G., Newall A.B., General and inorganic chemistry, Cambridge University Press, 2nd ed., pp. 341-357, 1970.
4. Cox P.A., The elements on Earth. Inorganic Chemistry in the Environment, University of Oxford Press, pp. 105-107, first published 1995, reprinted 1997.
5. http://www.hc-sc.gc.ca/ewh-semt/pubs/contaminants/pls2-lsp2/aluminum/aluminum_2_e.html
6. Birkeland, P.W., Soils and geomorphology. *Oxford University Press, New York, N.Y,* 1984.
7. Courchesne, F. and W.H. Hendershot., *Géog. Phys. Quat.* 51: 235, 1997.
8. Sposito G., The environmental chemistry of aluminum. *2nd edition. CRC Press, Boca Raton, Florida.* pp. 363–418, 1996.
9. Ritchie, G.S.P., *Plant Soil* 171: 17, 1995.
10. Sposito G., The environmental chemistry of aluminum. *2nd edition. CRC Press, Boca Raton, Florida.* pp. 39–80, 1995.
11. Lindsay, W.L., P.L.G. Vlek and S.H. Chien. 1989. Phosphate minerals. *In*: Dixon J.B., Weed S.B., Minerals in soil environments. *Soil Science Society of America, Madison, Wisconsin.* pp. 1089–1130, 1989.
12. Brown, B.A. and C.T. Driscoll., *Science* 256: 1667, 1992.
13. Stumm, W. and J.J. Morgan., Aquatic chemistry. An introduction emphasizing chemical equilibria in natural waters. *John Wiley and Sons, New York, N.Y.*, 1981
14. Broekaert J.A.C., Guter S., Adams F.B., Metal speciation in the environment. *Springer-Verlag, Berlin.* pp. 545–569 *(NATO ASI Series G – Ecological Sciences,* Vol. 23, 1990.
15. Urban, N.R., E. Gorham, J.K. Underwood, F.B. Martin and J.G. Ogden., *Limnol. Oceanogr.* 35: 1516, 1990.
16. Brezonik, P.L., C.E. Mach, G. Downing, N. Richardson and M. Brigham., *Environ. Toxicol. Chem.* 9: 871, 1990.
17. Dillon, P.J., H.E. Evans and P.J. Scholer., *Biogeochemistry* 3: 201, 1988.
18. Astruc M., Lester J.N. (eds.), Heavy metals in the hydrological cycle. *Selper Ltd., London.* pp. 11–18, 1988.
19. Nriagu, J.O. and H.T.K. Wong., *Water Air Soil Pollut.* 31: 999, 1986.

20. McBride, M.B.. Environmental Chemistry of Soils. *Oxford University Press. New York,* 1994.

21. Jenny, H., *Soil Sci. Soc. Am. Proc.* 25:428, 1961.

22. Driscoll, C.T., and W.D. Schecher. 1989. Aqueous chemistry of aluminum. In: Aluminum and Health: A Critical Review, Gitelman H.J., Dekker Ed.M., *Inc., New York, NY,* pp. 27-65, 1989.

23. Srinivasan, P.T., T. Viraraghavan, and K.S. Subramanian.,*Water S.A.* 25(1):47, 1999.

24. IPCS (International Programme on Chemical Safety). Aluminum. *Environmental Health Criteria 194. World Health Organization, Geneva, Switzerland,* pp. 270, 1997.

25. ATSDR (Agency for Toxic Substances and Disease Registry). Toxicological Profile for Aluminum. *ATSDR, Public Health Service, U.S. Department of Health and Human Services, Atlanta, GA.* pp. 368, 1999.

26. Yokel, R.A., Golub M.S., Research Issues in Aluminum Toxicity. *Eds. Taylor and Francis, Washington, DC,* 17-45, 1997.

27. Masion, A., J. Rose, A. Volge-Ritter, and J.-Y. Bottero., *Div. Environ. Chem. Prepr. Ext. Abstr.* 40(1):434, 2000.

28. C. Chambers, A. K. Holliday, Modern inorganic chemistry, *Great Britain, Butterwork & Co (Publishers) Ltd,*1975

29. Nieboer, E., Gibson, B.L., Oxman, A.D. and Kramer, J.R., *Environ. Rev.*, 3: 29, 1995

30. Srinivasan, P.T., T. Viraraghavan, B. Kardash, and J. Bergman, Aluminum speciation during drinking water treatment. *Water Qual. Res. J. Canada,* 1998

31. Casdorph, H.R., and M. Walker. Toxic Metal Syndrome. *Avery Publishing Group, Garden City Park, NY,* pp. 413, 1995.

32. Masten S., *Review of Toxicological Literature Abridged Final Report,* 2000

33. Dewberry, F.L., McKinney, T.D. and Stone, W.J., *Am. Soc. Artif. Intern. Organs,* 3: 102, 1980.

34. Altmann, P., Hamon, C., Blair, J., Dhanesha, U., Cunningham, J. and Marsh, F., *Lancet,* ii: 7, 1989.

35. Aluminum in the Canadian environment. M. Havas and J.F. Jaworski (eds.). *NRCC No. 24759, National Research Council of Canada, Ottawa.* pp. 153–173, 1986.

36. Neri, L.C. and Hewitt, D., [letter to the editor]. *Lancet,* 338: 390, 1991.

37. Neri, L.C., Hewitt, D. and Rifat, S.L., *Neurobiol. Aging,* 13(1): S115, 1992.

38. Forbes, W.F., Hayward, L.M. and Agwani, N., [letter to the editor]. *Lancet,* 338: 1592, 1991.

39. Forbes, W.F., Hayward, L.M. and Agwani, N., *Can. J. Aging*, 11(3):269, 1992.

40. Brun, A., Dictor, M., *Acta Pathol. Microbiol. Scand. [A]* 89:193; 1981.

41. Candy, J. M., McArthur, F. K., Oakley, A. E., Taylor, G. A., Chen, C. P. L.-H., Mountfort, S. A., Thompson, J. E., Chalker, P. R., Bishop, H. E., Beyreuther, K., Perry, G., Ward, M. K., Martyn, C. N., Edwardson, J. A., *J. Neurol. Sci.* 107:210, 1992

42. Harrington, C. R., Wischik, C. M., McArthur, mF. K., Taylor, G. A., Edwardson, J. A., Candy, J. M., *Lancet* 343: 993; 1994

43. Scholtz, C. L., Swash, M., Gray, A., Kogeorgos, J., Marsh, F., *Clin. Neuropathol.* 6: 93; 1987

44. Letterman, R. D., Driscoll, C. T., *J. Am. Water Works Assoc.* 80(4):154, 1988

45. Gajdusek, D.C. and Salazar, A., *Neurology*, 32:107, 1982.

46. Perl, D.P., Gajdusek, D.C., Garruto, R.M., Yanagihara, R.T. and Gibbs, C.J., Jr., *Science*, 217:1053, 1982.

47. Ganrot, P.O.,*Environ. Health Perspect.*, 65: 363, 1986.

48. Doll, R. review, *Age Ageing*, 22: 138, 1993.

49. Agency for Toxic Substances and Disease Registry. Toxicological profile for aluminum (update). Draft for public comment. *Public Health Service, U.S. Department of Health and Human Services, Atlanta, GA*, 1997.

50. Parkinson, I.S., Ward, M.K. and Kerr, D.N.S., *J. Clin. Pathol.*, 34:1285, 1981.

51. Touam, M., Martinez, F., Lacour, B., Bourdon, R., Zingraff, J., Di Giulio, S. and Drüeke, T., *Clin. Nephrol.*, 19(6):295,1983.

52. Alfrey, A.C., LeGendre, G.R. and Kaehny, W.D., *N. Engl. J. Med.*, 294(4):184, 1976.

53. Starkey, B.J., *Ann. Clin. Biochem.*, 24: 337, 1987.

54. Banks, W.A., Kastin, A.J. and Banks, M.F., *Clin. Res.*, 35(1): 31A, 1987.

2 Indicators

2.1 Dyes

Dyes are substances that can be used to impart color to other materials, such as textiles, foodstuffs, and paper. Unlike pigments, dyes are absorbed to a certain extent by the material to which they are applied. The colors from some dyes are more stable than others, however. A dye that does not fade when the material it was applied to be exposed to conditions associated with its intended use is called a *fast dye*. Contrariwise, a dye that loses its coloring during proper usage is referred to as a *fugitive dye*. Some of the conditions that could cause such a change in the properties of a dye include exposure to acids, sunlight, or excessive heat as well as various washing and cleaning procedures. Certain dyes may be considered both fast and fugitive, depending on the material with which they are used [1].

2.2 Metal indicators

The color of organic dyes is due to the chromophore groups and the addition of a metal cation causes a change in the electron distribution of the dye molecule. The indicators in which this occurs are called by Schwarzenbach [2] and by Körbl and Přibil [3] *metal indicators* as opposed to indicators that form with metal ions colored complexes in which the metal ion is the chromophore. A third group of indicators comprises those metals with incomplete 3d shells which form colored ions in solution. As the color intensity of such solutions is low, these ions are only rarely employed as indicators in complexometric titrations. Přibil has taken as an additional group of indicators compounds that form precipitates or colloidal particles with metal ions. Metal indicators which form the first group have been called *metallochromic* indicators by Přibil, but also the name *chelatochromic* indicators has been employed [4].

Metal indicators are classified according to their chemical constitution. Also those compounds which form metal complexes in which the metal is the chromophore are included. Bellow, group A comprises indicators that contain an azo group. Group T comprises indicators that are triphenylmethane derivative. All other indicators are included in the group O. This division has also been employed by Přibil [5]. Each group includes several subgroups as shown in the following.

The azo group may be bound to various cyclic groups which form the basic of the following classification:

A. Azo dyes

	Subgroup	*Azo group between*
ABB		two benzene rings
	ABI	a benzene and an imidazole ring
	ABN	a benzene and a naphthalene ring
	ABP	a benzene and a pyridine or pyrazoline ring
	ABQ	a benzene and a quinoline ring
	ABT	a benzene and a thiazole ring
	ANI	a naphthalene and an imidazole ring
	ANN	two naphthalene rings
	ANP	a naphthalene and a pyridine or pyrazoline ring
	ANQ	a naphthalene and a quinoline ring
	ANT	a naphthalene and a thiazole ring
APQ		a pyridine and a quinoline ring
T. Triphenylmethane Dyes		
TP		phthaleins
TS		sulphonephthaleins
O. Other Dyes		
	OA	anthracene derivatives
	OB	benzene derivatives
	ON	naphthalene derivatives
	OO	redox indicators and other unclassified dyes

Substances, whose fluorescent properties in solution are influenced by change in hydrogen ion concentration, oxidation potential or metal ion concentration, may be used as *'fluorescent indicators'* in titration in which a well-defined change in one of these properties occurs at the equivalence point.

A number of organic compounds which form complexes with cations in solution with a consequent quenching or appearance of fluorescence have been employed as indicators in complexiметric titrations. As indicators these compounds fuction in a similar manner to metallochromic indicators. The term *'metallofluorescent indicators'* proposed by Körbl [6] for these compounds has been adopted by IUPAC [7].

2.3 Mechanism of Azo Dye Formation

2.3.1 Mechanism of Diazotization [8, pp 414-430]

Nitrous acid is made in situ, most often by mixing hydrochloric acid with sodium nitrite. It dissociates to produce *nitrosonium ion* NO^+ rather than H^+ (although the solution is acidic because HCl is also present).

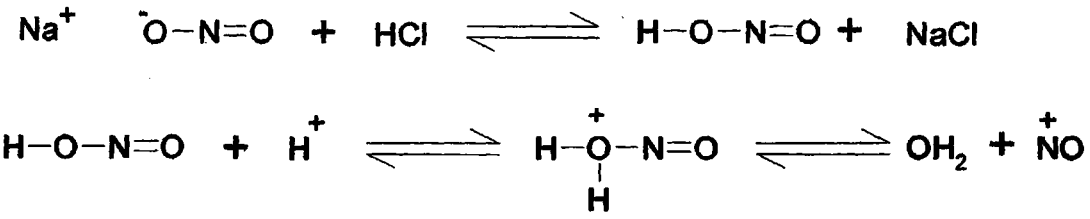

The nucleophilic amine, which is present in the reaction mixture from the beginning, reacts with the electrophilic nitrosonium ion, producing the *diazonium ion* by a series of acid-base and elimination reactions:

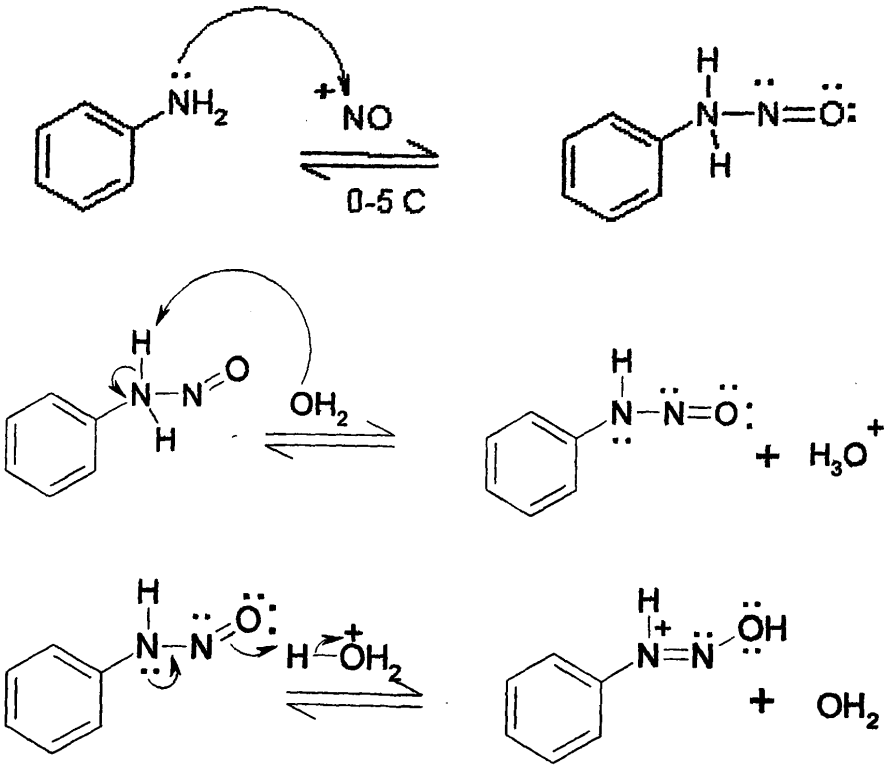

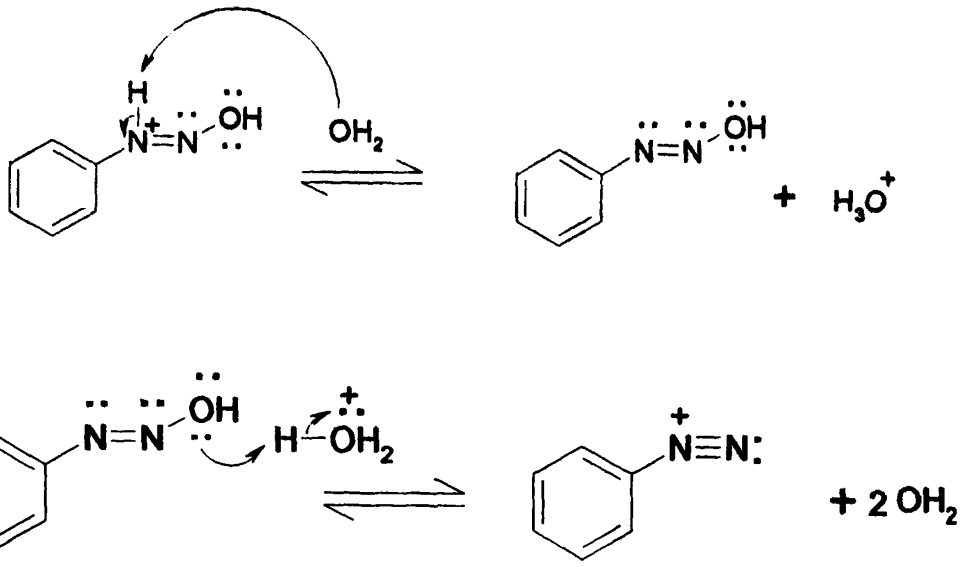

Aryl diazonium salt

2.3.2 Mechanism of Coupling Reaction

The diazonium ion has another resonance contributor, however, in which the terminal nitrogen atom bears the positive charge.

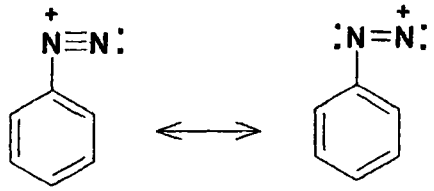

If an actived aromatic compound is added to a solution of the diazonium salt, then electrophilic substitution occurs. The electrophile in this case is the diazonium ion itself, rather than a simpler electrophile like NO_2^+ or Br^+. Only the most actived arenas, like a phenol or dialkylaniline, can be employed for this reaction, because the diazonium salt is a weak electrophile. The transformation occurs in two stages, the first of which involves reaction between the nucleophilic ring and the electrophilic nitrogen atom.

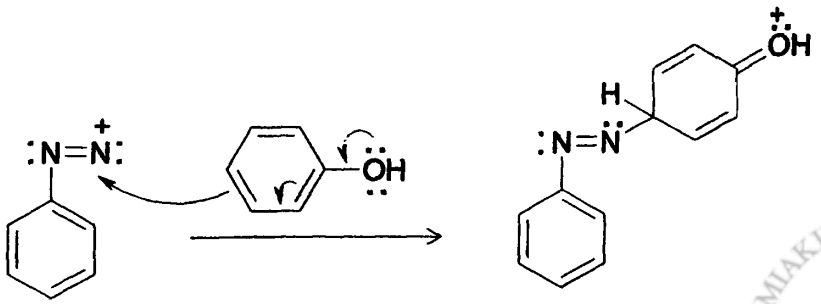

The second step in the regeneration of the aromatic π system.

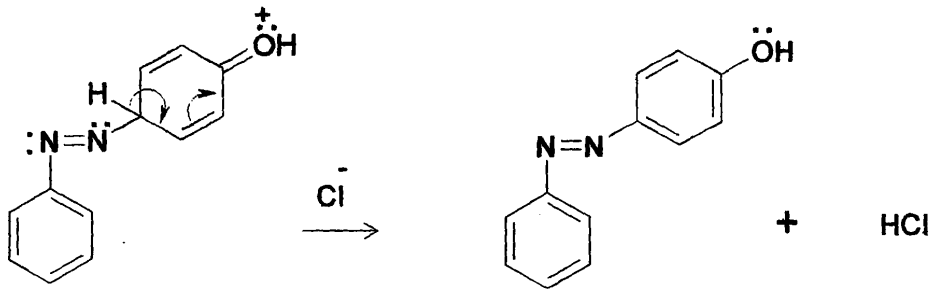

This coupling reaction produces molecules that are brightly colored as a result of extended conjugation of the π systems across the nitrogen-nitrogen double bond. Such compounds find applications as dyes [9, pp. 1171-1178].

2.4 Isomerism in azo dyes

2.4.1 Geometrical isomerism

As with any double bond, the planar -N=N- bond shows geometrical isomerism:

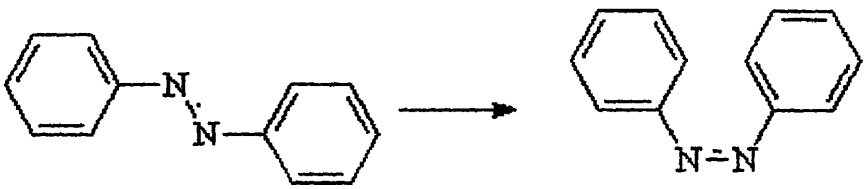

This change from trans (preferred) to cis can be effected by exposure to UV radiation. This can lead to *photochromism*, a light-induced reversible color change in some dyes, for example C.I. Disperse Red 1. This effect was considered a nuisance and has largely been eliminated by careful development of more stable dyes. But photochromic dyes are beginning to make a comeback in technology like sunglasses and sunroofs in cars.

2.4.2 Tautomerism

Following the discovery in 1870 of the coupling reaction between diazonium salts and phenols [10] the colored products were believed to be hydroxyazo compounds. The first challenge to this was made in 1883 by Liebermann [11] who postulate that the hydroxyl proton of 1-phenylazo-2-naphthol, II (R=H), was labile and could be capable of bonding with a nitrogen atom of the azo group. Evidence to support Liebermann's assertion came the

following year when Zincke and Bindewald [12] reported that they obtained the same product either by coupling the benzene diazonium ion with 1-naphthol or by condensing phenylhydrazine with 1,4-naphthoquinone. Kuhn and Bär [13] proved the existence of a rapidly formed tautomeric equilibrium of the type I(R=H) between the azo and hydrazo forms. It is know that this equilibrium is influenced by both structural factors within the molecule and by the nature of the medium surrounding the molecule.

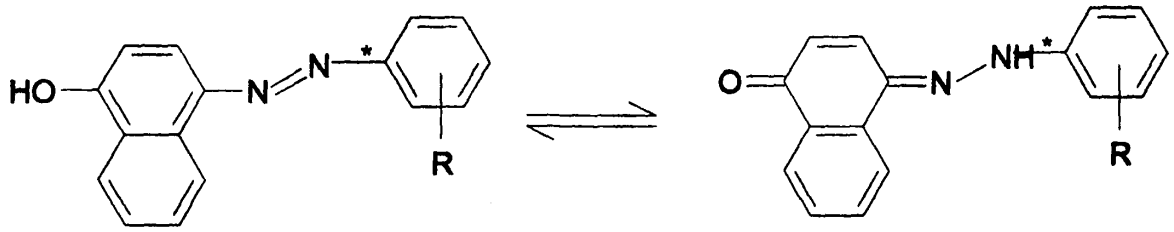

I 4-Phenylazo-1-naphthol[14]

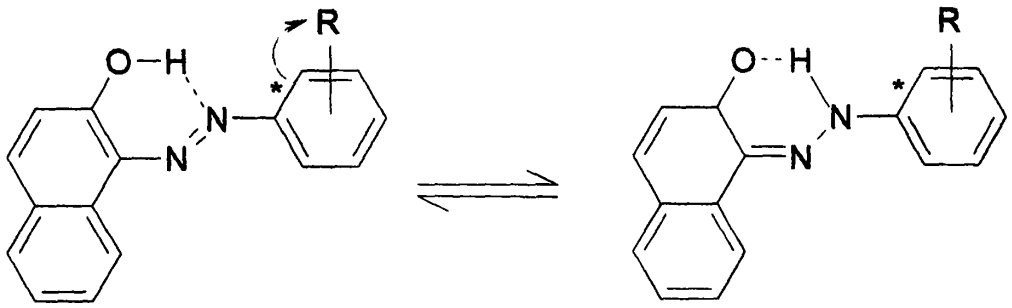

II 1-Phenylazo-2-naphthol[14]

Most azo phenol dyes exist in the azo form because of the resonance stabilization energy of the aromatic ring system. The loss in energy in going from hydroxyl naphthalene to naphtha quinine is less than in going from hydroxyl benzene to benzo quinine. Thus in azo-naphthol-dyes, the hydrazo form prevails [15].

References:

1 http://greatvistachemicals.com/

2 Schwarzenbach, G., Experientia Suppl. V, 1956, 162

3 Körbl, J. and Přibil, R., *Coll. Czech. Chem. Comms.*, 1957, 22, 1122.

4 Püschel, R. and Lassner, E., *Chemist Analyst*, 1960, 49, 58.

5 Přibil, R., Komplexometrie, Band I, *VEB Deutscher Verlag für Grundstoffindustrie, Leipzig*, 1960.

6 Körbl, J. and Svoboda, V., *Talanta*, 1960, 3, 370.

7 Bishop E., Indicators, *Pergamon Press*, 1972.

8 Norman R.O.C., Principles of organic synthesis, *Methuen & CO. LTD and Science Paperbacks*, pp 414-430, 1968.

9 Sorell T.N., Organic Chemistry, *University Science Books*, pp. 1171-1178, 1999.

10 Kekule A., Hidegh C., Chem Ber., 3, 233, 1870

11 Liebermann C., Chem Ber., 16:2858-2864, 1883

12 Zincke T., Bindewald H., Chem Ber., 17, 3026, 1884

13 Kuhn R., Bär F., Annalen., 516, 143-155, 1935

14 Ball P. and Nicholls C.H., Azo-Hydrazone Tautomerism of Hydroxyazo Compounds- a review, Dyes and Pigments 3 (1982) 5-26

15 Dakiky M., Manassra A., Abdul Kareem M., Jumean F., Khamis M., *Dyes and Pigments 63 (2004) 101-113*

3. Molecular Absorption Spectrometry

3.1 Interaction of electromagnetic radiation with matter [1].

In spectrometric methods, the sample solution absorbs electromagnetic radiation from an appropriate source, and the amount absorbed is related to the concentration of the analyte in solution.

Electromagnetic radiation can be considered a form of radiant energy that is propagated as a transverse wave. It vibrates perpendicular to the direction of propagation, and this imparts a wave motion to the radiation.

The wave is described either in terms of its *wavelength*, the distance of a complete cycle, or in terms of the *frequency,* the number of cycles passing a fixed point per unit time. The reciprocal of the wavelength is called the *wavenumber* and is the number of waves in a unit length or distance per cycle.

The relationship between the wavelength and frequency is:

$$\lambda = \frac{c}{\nu} \qquad (3.1)$$

where λ is the wavelength in centimeters (cm), ν is the frequency in reciprocal seconds (s^{-1}), or hertz (Hz), and c is the velocity of the light (3×10^{10}cm/s). The wavenumber is represented by $\bar{\nu}$, in cm^{-1}:

$$\bar{\nu} = \frac{1}{\lambda} = \frac{\nu}{c} \qquad (3.2)$$

The wavelength unit preferred for the ultraviolet and visible regions of the spectrum is nanometer, while the unit micrometer is preferred for the infrared region.

In this last case, wavenumbers are often used in place of wavelength, and the unit is cm^{-1}.

Electromagnetic radiation processes a certain amount of energy. The energy of a unit of radiation, called the *photon,* is related to the frequency or wavelength by

$$E = h\nu = \frac{hc}{\lambda} \qquad (3.3)$$

where E is the energy of the photon in ergs and h is Planck's constant, 6.62×10^{-34} joule-second (J-s).

3.2 Absorbance of Electromagnetic Radiation [2, pp. 380-381].

In absorption spectroscopy a beam of electromagnetic radiation passes through a sample. Much of the radiation is transmitted without a loss in intensity. At selected frequencies, however, the radiation's intensity is attenuated. This process of attenuation is called *absorption*. Two general requirements must be met if an analyte is to absorb electromagnetic radiation. The first requirement is that there must be a mechanism by which the radiation's electric or magnetic field interacts with the analyte. For ultraviolet and visible radiation, this interaction involves the electronic energy of valence electrons. The second requirement is that the energy of the electromagnetic radiation must exactly equal the difference in energy, ΔE, between two of the analytes quantized energy states. The energy level diagram in Figure 3.1 explains an absorbance spectrum. The thick lines labelled E_0 and E_1 represent the analyte's ground (lowest) electronic state and its first electronic excited state. Superimposed on each electronic energy level is a series of lines representing vibrational energy levels.

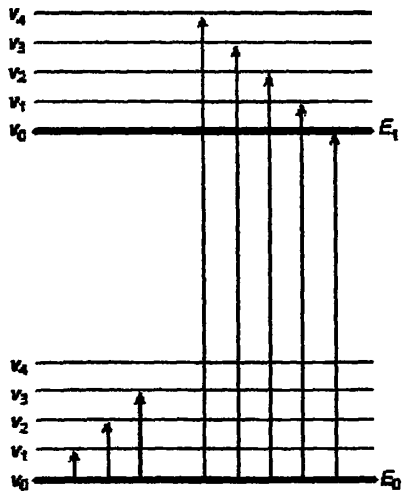

Figure 3.1 *Energy level diagram showing difference between the absorption of infrared radiation (left) and ultraviolet-visible radiation (right)*

3.3 Beer's Law

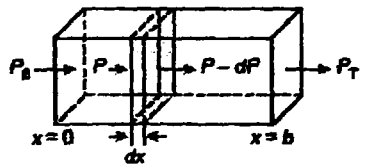

Figure 3.2 *Factors use in deriving the Beer-Lambert Law*

When monochromatic electromagnetic radiation passes through an infinitesimally thin layer of sample, of thickness *dx,* it experiences a decrease in power of *dP* (Figure 3.2). The fractional decrease in power is proportional to the sample's thickness and the analyte's concentration, *C;* thus

$$\frac{-dP}{P} = \alpha C dx \qquad (3.4)$$

where P is the power incident on the thin layer of sample, and α is a proportionality constant. Integrating the left side of Equation 3.4 from $P=P_0$ to $P=P_T$, and the right side from $x=0$ to $x=b$, where b is the sample's overall thickness

$$-\int_{P=P_0}^{P=P_T} \frac{dP}{P} = \alpha C \int_{x=0}^{x=b} dx \qquad (3.5)$$

gives

$$\ln\left(\frac{P_0}{P_T}\right) = \alpha b C \qquad (3.6)$$

Converting from ln to log, and substituting Equation 3.6, gives

$$A = abC \qquad (3.7)$$

where a is the analyte's absorptivity with units of cm^{-1} $conc^{-1}$. When concentration is expressed using molarity, the absorptivity is replaced by the molar absorptivity, ε (with units of cm^{-1} M^{-1})

$$A = \varepsilon b C \qquad (3.8)$$

The absorptivity and molar absorptivity give, in effect, the probability that the analyte will absorb a photon of given energy [2, pp.385].

Both absorbance and absorptivity are wavelength dependent. Actually a spectrophotometer does not measure the absorbance directly, but rather it must be calculated by taking the negative logarithm of the fraction of light transmitted through the sample. If P_T is the power of the light passing through a sample and P_0 is the power of the light detected when the concentration of absorbing material is zero, the fraction of the light transmitted is defined as the ratio of the electromagnetic radiation's power exiting the sample, P_T, to that incident on the sample from the source, P_0 and is given by:

$$T = \frac{P_T}{P_0} \qquad (3.9)$$

where T is the transmittance, often given as $\%T$. Absorbance is given by:

$$A = -\log T = \log \frac{P_0}{P_T} \qquad (3.10)\ [3]$$

3.3.1 Fundamental limitations to Beer's Law

Beer's law is a limiting law that is valid only for low concentrations of analyte [4]. Both chemical and instrumental deviations from Beer's Law may occur.

Chemical deviations are caused by reactions such as molecular dissociation or the formation of a new molecule. The most prevalent cause is some type of association caused by hydrogen bonding. For example, at very low concentrations in an inert solvent, alcohol exist as monomers, but as the concentration is increased the monomers combine to form dimmers, trimers, etc. Thus the concentrations and absorbances due to the monomers do not increase linearly with the total concentration of the species.

There are two *instrumental sources of deviation* from Beer's Law.

The first has to do with the fact that the Law was derived from monochromatic radiation [1].

Consider a beam consisting of just two wavelengths λ' and λ''. Assuming that Beer's law applied strictly for each of these individual wavelengths, we may write for radiation λ'

$$A' = \log \frac{P'_0}{P_T'} = \varepsilon' bC \qquad (3.11)$$

or

$$\frac{P'_0}{P_T'} = 10^{\varepsilon' bC} \qquad (3.12)$$

and

$$P_T' = P'_0 10^{-\varepsilon' bC} \qquad (3.13)$$

Similarly, for λ''

$$P_T'' = P''_0 10^{-\varepsilon'' bC} \qquad (3.14)$$

When an absorbance measurement is made with radiation composed of both wavelengths, the power of the beam emerging from the solution is given by $P_T'+P_T''$ and that of the beam from the solvent by $P'_0+P''_0$. Therefore, the measured absorbance is:

$$A = \log \frac{P'_0 + P''_0}{P'_0 10^{-\varepsilon' bC} + P''_0 10^{-\varepsilon'' bC}} \qquad (3.15)$$

When $\varepsilon' = \varepsilon''$, Equation 3.15 simplifies to

$$A = \varepsilon' bC \qquad (3.16)$$

and Beer's Law is followed.

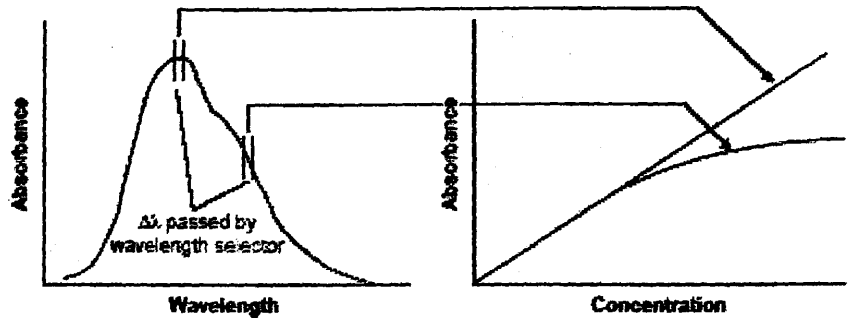

Figure 3.3 *Effect of wavelength on the linearity of a Beer's law calibration curve*

However, nonlinearity can occur at higher concentrations if there is a significant difference between ε' and ε'', as shown in Figure 3.3 [5, pp.305-306].

Stray radiation is the *second* contribution to instrumental deviations from Beer's law. Stray radiation arises from imperfections within the wavelength selector that allows extraneous light to 'leak' into the instrument. Stray radiation adds an additional contribution, P_{stray}, to the radiant power reaching the detector; thus

$$A = \log \frac{P_0 + P_{stray}}{P_T + P_{stray}} \qquad (3.17)$$

For small concentrations of analyte, P_{stray} is significantly smaller than P_0 and P_T, and the absorbance is unaffected by the stray radiation. At higher concentrations of analyte, however, P_{stray} is no longer significantly smaller than P_T and the absorbance is smaller than expected. The result is a negative deviation from Beer's law [2, pp.386-388].

References:

1. Gary D.Christian., Analytical Chemistry, 6th ed., John Wiley & Sons Inc., 2004
2. Harvey D., Modern Analytical Chemistry, McGraw-Hill Higher Education, pp. 385, 2000
3. Ewing G.W., Analytical instrumentation handbook, Marcell Dekker Inc., New York, 2nd ed., 1997.
4. Kortum G., and Seiler M.T., Angew. Chem., 52, 687, 1939
5. D. A. Skoog, F. J. Holler, T. A. Nieman, Principles of instrumental analysis, fifth edition, pp. 305-306, 1998

4. Molecular Luminescence Spectrometry

4.1 Introduction to fluorescence

4.1.1 Electron spin

The Pauli Exclusion Principle states that no two electrons in an atom can have the same set of four quantum numbers (n-principal quantum number; l-angular momentum number; m-magnetic quantum number; s-spin quantum number [1]). This restriction requires that no more than two electrons can occupy an orbital and furthermore the two must have opposed spin state. Under this circumstance, the spin are said to be paired. Because of spin pairing, most molecules exhibit no net magnetic field and are thus said to be *diamagnetic*- that is, they are neither attracted nor repelled by static magnetic field. In contrast, free radicals, which contain unpaired electrons, have a magnetic moment and consequently are attracted into a magnetic field; free radicals are thus said to be *paramagnetic* [2, pp 356].

4.1.2 Singlet/ triplet excited states

A molecular *electronic* state in which all electron spins are paired is called a *singlet state*, and no splitting of electronic energy levels occurs when the molecule is exposed to a magnetic field. The ground state for a free radical, on the other hand, is a *doublet* state because the odd electron can assume two orientations in a magnetic field, which imparts slightly different energies to the system.

When one of the pair of electrons of a molecule is excited to a higher energy level, either a *singlet* or *triplet* state is formed. In the excited singlet state, the spin of the promoted electron is still paired with the ground-state electron; in the triplet state, however, the spins of the two electrons have become unpaired and are thus parallel. These states can be represented as follows where the arrows represent the direction of the spin:

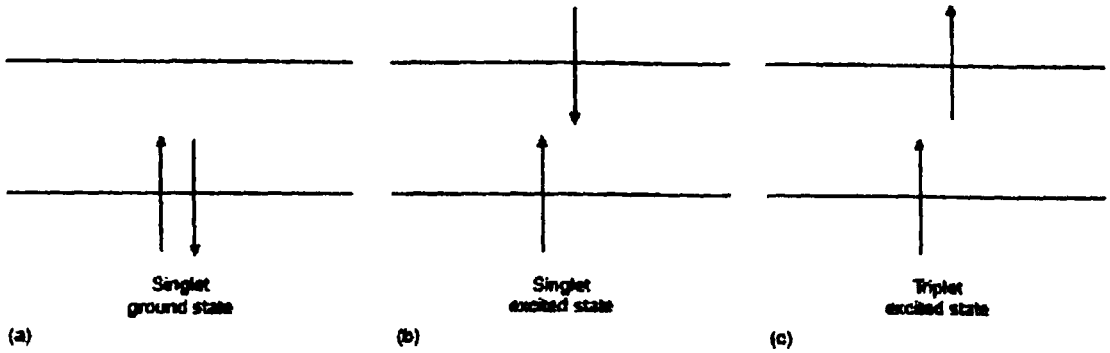

Figure 4.1. *Difference between singlet and triplet states*

Note that the excited triplet state is less energetic than the corresponding excited singlet state. The properties of a molecule in the excited triplet state differ significantly from those of the excited singlet state, for example: a molecule is paramagnetic in the triplet state and diamagnetic in the singlet state. More important, is the fact that a singlet/triplet transition (or the reverse), which also involves a change in electronic state, is a significantly less probable event than the corresponding singlet/singlet transition. As a consequence, the average lifetime of an excited triplet state may range from 10^{-4} to several seconds, as compared with an average lifetime of 10^{-5} to 10^{-8} s for an excited singlet state. Furthermore, radiation-induced excitation of a ground-state molecule to an excited triplet-state has a low probability of occurring, and absorption peak due to this process are several orders of magnitude less intense than the analogous singlet/singlet transition [2, pp 356-357].

4.1.3 Energy-level diagrams for photoluminescent molecules

The Figure 4.2 is a partial energy-level diagram for a typical photoluminescent molecule.

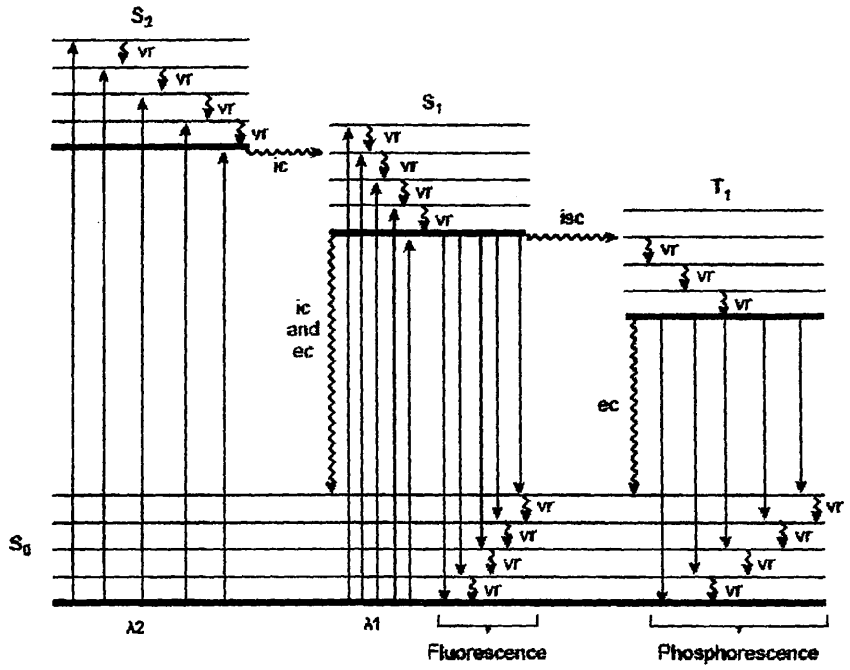

Figure 4.2. *Partial energy diagram for a photoluminescence system (one form of a Jabłoński diagram), vr is vibrational relaxation, ic is internal conversion, ec is external conversion and isc is intersystem crossing. The lowest vibrational energy level for each electronic state is indicated by thicker line* [3, p.423-425].

The lowest heavy horizontal line represents the ground-state energy of the molecule, which is normally a singlet state and is labeled S_0. At room temperature, this state represents the energies of essentially all of the molecules in solution. The upper heavy lines are energy levels for the ground vibrational level of three excited electronic states. The two lines on the left represent the first (S_1) and second (S_2) *electronic* singlet states. The one on the right (T_1) represents the energy of the first electronic *triplet* state. Numerous vibrational energy levels are associated with each of the four electronic states, as suggested by the lighter horizontal lines. As shown in Figure 4.2, excitation of this molecule can be brought about by absorption of two bands of radiation, one centered about the wavelength λ_1 (S_0-S_1) and the second around the shorter wavelength λ_2 (S_0-S_2). The excitation process results in conversion of the molecule to any of the several excited vibrational states. The rate at which a photon of radiation is absorbed is enormous, the process requiring on the order of 10^{-14} to 10^{-15} s.

Note that direct excitation to the triplet state is not shown because this transition does not occur to any significant extent since this process involves a change in multiplicity, an event which has a low probability of occurrence (a low-probability transition of this type is called '*forbitten*') [2, pp 357-358].

4.1.4 Deactivation processes

An excited molecule can return to its ground state by a combination of several mechanistic steps. As shown in Figure 4.2, two of these steps, *fluorescence* and *phosphorescence*, involve the emission of a photon of radiation. Fluorescence is a radiational transition between electronic states of the same multiplicity. Fluorescence usually occurs from the ground vibrational state of S_1 to various vibrational levels in S_0 ($S_1 \rightarrow S_0 + h\nu$). Typically, fluorescence requires 10^{-10} to 10^{-6} s to occur. Fluorescence usually appears at longer wavelengths than absorption because absorption transitions are to higher excited electronic states or to higher vibrational levels in the S_1 manifold. Fluorescence can occur from higher electronic states in rare instances. *Azulene* and its derivatives exhibit $S_2 \rightarrow S_0$ fluorescence.

The radiational deactivation process between electronic states of different multiplicity is called phosphorescence (typically, $T_1 \rightarrow S_0 + h\nu$). Usually, phosphorescence takes 10^{-4} to 10 s to occur because the process is spin forbidden. The wavelengths of phosphorescence for a given molecule are generally longer than those for fluorescence because the energy of T_1 is less than S_1, due to the electrons being unpaired and in different molecular orbitals. Phosphorescence is usually not seen in fluids solutions at room temperature. This is because there are many deactivation processes which compete with emission, such as nonradiative decay and quenching process [4, pp 5-6].

Fluorescence caused by direct excitation to the S_1 state or internal conversion to the S_1 state is called more precisely *prompt fluorescence*. *Delayed fluorescence* has a longer lifetime than prompt fluorescence because S_1 is populated by indirect mechanisms. For example, in *E-type delayed fluorescence*, S_1 is populated by thermally assisted intersystem crossing ($T_1 \rightarrow S_1$) back from a triplet state originally derived from an S_1 state; *P-type delayed fluorescence* involves a bimolecular reaction between triplet state followed by triplet-triplet annihilation ($T_1 + T_1 \rightarrow S_1 + S_0$). The term *photoluminescence* is used to describe any emission of photons after photon excitation. For molecules, photoluminescence includes prompt and delayed fluorescence as well as phosphorescence [5].

The first observation of fluorescence from a quinine solution in sunlight was reported by Sir John Frederick William Herschel in 1845 [6].

An important feature of fluorescence is high-sensitivity detection. The sensitivity of fluorescence was used in 1877 to demonstrate that the rivers Danube and Rhine were connected by underground streams. This connection was demonstrated by placing fluorescein into Danube river. Some 60 hours later, its characteristic green fluorescence appeared in a small river which led to the Rhine [7].

The other deactivation steps are radiationless processes. The favored route to the ground state is the one that minimizes the lifetime of the excited state. Thus, if deactivation by fluorescence is rapid with respect to the raditionless processes, such emission is observed. On the other hand, if a radiationless path has more favorable rate constant, fluorescence is either absent or less intense.

4.1.4.1 Vibrational relaxation (vr)

As shown in Figure 4.2, a molecule may be promoted to any of several vibrational levels during the electronic excitation process. In solution, however, the excess vibrational energy is immediately lost as a consequence of collisions between the molecules of the excited species and those of the solvent; the result is an energy transfer and a minuscule increase in temperature of the solvent. This relaxation process is so efficient that the average lifetime of a *vibrationally* excited molecule is 10^{-12}s or less, a period significantly shorter than the average lifetime of an *electronically* excited state. As a consequence, fluorescence from solution, when it occurs, always involves a transition *from the lowest vibrational level of an excited electronic state*. Several closely spaced peaks are produced, however, since the electron can return *to any one of the vibrational levels of the ground state* (Figure 4.2), whereupon it will rapidly fall to the lowest vibrational level of the ground electronic state by further vibrational relaxation.

A consequence of the efficiency of vibrational relaxation is that the fluorescence band for a given electronic transition is displaced toward lower frequencies or longer wavelengths from the absorption bands (the *Stoke's shift*); overlap occurs only for the resonance peak involving transitions between the lowest vibrational level of the ground state and the corresponding level of an excited state [2, pp 356-358].

4.1.4.2 Internal conversion (ic)

The crossover between two states of the same multiplicities is a nonradiative electron state transition called *internal conversion*. This is likely to occur when the potential energy curves for two electronic states cross such that the lower vibrational levels of the higher electronic state are approximately of the same energy as higher vibrational level of the lower electronic singlet state. Internal conversion can occur between excited states (e.q., $S_2 \rightarrow S_1$) or between the first excited electronic state and the ground electronic state ($S_1 \rightarrow S_0$). Generally, internal conversion between excited electronic states is rapid (10^{-12} s). Internal conversion from the S_1 to the S_0 state depends on the molecule but is often less efficient if there is a wide energy separation between S_1 and S_0, so that there is no overlap of the potential energy wells. After internal conversion, the excess vibrational energy is rapidly dissipated through vibrational relaxation to the ground vibrational level of the lower electronic state [5, pp 339].

4.1.4.3 External conversion (ec)

Deactivation of an excited electronic state may involve interaction and energy transfer between the excited molecule and the solvent or other solute. These processes are called collectively *external conversion*, or *collisional quenching*. Evidence for external conversion includes the marked effect upon fluorescence intensity exerted by the solvent; furthermore, those condition that tend to reduce the number of collisions between particles (low temperature and high viscosity) generally lead to enhanced fluorescence. Radiationless transitions to the ground state from the lowest excited singlet state and triplet state (Figure 4.2) probably involved external conversion, as well as internal conversion [2, pp 360].

4.1.4.4 Intersystem crossing (isc)

Intersystem crossing is a process in which the spin of an excited electron is reversed, and a change in multiplicity of the molecule results. As with internal conversion, the probability of this transition is enhanced if the vibrational levels of the two states overlap.

Intersystem crossing is most common in molecules that contain heavy atoms, such as iodine or bromine (the *heavy - atom effect)*. Spin/orbital interactions become large in the presence of such atoms, and a change in spin is thus more favorable. The presence of paramagnetic species such as molecular oxygen in solution also enhances intersystem crossing and a consequent decrease in fluorescence [2, pp 360].

4.2 Fluorescence [2p.425-426]

Fluorescence occurs when a molecule in the lowest vibrational energy level of an excited electronic state returns to a lower energy electronic state by emitting a photon. Since molecules return to their ground state by the fastest mechanism, fluorescence is only observed if it is a more efficient means of relaxation than the combination of internal conversion and vibrational relaxation. A quantative expression of the efficiency of fluorescence is the *fluorescent quantum yield,* Φ_F, which is the fraction of excited molecules returning to the ground state by fluorescence. Quantum yields range from 1, when every molecule in an excited state undergoes fluorescence, to 0 when fluorescence does not occur.

4.2.1 Quantum yield [2, pp360-361]

The *quantum yield,* or *quantum efficiency,* for fluorescence and phosphorescence is simply the ratio of the number of molecules that luminescence to the total number of excited molecules. For a highly fluorescent molecule such as fluorescein, the quantum efficiency under some conditions approaches unity. Chemical species that do not fluorescence appreciably have efficiencies that approach zero.

The fluorescence quantum yield Φ_F for a compound is determinated by the relative rate constants k_x for the processes by which the lowest excited singlet state is deactivated-namely, fluorescence (k_f), intersystem crossing (k_i), external conversion (k_{ec}), internal conversion (k_{ic}), predissociation (k_{pd}), and dissociation (k_d).We may express these relationships by the Equation

$$\Phi_F = \frac{k_f}{k_f + k_i + k_{ec} + k_{ic} + k_{pd} + k_d} \qquad (4.1)$$

where the k terms are the respective rate constants for the several processes enumerated above. Equation (4.1) permits a qualitative interpretation of many of the structural and environmental factors that influence fluorescence intensity. The magnitude of k_f, the predissociation rate constant k_{pd}, and the dissociation rate constant k_d are mainly dependent upon chemical structure; the remaining constants are strongly influenced by environment and to a somewhat lesser extent by structure.

4.2.2 Transition types in fluorescence [2, pp361]

The fluorescence seldom results from absorption of ultraviolet radiation of wavelengths lower than 250 nm because such radiation is sufficiently energic to cause deactivation of the

excited state by predissociation or dissociation. Fluorescence due to $\sigma^* \rightarrow \sigma$ transitions is seldom observed; instead, such emission is confined to the less energetic $\pi^* \rightarrow \pi$ and $\pi^* \rightarrow n$ processes.

As we have noted, an electronically excited molecule ordinarily returns to its *lowest excited state* by a series of rapid vibrational relaxations and internal conversions that produce no emission of radiation. Thus, fluorescence most commonly arises from a transition from the lowest vibrational level of the first excited electronic state to one of the vibrational levels of the ground state. For the majority of fluorescent compounds, then, radiation is produced by either an $n \rightarrow \pi^*$ or a $\pi \rightarrow \pi^*$ transition, depending upon which of these is the less energetic.

4.2.3 Quantum efficiency and transition type [2, pp361]

It is observed empirically that fluorescence is more commonly found in compounds in which the lowest energy transition is of a $\pi \rightarrow \pi^*$ type than in compounds in which the lowest energy transition is of the $n \rightarrow \pi^*$ type.

The greater quantum efficiency associated with the $\pi \rightarrow \pi^*$ state can be rationalized in two ways. First, the molar absorptivity of $\pi \rightarrow \pi^*$ transition is ordinarily 100- to 1000-fold greater than for an $n \rightarrow \pi^*$ process, and this quantity represents a measure of transition probability in either direction. Thus, the inherent lifetime associated with a $\pi \rightarrow \pi^*$ transition is shorter (10^{-7} to 10^{-9} s compared with 10^{-5} to 10^{-7} s for an $n \rightarrow \pi^*$ transition) and k_f in Equation (4.1) is larger.

Second, the rate constant for intersystem crossing k_i is smaller for $\pi \rightarrow \pi^*$ excited state because the energy difference between the singlet/triplet state is larger, that is, more energy is required to unpair the electron of the π^* excited state.

The *intensity of fluorescence*, I_f, is proportional to the amount of the radiation from the excited source that is absorbed and the quantum yield for fluorescence.

$$I_f = k\Phi_F(P_0 - P_T) \qquad (4.2)$$

where k is a constant accounting for the efficiency of collecting and detecting the fluorescence emission. From Beer's law we know that

$$\frac{P_T}{P_0} = 10^{-\varepsilon bC} \qquad (4.3)$$

where C is the concentration of the fluorescing species.

We obtain:

$$I_f = k\Phi_F P_0(1 - 10^{-\varepsilon bC}) \qquad (4.4)$$

For low concentrations of the fluorescing species, when εbC is less than 0.01, this Equation simplifies to

$$I_f = 2.303k\Phi_F P_0 \varepsilon bC \qquad (4.5)$$

The intensity of fluorescence therefore, increases with an increase in quantum efficiency, incident power of the excitation source, the molar absorptivity and concentration of the fluorescing species.

Fluorescence is generally observed with molecules where the lowest energy absorption is a $\pi \rightarrow \pi^*$ transition, although some $n \rightarrow \pi^*$ transitions show weak fluorescence. Most unsubstituted, nonheterocyclic aromatic compounds show favorable fluorescence quantum yields, although substitution to the aromatic ring can have a significant effect on Φ_F.

For example, the presence of an *electron-withdrawing* group, such as $-NO_2$, decreases Φ_F, whereas adding an *electron-donating* group, such as –OH, increases Φ_F. Fluorescence also increases for aromatic ring systems and for aromatic molecules with planar structures. A molecule's fluorescence quantum yield is also influenced by external variables such as temperature and solvent. Increasing temperature generally decrease Φ_F because more frequent collisions between the molecule and the solvent increases external conversion. Decreasing the solvent's viscosity decreases Φ_F for similar reasons. For an analyte with acidic or basic functional groups, a change in pH may change the analyte's structure and, therefore, its fluorescent properties. Changes in both wavelength and intensity of fluorescence may be affected. Fluorescence may return the molecule to any of several vibrational energy levels in the ground electronic state. Fluorescence, therefore, occurs over a range of wavelengths. Because the change in energy for fluorescent emission is generally less than that for absorption, a molecule's fluorescence spectrum is shifted to higher wavelengths than its absorption spectrum [2, 360-361].

4.3 Excitation versus Emission Spectra [2, p.427]

Photoluminescence spectra are recorded by measuring the intensity of emitted radiation as a function of either the excitation wavelength or the emission wavelength. An *excitation spectrum* is obtained by monitoring emission at a fixed wavelength while varying the excitation wavelength. Figure 4.3 shows the excitation spectrum for the hypothetical system described by the energy level diagram in Figure 4.2 when corrected for variations in source intensity and detector response, a sample's excitation spectrum is nearly identical to its

absorbance spectrum. The excitation spectrum provides a convenient means for selecting the best excitation wavelength for a quantitative or qualitative analysis. In an *emission spectrum* a fixed wavelength is used to excite the molecules, and the intensity of emitted radiation is monitored as a function of wavelength (nanaometers) or wavenumber (cm^{-1}). Although a molecule has only a single excitation spectrum, it has two emission spectra, one for fluorescence and one for phosphorescence. The corresponding emission spectra for the hypothetical system in Figure 4.2 are shown in Figure 4.3.

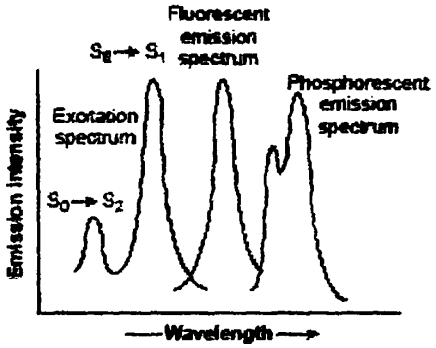

Figure 4.3. *Example of molecular excitation and emission spectra.*

4.3.1 Stokes'Shift

Examination of the Jablonski diagram (Figure 4.2) reveals that the energy of the emission is typically less than that of absorption. Hence, fluorescence typically occurs at lower energies or longer wavelengths. This phenomenon was first observed by Sir G. G. Stokes in 1852 in Cambridge [8].

One common cause of the Stokes'shift is the rapid decay to the lowest vibrational level of S_1. Furthermore, fluorophores generally decay to higher vibrational levels of S_0, resulting in further loss of excitation energy by thermalization of the excess vibrational energy. In addition to these effects, fluorophores can display further Stokes'shifts due to the solvent effects, excited-state reactions, complex formation, and/or energy transfer [4, pp 6].

4.3.2 Emission spectra are typically independent of the excitation wavelength

Another generally property of fluorescence is that the same fluorescence emission spectrum is generally observed irrespective of the excitation wavelength, because of rapid vibrational relaxation. This is known as Kasha's rule [9].

Although Vavilov reported in 1926 that quantum yields were generally independent of excitation wavelength [7].

The generally symmetric nature (the mirror image rule) of these spectra (absorption and emission spectra) is a result of the same transitions being involved in both absorption and emission and the similarities of the vibrational energy levels of S_0 and S_1.

4.3.3 Exception to the Mirror Image rule

Deviations from the mirror image rule usually indicate a different geometric arrangement of nuclei in the excited state as compared to the ground state. Nuclear displacement can occur prior to emission because of the relatively long lifetime of the S_1 state, which allows time for motion following the instantaneous process of absorption [4, pp 8].

4.4 Structural factors

Fluorescence is expected in molecules that are aromatic or contain multiple-conjugated double bonds with a high degree of resonance. Both classes of substances have delocalized π-electrons that can be placed in low-lying excited singlet states. In polycyclic aromatic system where the number of π-electrons available is greater than in benzene, these compounds and their derivatives are usually much more fluorescent than benzene and its derivatives [10].

The nature of substituent groups (especially chromophoric ones) of aromatic compounds play an important role in the nature and extend of a molecule's fluorescence, as summarized in Table 4.1

Table 4.1 *Effects of substituents on luminescence of aromatic compounds* [11, pp 88-92]

Substituent	Effect on frequency of emission	Effect on intensity
Alkyl	None	Very slight increase or decrease
Hydroxyl (OH), methoxyl (OCH_3)	Decrease	Increase
Carboxyl (CO_2H), keto (COR)	Decrease	Large decrease
Nitro (NO_2), nitroso (NO)	Large decrease	Large decrease
Primary (NH_2), secondary (NHR), or tertiary amine (NR_2)	Decrease	Increase
Cyanide (CN)	None	Increase
Sulphydryl (SH)	Decrease	Decrease
Soulphonic acid (SO_3H)	None	None
F ↓	Decrease	Decrease
Cl		
Br		
I		

A simple generalization is that ortho-para-directing substituents often enhance fluorescence, whereas meta-directing groups repress it. Many of the common meta-directing substituents possess low-lying (n,π^*) singlets. The lowest-lying (n,π^*) singlet increase the extent of singlet→triplet intersystem crossing relative to that in the parent hydrocarbon [12].

In contrast, the –CN substituent is meta-directing, yet cyanosubstituted aromatics often fluoresce more intensely than the parent hydrocarbon. Evidently (n,π^*) singlet states in cyanoaromatics are sufficiently higher in energy than the lowest (π,π^*) singlet for the former to have no significant perturbing effect [13].

Some ortho-para-directing substituents (-OH, $-NH_2$, $-OCH_3$) tend to enhance the fluorescence of aromatic compounds, whereas, they have a strong tendency to hydrogen-bond with solvent or occasionally with other solutes, hence increasing the efficiency of $S_1^* \rightarrow S_0$ internal conversion.

The trends for luminescence yields in haloaromatics are usually rationalized by postulating that heavy-halogen substitution ('heavy-atom' effect [14,15 pp 40-43]) increases the rates of $S_1^* \rightarrow T_1^*$ intersystem crossing and $T_1^* \rightarrow S_0$ phosphorescence.

Molecular rigidity reduces the interaction of a molecule with its medium and thus reduces the rate of collisional deactivation (internal conversion). This reduced rate of deactivation by nonradiative processes leads to a greater probability of luminescence.

The quantum efficiency of fluorescence in most molecules decreases with increasing temperature because the increased frequency of collisions at elevated temperatures improves the probability for deactivation by external conversion [2, pp 363].

The fluorescence of a molecule is decreased by solvent containing heavy atoms or other solute with such atoms in their structure. Heavy-atoms solvents usually induce a significant decrease in Φ_F and a concomitant in the efficiency of $S_1^* \rightarrow T_1$ intersystem crossing [16].

The heavy-atom effect increases the rates of both intersystem crossing $T_1^* \rightarrow S_0$ and phosphorescence, but the effect on the latter is usually greater [17].

The fluorescence spectra of most aromatic compounds containing acidic or basic functional groups are very sensitive to the pH of the solvent. Most proton-transfer reactions in polar solvents are very fast, such that Brőnsted acid-base reactions can occur during the lifetime of an excited-singlet state of an aromatic molecule. Brőnsted acidity differences between the ground and lowest excited singlet states of organic molecules are large, commonly ranging 4-9 pK units. Some compounds classes, especially phenols, thiols, and aromatic amines, become much stronger acid on excitation, whereas others (nitrogen and

sulfur heterocyclics, carboxylic acids, aldehydes, and ketones) with lowest (π,π^*) singlets becomes much more basic (Table 4.2).

Table 4.2. *Excited-state acidities for some aromatic compounds* [a]

Compound	*pK_a*		
	Ground	*Singlet*[b]	*Triplet*[c]
Phenol	10.00	4.0	8.5
4-Methoxyphenol	10.21	5.6	8.6
2-Naphthol	9.5	3.1	7.7
1-Naphthoic acid	3.7	~11	4.6
2- Naphthoic acid	4.2	~11	4.2
Quinolinium ion	5.1	10.5	5.8
Acridinium ion	5.5	10.6	5.6
2-Naphthylammonium ion	4.1	~-2	3.1

[a] Data from Jackson and Porter [18], Weller [19], and Wehry and Rogers [20]

[b] First excited-singlet state

[c] Lowest triplet state.

The formation of chelates with metal ions, in general, also promotes fluorescence by promoting rigidity and minimizing internal vibrations. When a fluorescence ligand is complexed with a *closed-shell*, diamagnetic, metal ion, such as Al^{3+}, Zn^{2+}, Mg^{2+}, Cd^{2+}, Ga^{3+}, In^{3+}, and Tl^{3+}, the complex is likely to fluoresce; its fluorescence spectrum will tend to resemble that of the free ligand. For this behavior to be observed, the lowest energy spin-allowed ligand-localized $\pi\rightarrow\pi^*$ transition (i.e., $S_0\rightarrow S_1$) must be lower in energy than any of the metal-centered transitions [21, pp 109-110].

The introduction of paramagnetic metal ions, such as Cu^{2+} and Ni^{2+}, in a sample tends to quench the fluorescence of fluorescent molecules and to increase the efficiencies of $S_1^*\rightarrow T_1^*$ intersystem crossing and spin-forbidden radiative process (both phosphorescence and $S_0\rightarrow T_1^*$ absorption) [15, pp 284].

The paramagnetism of most transition metal ions is a direct consequence of the fact that they have an *unfilled d subshell*. The color of many transition metal salt are due to spin-allowed *d-d* transitions, which usually occur at lower energies than the $\pi\rightarrow\pi^*$ transitions in aromatic ligands [22,23].

On the other hand, whereas paramagnetic species quench fluorescence, they strongly promote intersystem crossing so that those cations are observed to promote phosphorescence.

4.5 Quenching and excited-state reaction [3, p.343-344]:

The luminescence signals observed can be reduced by the presence of concomitants through several mechanisms. Reabsorption of emitted radiation by other species (or even other analyte molecules) is sometimes called *trivial quenching.*

4.5.1 Dynamic quenching.

Quenching normally refers to nonradiative energy transfer from excited species to other molecules. Dynamic quenching or collisional quenching requires contact between the excited lumophore and the quenching species, the quencher (Q). The rate of quenching is diffusion controlled and depends on the temperature and viscosity of the solution. The quencher concentration must be high enough that the probability of collision between the analyte and the quencher is significant during the lifetime of the excited species.

If the magnitude of the quenching depends linearly on the concentration of the quencher, then the quenching is said to obey *Stern-Volmer kinetics* and follows the Stern-Volmer Equation:

$$\frac{\Phi_0}{\Phi_q} = 1 + k_q \cdot [Q] \qquad (4.6)$$

where k_q is the Stern-Volmer quenching constant, Φ_0 is the fluorescence quantum yield when no quencher is present, and Φ_q is the quantum yield in the presence of a quencher concentration of Q moles per liter. When the quenching process is a collisional process and diffusion controlled, the Stern-Volmer Equation can be written in the form

$$\frac{\Phi_0}{\Phi_q} = 1 + \tau_M \cdot k_{diff} \cdot [Q] \qquad (4.7)$$

where τ_M is the fluorescence lifetime in the absence of Q and k_{diff} is the rate parameter of the diffusion-controlled quenching process. In the case of concentration quenching or self-quenching, a diffusion-controlled process as well, the solute fluorescence is decreased with increase of solute concentration. The Stern-Volmer law can be applied here and written as:

$$\frac{\Phi_0}{\Phi_q} = 1 + k \cdot [X] \qquad (4.8)$$

where k is the Stern-Volmer coefficient of concentration quenching and X is the solute concentration [24].

4.5.2 Static quenching.

Another form of quenching is *static quenching* in which the quencher and the fluorophore in the ground state form a stable complex (i. e. the dark complex). Fluorescence is only observed from the unbound fluorophore.

4.5.3 Long-Range Quenching

Energy transfer can occur between molecules without collisions. This type of nonradiational deactivation is called *long-range quenching* or *Förster quenching.* It can be considered to be due to dipole-dipole coupling between a donor (the excited lumophore) and an acceptor (the quencher). The rate of energy transfer (k_T) to a specific acceptor is given by

$$k_T = \tau_D^{-1} \left(\frac{R_0}{R} \right)^6 \qquad (4.9)$$

where τ_D is the luminescence lifetime of the donor, R is the average distance between the donor and acceptor molecules, and R_0 is the Förster distance. The Förster distance for efficient quenchers is often in the range 20 to 50 Å and can be as large as 100 Å. Efficient long-range energy transfer is favored in situations where the emission spectrum of the donor and the absorption spectrum of the acceptor overlap and the molar absorptivity of the donor is relatively high in the overlap region. The rate of energy transfer increases with acceptor concentration as the average distance between molecules decreases. The dependence of the degree of quenching on the quencher concentration is complex and does not follow the Stern-Volmer model.

References:

1. Mingos, D.M.P., *Essential Trends in Inorganic Chemistry*, Oxford University Press, pp. 1-6, 1998.
2. D. A. Skoog, F. J. Holler, T. A. Nieman, *Principles of instrumental analysis, fifth edition*, 1998
3. Harvey D., *Modern Analytical Chemistry*, McGraw-Hill Higher Education, 2000.
4. Lakowicz J., R., *Principles of fluorescence Spectroscopy*, 2nd ed., Kluwer Academic/Plenum Publishers, New York, p.5-6, 1999
5. J. D. Ingle, jr. S. R. Crouch, *Spectrochemical analysis*, Prentice-Hall International Edition, 1988
6. Herschel, Sir J.F.W., *Phil. Trans. R. Soc. London* 135:143, 1845.
7. Berlman I.B., *Handbook of fluorescence spectra of aromatic molecules*, 2nd ed., Academic Press, New York, pp. 4, 1971
8. Stokes G.G., *Phil. Trans. R. Soc. London* 142;463, 1852
9. Kasho M., *Disc. Faraday Soc.*, 9:14, 1950.
10. Willard H.H., Merritt Jr.L.L., Dean J.A., Settle Jr.F.A., *Instrumental methods of analysis*, 7th ed., Wadsworth publishing company, USA, 1988.
11. Guilbault G.G., *Practical Fluorescence theory, methods, and techniques*, New York, pp. 88-92, 1973
12. Hurley R. and Testa A.C., *J. Amer. Chem. Soc.*, 90:1949, 1968.
13. Parker A., *Photoluminescence of Solutions*, Elsevier, Amsterdam, pp.435, 1968
14. El-Sayed M.A., *Acc. Chem. Res.*, 1:8, 1968.
15. McGlynn S.P., Azumi T., and Kinoshita M., Molecular Spectroscopy of the Triplet State, Prentince-Hall, Englewood Cliffs, N.J., pp.40-43, 1969.
16. Medinger T. and Wilkinson F., *Trans. Faraday Soc.*, 61:620, 1965.
17. Gianchino G.G. and Kearns D.R., *J. Chem. Phys.*, 52: 2964, 1970.
18. Jackson G. Porter G., *Proc. Roy. Soc. (London)*, A260:13, 1961.
19. Weller A., *Progr. React. Kinet.*, 1:189 ,1961.
20. Wehry E.L., and Rogers L.B., *J. Amer. Chem. Soc.*, 87:4234, 1965.
21. Guilbault G.G., *Practical Fluorescence*, 2nd edition, revised and expanded, New York , p.109-110, 1990.
22. Porter G.B., *Concepts of Inorganic Photochemistry*, John Wiley and Sons, New York, pp. 38, 1975.

23. Crosby G.A., *J. Chem. Ed.,* 60: 791, 1983.

24. Schulman S.G., *Molecular Luminiscence Spectroscopy. Methods and Applications: Part 1*, vol.77, John Wiley & Sons, pp. 32-33, 1985.

5. Analytical methods of aluminum measurements in pharmaceutics, environmental and biological samples

Large amounts of toxic elements such as metal ions have been and are nowadays discharged into the environment as a consequence of human activities. Exposure to these compounds is of great concern as it poses not only severe carcinogenic risks to humans, but also potentially unacceptable ecological risk to plants, animals and microorganisms. Therefore, it is necessary to ensure a timely warning for possible accumulation of polluting trace metal in natural waters in order to protect public health. The accurate determination of trace metals in a variety of environmental samples at the low 10^{-8} M levels according to the tolerable levels imposed by European directives is thus required, along with the development of speciation schemes to discriminate between different chemical forms.

Although aluminum is the third most abundant element in the Earth's crust, its concentration in natural waters is low because of the relatively low solubility of aluminum minerals (viz. feldspars). In spite of this fact, the possible relationship between environmental aluminum exposure and Alzheimer's disease prompted an increased awareness of aluminum levels in the environment and forced the development of analytical methodology suitable for ultratrace detection of the target element [1].

An intractable chemical nature coupled with the lack of specific reagents combine to make aluminum one of the most difficult of the commonly occurring elements to determine chemically. Any sample taken from the environment will contain a wide range of inorganic substances, among which there will be present almost always a metal ion or counterion to cause interference effects. Therefore, separation, masking, critical control of pH, etc., must be performed routinely during chemical analysis for aluminum [2].

Table 5.1 Analytical Methods for determining aluminium in environmental samples

Analytical method	*Detection technique*	*Reagent/characteristics*	*Linear range*	*Detection Limit*	*Matrix sample*	*Ref.*
GFAAS	-	-	$(2.22\text{-}7.4)\times10^{-6}$ M $(1.41\text{-}7.4)\times10^{-6}$ M	6.6×10^{-7} M 4.1×10^{-7} M	soft drinks	4
SIA	ETAAS	co-surfactant (sec-butanol)	7.7-120 p,gAll(-1)	2.3μg All(-1)	lubricating oils	5
GFAAS	-	-	-	0.6 μg/g	solid samples	6
GFAAS	-	-	$7.4\times10^{-8}\text{-}1.85\times10^{-6}$ M	3.7×10^{-8} M	wine	7
ETAAS	-	ruthenium, permanent modifier	$(0.037\text{-}3.7)\times10^{-6}$ M	1.5×10^{-8} M	urine and serum samples	8
FIA – ETAAS	-	8-Q	$1.85\times10^{-9}\text{-}0.11\times10^{-6}$ M	$(0.55\text{-}1.48)\times10^{-9}$ M	potable, fresh, river and sea water	9
GFAAS	-	-	$(9.3\text{-}94.5)\times10^{-6}$ M	5.55×10^{-8} M	wines	10
ETAAS	-	-	$7\times10^{-8}\text{-}2.96\times10^{-6}$ M	7×10^{-8} M	bottled mineral waters	11
SE+GFAAS	-	pyrocatechol violet	(1-0.40)μg/250 mL	7.8×10^{-10} M	natural waters	12
HPF/HHPN	FAAS	-	2.5-25 μg/g	0.1-1 μg/g	drinking water	13
INAA	-	-	$(2.95\text{-}6.3)\times10^{-6}$ M	100 ng	drinking water	14
UV	λ = 561nm	MCPF + surfactant	$(0.11\text{-}5.18)\times10^{-6}$ M	-	novel chemical probe	15
UV	-	PCV	-	10^{-8} M	water	16
UV	-	Bisfol	-	3.7×10^{-7} M	river and well water	17
UV	λ = 600nm	Chromazol-KS	1-150μgAl_2O_3/100 mL	-	rock, gypsum, water glass , phosphoric acid, waste effluents, Deep-well water	18
UV	λ = 580 nm	SPADNS	-	$(2.96\text{-}11.86)\times10^{-6}$ M	-	19
UV Derivative UV	λ = 569nm	HNB	$(1.11\text{-}59.3)\times10^{-7}$ M $(2.96\text{-}11.86)\times10^{-6}$ M	3.78×10^{-7} M 1.3×10^{-7} M	alloy, ore, cement, dolomite, feldspar, limestone	20
UV	λ= 625 nm	Gallocyanine	$0\text{-}7.4\times10^{-6}$ M	4.44×10^{-8} M	human hair, tea, water	21

UV	λ = 380 nm	8-Q	1-150 μg/25 cm^3	-	aqueous solution	22
FIA	UV	Methyl thymol blue	(9.3-74.1)×10^{-6} M	1.11×10^{-6} M	Silicate materials and ores	23
HPLC	UV(λ=290nm)	PMBP	0-1.8×10^{-4} M	5×10^{-7} M	-	24
IP-RP-HPLC	UV	SO(2)CAS	-	8.9×10^{-9} M	river and tap water	25
RP-HPLC +E	UV (λ= 390nm)	8-HQ	(1.4-37.1)×10^{-9} M	0-08ng	drinking , natural waters	26
PR-HPLC	UV	8-HQ	7.4×10^{-8}-22.2×10^{-6} M	3.7×10^{-8} M	water	27
SPE/SCX-ICP-AES	UV	PCV	-	-	soil and freshwater sample	28
E-K	UV	H_2O_2-Cu(II)-o-aminophenol/$CHCl_3$	(1.4-92)×10^{-7} M	5.9×10^{-8} M	water, tea	29
RP-HPLC	UV	8-HQ	7.4×10^{-11}-1.1×10^{-8} M	7.4×10^{-8} M	real drinking and natural water	30
IC	UV	-	0-3.7×10^{-3} M	1.8×10^{-6} M	natural and tap waters	31
IC	UV	Tiron	(0.74-74)×10^{-6} M	-	natural waters	32
CFA FIA	UV	Triphenylmethane azo dyes	(1.8-29.6)×10^{-6} M	-	drinking water	33
RPLC	UV (λ=390nm)	8-Q	-	10^{-8} M	natural waters	34
CKS	λ = 360 nm	PCV	(1.48-74.1)×10^{-7} M	3×10^{-8} M	water, tea samples	35
DRS	-	Eriochrome cyanine R	-	1.48×10^{-7} M	water	36
DRS	(speciation)	Eriochrome cyanine R	0.2-2 μg/50 mL	1.48×10^{-7} M	surface water	37
DRS	-	eriochrome cyanine R	(1.3-40)×10^{-5} M	1×10^{-5} M	aqueous samples	38
AdCSV	-	DASA	<LOD-3.3×10^{-8} M	2.9×10^{-8} M	dialysis concentrates	39
AdPV	-	DA	(4-800)×10^{-7} M	1.4 ×10^{-7} M	drinking water	40
AdSV	-	-	10^{-5}-10^{-7} M	-	Waters	41
Indirect-DPV	-	L-dopa	(2-18)×10^{-7} M	7.6×10^{-8} M	mineral water	42
DPV	-	PCV	10^{-8}-10^{-7} M 10^{-7}-10^{-6} M	5×10^{-9} M	drinking water	43
Indirect-DPV	-	PCV	10^{-8}-10^{-7} M	5×10^{-9} M	water	44
V	-	ARS	(1.4-14)×10^{-7} M	8×10^{-8} M	water samples	45
V	-	Alizarin	0-1×10^{-5} M	1.5×10^{-7} M	Soil samples	46
A.C.OP	-	Solochrome violet RS	10^{-7}-6×10^{-6} M	5×10^{-8} M	natural and drinking	47

					waters	
A.C.OP	-	Solochrome violet RS	$(5\text{-}600)\times10^{-7}$ M	2×10^{-7} M	real water	48
A.C.OP	-	-	5×10^{-6}-8×10^{-5} M	5×10^{-6} M	drinking waters	49
A.C.OP	-	1,2dihydroxyanthraquinone-3-sulfonic acid	5×10^{-6}-5×10^{-5} M	1×10^{-6} M	natural and drinking waters	50
FIA, P, V	-	4-nitrocatechol	-	0.08×10^{-6} M	soil-derived fluvic acid	51
P	-	ETPTP	10^{-5}-10^{-1} M	-	rocks	52
P	-	EDTA	10^{-5}-10^{-1} M	-	aqueous solutions	53
Adsorption chrono-potentiometry	-	cupferon	2×10^{-9}-9×10^{-7}M	1×10^{-9} M	drinking waters	54
Chronopotentiometry	-	solochrome violet RS	10^{-8}-10^{-6} M	5.2×10^{-9} M	real water samples	55
SS	-	Lumogallion Silica modified	$(3.7\text{-}48.2)\times10^{-7}$ M	2.6×10^{-6} M 1.11×10^{-6} M	alcohol-free beverages	56
EIA	-	Xylenol Orange	$(3.7\text{-}74.1)\times10^{-6}$ M	-	water	57
ISE	-	-	1×10^{-5}-1×10^{0} M	1×10^{-6} M	electroplating electrolytes	58
FIS	-	methyl thymol blue	$(9.2\text{-}74.1)\times10^{-6}$ M	1.11×10^{-6} M	silicate materials, ores	59
IPRPP	HPLC	2,2'-dihydroxyazobenzene	-	7.4×10^{-9} M	water samples	60

Table 5.2 *Analytical methods for determining aluminum in biological materials*

Analytical method	*Detection technique*	*Reagent/characteristics*	*Linear range*	*Detection Limit*	*Matrix sample*	*Ref.*
GFAAS	-	-	-	0.01 μg/g	liver from reindeer, moose, sheep	61
ET-AAS	-	-	-	-	shellfish	62
AAS	-	-	-	-	plants	63
ET-AAS	-	slurry sample introduction	-	-	chewing gum	64
ET-AAS	-	with a tungsten tube atomizer	-	1.9×10^{-9} M	biological-materials	65
Zeeman AAS	-	-	0.9 -3.04 M	-	serum, urine	66
STP-GFAAS	-	-	0.24-250 ng	0.24 ng	food samples	67
ETAAS	-	-	-	3-58 ng/g	tissues of the rat	68
THGA furnace	-	-	-	7.78×10^{-10} M	plasma, urine	69
FIA	FAAS	-	$(2.6\text{-}231.6)\times10^{-6}$ M	10^{-8} M	leaf	70
ETAAS	-	-	-	5.55×10^{-8} M	serum	71
ETAAS	-	-	-	-	brain tissue	72
FAAS	-	-	-	-	serum, urine, CSF	73
MAOP	GFAAS	-	$(0\text{-}2.22)\times10^{-6}$ M	3.7×10^{-8} M	Fish, Human blood, cerebrospinal fluid	74
FIAS	ETAAS	-	-	3.7×10^{-8} M	dialysis concentrates	75
SE	GFAAS	pyrocatechol violet	(1-0.40)μg/ 250 mL	7.78×10^{-10} M	haemodialysis fluids, microwave, digested red wine samples	12
ICPOES	λ = 167 nm	-	-	-	Serum	76
ETV-ICPAES	-	PTFE as chemical modifier	-	7.4×10^{-6} M	biological materials	77
ICPAES	λ = 167, 237, 394, 396nm	-	-	4.45;32.6;37.1;17.4; $>37.1\times10^{-8}$ M	infusion solution for parenteral, nutricion	78
ICPAES	-	-	-	1.5×10^{-8} M	bone in hemodialysed patients	79
INAA	-	-	-	-	Serum, RBC	80
INAA	-	-	-	-	human brain	81

UV	$\lambda = 421$nm	Morin	-	-	human blood, urine, gallstone	82
Multicommutated flow system	UV	Chrome azurol S	(1.8-370) $\times 10^{-5}$ M	3.7×10^{-6} M	Crystallized fruit	83
PR-HPLC	UV	8-HQ	7.2×10^{-8}-2.2×10^{-5} M	3.7×10^{-8} M	biomedical samples	27
FBA	UV	ECR	(9.2-222.4) $\times 10^{-6}$ M	-	plant tissue	84
AdSV	-	Calmagite	-	2.7×10^{-9} M	plant	85
AdPV	-	DA	(5-40) $\times 10^{-8}$ M (4-72) $\times 10^{-7}$ M	1.9×10^{-8} M	biological fluids	86
AdPV	-	DA	(4-800) $\times 10^{-7}$M	1.4×10^{-7} M	renal dialysate, Ringer's solution,	40
DPV	-	L-dopa	(1-16) $\times 10^{-6}$ M	8.9×10^{-7} M	urine, hair, pork organs, Synthetic renal dialysate	87
DPV	-	1,2-dihydroxyantraquinone 3-sulfonic acid	(2.4-111.2) $\times 10^{-8}$ M	7.4×10^{-9} M	Hemodialysis concentrates	88
DPAdSV	-	Solochrome Violet RS Palatine Chrome Black BN Chromazurol S Eriochrome Black T	-	10^{-8}M	peritoneal and hemodialysis fluids	89
Indirect-DPV	-	L-dopa	(2-18) $\times 10^{-7}$M	7.6×10^{-8}M	urine, hair	42
Indirect-DPV	-	L-dopa	(4-52) $\times 10^{-7}$M (7.2-45) $\times 10^{-6}$M	3.5×10^{-7}M	urine	90
Indirect V	-	DFO, Hdmp, Hma, DHP	5×10^{-7}-3×10^{-5}M	2×10^{-7}M	Serum and biological samples	91
RAA	-	-	-	-	biological material	92

A variety of analytical methods have been used to measure aluminum levels in biological materials and environmental samples, including *graphite furnace atomic absorption spectrometry (GFAAS), flame atomic absorption spectrometry (FAAS), neutron activation analysis (NAA), inductively coupled plasma-atomic emission spectrometry (ICP-AES), inductively coupled plasma-mass spectrometry (ICPMS), laser ablation microprobe mass analysis (LAMMA), emission spectroscopy (ES), titrimetry (T), voltammetry (V), polarography (P), fluorescence (F), X-ray fluorescence (XrF)* and other methods (see Table 5.1 and Table 5.2). Front end separation techniques such as chromatography are frequently coupled with analytical methods.

Atomic absorption/emission spectroscopic methods are based on the fact that atoms in the ground state can absorb or emit light at characteristic wavelengths. In atomic absorption spectrometry *(AAS)*, absorption of the light by ground state atoms in a flame *(FAAS)* or furnace *(GFAAS)* is measured. In emission spectrometry, emission of the atoms excited at high temperature is measured. In these methods, the aluminum compounds and complexes are thermally decomposed, thereby allowing the measurement of total aluminum without sample pre-treatment. However, in the case of more refractory materials such as suspended aluminous minerals, the decomposition may not be complete.

Two types of *AAS* analysis are distinguished by whether or not a flame or a furnace is used to vaporize and atomize the sample. Aluminum can be determinate using a nitrous oxide-acetylene flame [13,73], but for most natural waters this method lacks sufficient sensitivity without pre-concentration[3].

Aluminum is more commonly determined using the most sensitive *graphite furnace (flameless) techniques. GFAAS* is used for the determination of low levels of aluminum in biological tissues [61,64,65,67,68,71,72,73] and in environmental samples [4,6,7,8,10,11]. This is because GFAAS offers the best combination of sensitivity, simplicity, and low cost. Detection limit of (1.5-7.0) $\times 10^{-8}$ M were reported. *Flow injection system (FIA)* using *ETAAS* detection have been used to monitor aluminum levels in water and biological material, with detection limits as low as $(5.6\text{-}14.8)\times 10^{-7}$ M in aqueous solution [9] and 3.7×10^{-8} M in dialysis concentrates [75]. When solid-phase extraction method is used to separate and preconcentrate trace quantities of aluminum, GFAAS can detects low level of aluminum as 7.8×10^{-10} M[12].

The *atomic emission* measurement of aluminum in different samples is accomplished generally by using *inductively coupled plasma (ICP)* as the excitation source.

The *ICP-AES* technique, also referred to as *ICP-optical emission spectroscopy (ICP-OES),* has been reported for the measurement of aluminum in biological materials and is an excellent alternative to GFAAS for those laboratories possessing the appropriate instrumentation[76,78,79]. ICP-AES is a multi-elemental technique that is relatively free of chemical interferences. The matrix problems that can exist in atomic absorption spectrometry (AAS) are minimized in ICP-AES due to the very high excitation temperature of the sample. The limits of detection for ICP-AES method have been reported to be about 1.5×10^{-8} M [79] of aluminum in bone in hemodialysed patients. A major problem with using the ICP-AES technique is the intense and broad emission of calcium which increases the aluminum background and can raise the detection limit of this element. Titanium also interferes with aluminum analysis. Also the relatively high cost and complexity of this technique can limit its routine use in many laboratories. Flame emission *(FEAS)* is rarely used for aluminum determination analysis because of low sensitivity. Another type of plasma, direct current plasma *(DCP),* is sometimes employed as the source. In principle its use is very similar to that of ICP. In this method the most commonly used spectral line for the determination of aluminum is 309.3 nm.

Instrumental neutron activation analysis (INAA) has been used to determine low levels of aluminum in biological tissues, serum and drinking water [14, 80, 81]. INAA involves the bombardment of a sample with neutrons, which transforms some of the stable ^{27}Al atoms into several radioactive aluminum isotopes beginning with ^{28}Al, and measurement of the induced radioactivity. Advantages of INAA include good sensitivity and relative independence from matrix (or media) effects and interferences. Moreover, this technique can be used to detect almost all elements of environmental concern in the same samples. One major problem with INAA with aluminum is the need to correct for interfering reaction with phosphorous and silicon, which produce the same radioisotope (^{28}Al) of aluminum. Other disadvantage of this technique include its high cost, the limited availability of nuclear reactors for INAA, the short 2.25 minute half-life of ^{28}Al that requires prompt analysis of the sample following bombardment with neutrons, and disposal problem of radioactive waste.

Determination of aluminum by reacting with an organic reagent and measuring the light absorbed by the aluminum-organic complex is very common. These methods are categorized under *'molecular absorption methods'* and are widely used. It is based on the absorption of ultraviolet-visible radiation by molecular species, which are usually formed by controlled complexation of the analyte with various organic and inorganic ligands. The

complexing reagents are not always specific for aluminum. They may react with other cations as well. Iron is probably the most common seriously interfering cation, but other cations may also interfere. Cation interference is generally reduced by either adding another reagent to complex the interfering ion or by extracting interfering ions into an organic phase using a complexing agent. Anions that complex aluminum may interfere with formation of the analyte complex. F^- , PO_4^{3-} and organic anions are the most important interfering anions. These interferences can sometimes be minimized by adjusting the pH value of the reacting solution. Organic compounds may be removed by oxidation before reaction. Aluminum can also forms hydroxypolimers, which react only slowly with the organic complexing agents. Some of the most commonly used complexing agents for aluminum determination using molecular absorption methods are: m-carboxyphenylfluorone (MCPF)[15], pyrocatechol violet (PCV)[16,28,35], 8-hydroxylquinoline (8-HQ)[26,27,30], bisfol[17], Chromazol-KS[18], 4,5 dihydroxyl-3-(p-sulphophenylazo)-2,7-naphthalene-disulphonic acid trisodium salt (SPADNS)[19], hydroxynaphtol blue (HNB)[20], gallocyanine[21], Tiron[32], 8-quinolinol (8-Q)[9,14], Chrome azurol S[83], 3,5,7,2'-4' pentahydroxy flavone (Morin)[82], eriochrome cyanine R (ECR)[84]. The limits of detection for UV-VIS method have been reported to be about 4.4×10^{-8} M [21].

In order to decrease the detection limit, *UV-VIS method* is often combined with front-end separation and pre-concentration techniques such as high-performance liquid chromatography.

Reverse-phase high-performance liquid chromatography (RP-HPLC) using *UV-VIS* detection can detect aluminum in aqueous and biomedical samples of $(3.7\text{-}7.4)\times10^{-8}$ M [27,30], while *ion pair reverse-phase high-performance liquid chromatography (IP-RP-HPLC)* using spectrophotometric detection had a detection limit of 8.9×10^{-9} M aluminum in water[25] .

Catalytic kinetic spectrophotometry (CKS) has been used to measure 2.9×10^{-8} M concentration of aluminum in water and tea samples [35]. The method involved separation of extraction of dithizone-carbon tetrachloride solution.

Additionally, *diffuse reflectance spectrometry (DRS)* have been used to measure aluminum level in water of $(1.48\text{-}3.7)\times10^{-7}$ M [36,37,38].

Anodic stripping voltammetry (ASV) as well as *adsorptive stripping voltammetry (AdSV)* are very powerful techniques for the determination of aluminum traces; detection limits in the range of $(0.37\text{-}3.7)\times10^{-9}$ M of aluminum were reported [39,40,41,85,89]. The

same range of detection limits was obtained using methods, such as *differential pulse voltammetry (DPV)* [42,43,44,87,88,90] and *oscillo-polarography (OP)* [47.48,49,50].

Also, other methods, such as *ion selective electron (ISE)* [58] and *chronopotentiometry* [55] have been employed for measuring aluminum levels of 10^{-9} M in water samples.

References:

1. Miró M., Estela J. M., Cerdà V., *Talanta* 63:201, 2004
2. Sorenson R. J., Campbell R., Tepper L. B., Lingg R. D., *Environmental Health Perspectives*, 8:3, 1974
3. Srinivasan P.T., Profile and characterization of aluminium during water treatment, September, 2000
4. de Amorim F.V., Bof C., Franco M.B., da Silva J.B.B., Nascentes C.C., *Microchemical Journal*, 82 (2):168, 2006
5. Burguera J.L., Burguera M., Anton R.E., Salager J.L., Arandia M.A., Rondon C., Carrero P., de Pena Y.P., Brunetto R., Gallignani M., *Talanta* 68 (2):179, 2005
6. Minami H., Yada M., Yoshida T., Zhang Q.B., Inoue S., Atsuya I., *Analytical Sciences* 20 (3): 455, 2004
7. Catarino S., Curvelo-Garcia A.S., de Sousa R.B., *Atomic Spectroscopy* 23(6);196, 2002
8. Magalhaes C.G., Lelis K.L.A., Rocha C.A., da Silva J.B.B., *Analytica Chimica Acta*, 464 (2): 323, 2002
9. Yuan D.X., Shuttler I.L., *Analytica Chimica Acta* 316 (3): 313,1995
10. Larroque M., Cabanis J.C., Vian L., *Journal of Aoacc International*, 77(2): 463, 1994
11. Plessi M., Monzani A., *Journal of Food Composition and Analysis* 8:21, 1995
12. Narin I., Tuzen M., Soylak M., *Talanta* 63: 411, 2004
13. Berndt H., Muller A., Schaldach G., *Fresenius Journal of Analytical Chemistry*, 346 (6-9): 711, 1993
14. Lavin N., Neeman E., Nirel Y., *Journal of Radioanalytical and Nuclear Chemistry-articles*, 163 (2): 307, 1992
15. Kamino S., Yamaguchi T., Mori T., Miyamoto M., Kusumi Y., Fujita Y., *Analytical Sciences*, 21 (12): 1549, 2005
16. Maeda T., Takizawa T., Uchiyama K., Hobo T., *Bunseki Kagaku* 53 (9): 987, 2004
17. Dedkova V.P., Shvoeva O.P., Savvin S.B., *Journal of Analytical Chemistry*, 53 (9): 810, 1998
18. Basargin N.N., Rozovski Y.G., Repenkova T.G., *Industrial Laboratory*, 60 (12): 695, 1994
19. Rizk M., Zakhari N.A., Toubar S.S., Elshabrawy Y., *Microchimica Acta* 118 (3-4): 239, 1995

20. Ferreira S.L.C., Leite N.O., Dantas A.F., Deandrade J.B., Costa A.C.S., *Talanta* 41 (10): 1631, 1994

21. He R., Wang J., *Analytica Chimica Acta* 412: 241, 2000

22. Nishida H., *Bunseki Kagaku,* 45 (5): 293, 1993

23. Cassella R.J., Santelli R.E., Branco A.G., Lemos V.A., Ferreira S.L.C., de Carvalho M.S., *Analyst* 124 (5): 805, 1999

24. Akama Y., Tong A., *Analytical Science* 7(5): 745, 1991

25. Matsumiya H., Iki N., Miyano S., *Talanta* 62 (2): 337, 2004

26. Lian F.Z., Huang Q., Kang Y.F., Zou G.W., Bi S.P., Tian L.C., *Journal of Liquid Chromatography & Related Technologies,* 26(2): 273, 2003

27. Lian H.Z., Kang Y.F., Bi S.P., Chen Y.J., Moa L., Dai L.M., Cao M., Tian L.C., *Journal of Liquid Chromatography & Related Technologies,* 25(19): 3059, 2002

28. Tangen G., Wickstrom T., Lierhagen S., Vogt R., Lund W., *Environmental Science & Technology* 36 (24): 5421, 2002

29. Zhu Q.R., Sun D.M., Huang X.X., Zhu Q.F., *Chinese Journal of Analytical Chemistry,* 30(6):739, 2002.

30. Lian H.Z., Bi S.P., Chen Y.J., Dai L.M., Cao M., Li H.M., Tian L.C., *Journal of Liquid Chromatography & Related Technologies,* 24 (2): 215, 2001

31. Litvina M.L., Voloschik I.N., Rudenko B.A., *Journal of Chromatography A,* 706 (1-2): 307, 1995

32. Motellier S., Pitsch H., *Journal of Chromatography A* 660 (1-2): 211, 1994

33. Moskvin L.N., Slesar N.I., Moskvin A.L., Mozzhukhin A.N., Zakharenko V.M., *Industrial Laboratory,* 64 (3): 137, 1998

34. Nagaosa Y., Kawabe H., Bond A.M., *Analytical Chemistry,* 63 (1): 28, 1991

35. Sun D.M., Ji F., *Spectroscopy and Spectral Analysis* 23 (2): 351, 2003

36. Ivanov V.M., Ershova N.I., *Journal of Analytical Chemistry* 56 (12):1089, 2001

37. Ershova N.I., Ivanov V.M., *Analytica Chimica Acta* 408 (1-2): 145, 2000

38. Ahmad M., Narayanasw A.R., *Analytica Chimica Acta* 291 (3): 255, 1994

39. de Carvalho L.M., do Nascimento P.C., bohrer D., Stefanello R., Bertagnolli D., *Analytica Chimica Acta,* 546 (1): 79, 2005

40. Zang F.B., Yang L., Bi S.P., Liu J., Liu F., Wang X.L., Yang X.D., Gan N., Yu T., Hu J., Li H.Z., Yang T.M., *Journal of Inorganic Biochemistry,* 87 (1-2): 105, 2001

41. Dostal A., Duong H.B., Kalvoda R., *Chemicke List* 86 (11): 847, 1992

42. Zhang F.P., Bi S.P., Liu F., Bian N.S., *Chemical Journal of Chinese Universities-Chinese*, 21 (8): 1205, 2000
43. Bi S.P., Chen G., Liu J., Zou G.W., Gan N., *Acta Chimica Sinica* 58 (5): 494, 2000
44. Bi S.P., Chen G., *Chinese Chemical Letters* 10 (3): 247, 1999
45. Di J.W., Bi S.P., Yang T.Y., Zhang M., *Sensors and Actuators B-Chemical*, 99 (2-3): 468, 2004
46. Downard A.J., Powell H.K.J., Xu S.H., *Analytica Chimica Acta*, 251 (1-2): 157, 1991
47. Gan N., Bi S.P., Wei Z.B., Tan Y.X., *Chinese Journal of Analytical Chemistry*, 29 (2): 212, 2001
48. Bi S.P., Liu F., Ye L., Dai L.M., Cao M., Chen Y.J., Lian H.Z., *Chemical Papers-Chemicke Zvesti*, 53 (2): 93, 1999
49. BI S.P., Gong M., Nian H.Z., Dai L.M., Cao M., Chen Y.J., *Analytical Letters* 31 (4): 669, 1998
50. Bi S.P., Zhang Z.J., *Collection of Czechoslovak Chemical Communications*, 61 (12): 1745, 1996
51. Downard A.J., Lenihan R.J., Simpson S.L., OSullivan B., Powell K.J., *Analytica Chimica Acta*, 345 (1-3): 5, 1997
52. Saleh M.B., Hassan S.S.M., Gaber A.a.A., Kream N.A.A., *Analytica Chimica Acta* , 434 (2): 247, 2001
53. Agarwal H., Singh C.K., Chandra S., *Journal of the Indian Chemical Society* 82 (6): 507, 2005
54. Bi S.P., Gong Y., Ye L., Li J., *Chinese Chemical Letters*, 9(10): 949, 1998
55. Bi S.P., Song M.J., Xu D., *Analytical Letters*, 31 (11):1937, 1998
56. Nadzhafova O.Y., Zaporozhets O.A., Rachinska I.V., Fedorenko L.L., Yusupov N., *Talanta* 67 (4): 767, 2005
57. Markova O.I., Nikitina T.G., Moskvin L.N., Andreev V.P., *Journal of Analytical Chemistry*, 61 (2): 179, 2006
58. Evsevleeva L.G., Bykova L.M., Badenikov V.Y., *Journal of Analytical Chemistry*, 60 (9): 866, 2005
59. Cassella R.J., Santelli R.E., Branco A.G., Lemos V.A., Ferreira S.L.C., de Carvalho M.S., *Analyst* 124 (5): 805, 1999
60. Kaneko E., Hoshino H., Yotsuyanagi T., Watabe R., Seki T., *Bulletin of the Chemical Society of Japan*, 65 (11): 3192, 1992

61. Godal A., Langseth W., Sivertsen T., Lund W., *Science of the Total Environment,* **168** (3): 249, 1995

62. Arruda M.A.Z., Gallego M., Valcarcel M., *Journal of Analytical Atomic Spectrometry,* 10 (7): 501, 1995

63. Mercy G., Nyagah G., Murungi J.I., *Journal of environmental Science and Health Part A-Environmental Science and Engineering & Toxic and Hazardous Substance Control,* 30 (6):1145, 1995

64. Vinas P., Campillo N., Garcia I.L., Cordoba M.H., *Presenius Journal of Analytical Chemistry,* 351 (7): 695, 1995

65. Otha K., Yokoyama M., Itoh S., Kaneco S., Mizuno T., *Analytica Chimica Acta,* 291 (1-2): 115,1994

66. Wang S.T., Pizzolato S., Demshar H.P., *Journal of Analytical Toxicology,* 15 (2): 66, 1991

67. Wang Y., Lu C.H., Xiao Z.F., Wang G.J., Kuan S.S., Rigsby E.J., *Journal of Agricultural and Food Chemistry,* 39 (4): 724, 1991

68. Radunovic A., Bradbury M.W.B., Delves H.T., *Analyst* 118 (5): 533, 1993

69. Brandley C., Leung F.Y., *Clinical Chemistry,* 40 (3): 431, 1994

70. Salacinski H.J., Riby P.G., Haswell S.J., *Analytica Chimica Acta,* 269 (1): 1, 1992

71. Gayon J.M.M., Parajon J.P., Sanzmedel A., Fellows C.S., *Journal of Analytical Atomic Spectrometry,* 7 (5): 743, 1992

72. Xu N., Majidi V., Ehmann W.D., Markesebery W.R., *Journal of Analytical Atomic Spectrometry,* 7 (5): 749, 1992

73. Johnson K.E., Treble R.G., *Journal of Clinical Laboratory Analysis,* 6(5): 264, 1992

74. Ranau R., Oehlenschläger J., Steinhart H., *Fresenius J. Anal. Chem.,* 364: 599, 1999

75. Aceto M., Abollino O., Sarzanini C., Mentasti E., Mariconti F., *Atomic Spectroscopy* 15 (6): 237, 1994

76. Lyon T.D.B., Cunningham C., Halls D.J., Gibbons J., Keating A., Fell G.S., *Annals Clinical Biochemistry,* 32(2): 160,1995.

77. Hu B., Jiang Z.C., Zeng Y., *Analytica Chimica Acta* 296(2): 213, 1994

78. Recknagel S., Rosick U., Bratter P., *Journal of Analytical Atomic Spectrometry,* 9 (11):1293, 1994

79. Leflon P., Plaquet R., Morinibe P., Foumier A., *Clinica Chimica Acta,* 191: 31, 1990

80. Sharif A.A.M., Ghafourian H., Ahmadiniar A., Husain S.W., Saber-Tehrani M., Ghods H., *Journal of Radioanalytical and Nuctear chemistry*, 262(2): 473, 2004

81. Blotcky A.J., Claassen J.P., Roman F.R., Rack E.P., Badakhsh S., *Analytical Chemistry*, 64 (23): 2910, 1992

82. Ahmed M.J., Hossan J., *Talanta*, 42 (8):1135, 1995

83. Toth I.V., Rangel A.O.S.S., Santos J.L.M., Lima J.L.F.C., *Journal of Agricultural and Food Chemistry*, 52 (9):2450, 2004

84. Honorato R.S., Carneiro J.M.T., Zagatto A.G., *Analytica Chimica Acta*, 441: 309, 2001

85. Stryjewska E., Rubel S., Sadowska J., Karpiuk M., *Chemia Analityczna*, 38 (2):175, 1993

86. Zang F.B., Bi S.P., Liu J., Yang X.D., Wang X.L., Yang L., Yu T., Chen Y.J., Dai L.M., Yang T.M., *Analytical Science*, 18 (3): 293, 2002

87. Zang F.B., Bi S.P., Li H.Z., Chen Y.J., Dai L.M., *Electroanalysis*, 13(12): 1054, 2001

88. Carrera M.E., Rodriguez V., Toral M.I., Richter P., *Analytical Letters* 26(12): 2575, 1993

89. Locatelli C., *Electroanalysis* 15(17): 1397, 2002

90. Zhang F.P., Bi S.P., Liu F., Bian N.S., *Analytical Letters*, 33 (2):209, 2000

91. Di J.W., Zhang F., Zhang M., Bi S.P., *Electroanalysis* 16(8):644, 2004

92. Furnari J.C., Cohen I.M., *Biological Trace Element Research*, 43-5:503, 1994

6. Spectrofluorimetric method for determining aluminum in biological and environmental samples

Fluorescence continues to prove itself as an ultrasensitive and potentially selective analytical technique [1].

Good reviews, on the use of fluorescence in analytical chemistry, with data on the determination of Al(III) , appear every two years in Analytical Chemistry.

These reviews, in the Fundamental Review section of the journal, have been written by White C.(1960-1972), Weissler A.(1974), O'Donnell C.M. and Solie T.N.(1976, 1978).

Potential problems with the use of these methods include interfering fluorescence by humic substances (Figure 6.1), F^- or quenching by iron (III). These interferences could, however, be dealt by masking and extraction (Fe^{3+} is masked with 1,10-phenantroline (Figure 6.2), whereas F^- is masked with Be^{2+}). The presence of humic substances in natural waters can cause interference, if detection is made at a wavelength in the UV or lower visible range. There are at least two ways of minimising this interferences; either by using a reagent that forms complex with Al, absorbing at wavelengths at which humic has got a low absorption, or by extracting the complex formed into an organic solvent, to which the extraction of humic substances is not large enough to cause interference). Advantages of fluorescence include the possibility of obtaining a very good detection limit [2].

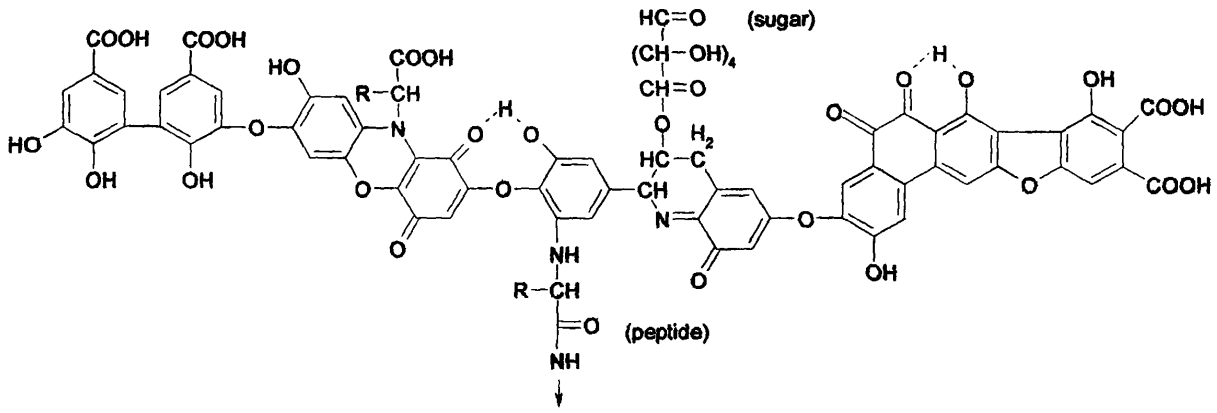

Figure 6.1 *Hypothetical model structure of humic acid* [3]

Table 6.1 *Spectrofluorimetric method for determining aluminum in biological and environmental samples*

Reagent/characteristics	***Analytical method***	***Detection technique***	***Linear range***	***Detection Limit***	***Matrix sample***	***Ref.***
Eriochrome Red B pH=6, 35 min 60°C	F	F(Ex=525, Em=595) nm	(0-7.4) $\times 10^{-7}$ M	3.7×10^{-9} M	tap water	5
Eriochrome Red B pH=6	FIA	F(Ex=525, Em=595) nm	(0-3.7)$\times 10^{-5}$ M	1.11×10^{-8} M	tap and mineral waters	6
Lumogallion pH=5.2, at temperature	FIA	F(Ex=500, Em=595) nm	0-37$\times 10^{-6}$ M	3.7×10^{-9} M	lakes waters	9
lumogallion	Automated non-Segmented continuous flow analysis	F	(0-1.1) $\times 10^{-4}$ M	4.44×10^{-7} M	Beverage	10
Lumogallion pH=5, 90 min room temperature	E	F(Ex=500, Em=580) nm	(0-5.93) $\times 10^{-9}$ M	0.25×10^{-9} M	natural waters	11
Lumogallion, pH=4.7	HPLC	F(Ex=500, Em=574) nm	-	1.85×10^{-9} M	tap and coastal sea-waters	12
Lumogallion	HPLC	F(Ex=505, Em=574) nm	-	3.7×10^{-9} M	Vitamins, glucose, lipide amino acids	13
Lumogallion	F	-	-	-	Human serum, whole blood	14
Lumogallion +surfactant	F	F(Ex=485, Em=590) nm	(0-3.7) $\times 10^{-9}$ M	7.4×10^{-10} M	fresh and saline waters	15
Lumogallion	Capillary zone electro-phoresis	LIF	-	$<10^{-8}$ M	Human serum	16
Morin	RP-HPLC	F	6×10^{-9}-6×10^{-5} M	2×10^{-9} M	environmental samples Biological samples	21
Morin	1st-derivative synchronous solid-phase spectrofluoro metry	F(Ex=445, Em=520) nm	(1.85-18.5)$\times 10^{-8}$ M	3.7×10^{-9} M	synthetic mixture, natural water	22

Eriochrome blue black R Morin 8-hydroxyquinoline	F (speciation)	-	10^{-6}-10^{-5} M (4-400) $\times10^{-8}$ M 10^{-6}-10^{-5} M	5×10^{-7} M 1×10^{-8} M 5×10^{-7} M	natural water	23
Morin pH=5.6	F assay	F(Ex=440,Em=510) nm	-	-	cultured cells of Nicotina tabacum cv BY-2	24
Morin pH=4.8	F	-	10^{-5}-10^{-4} M	10^{-6} M	-	25
Morin + surfactant(Tween-20), pH=4.5	SIA	F(Ex=425, Em=495) nm	(1.85-37) $\times10^{-6}$ M	1.12×10^{-7} M	natural water samples	26
Salicylaldehyde picolinoylhydrazone (SAPH), pH=5.4	F	F(Ex=384, Em=468) nm	(3.7-93) $\times10^{-8}$ M	9.8×10^{-9} M	seawater	29
Salicylaldehyde picolinoylhydrazone (SAPH), pH=5.4	rFIA	F(Ex=384, Em=468) nm	(1.85-11.12)$\times10^{-7}$ M	7×10^{-8} M	commercial drinking, soft drinking(CRM), tap water	30
Salicylaldehyde picolinoylhydrazone (SAPH)	FIA	F	7.4×10^{-8}-7.4×10^{-6} M	-	Waters	31
5-Br-SASH pH=5.4	F	F(Ex=370, Em=460) nm	(0-4.4) $\times10^{-6}$ M	4.1×10^{-8} M	glucose injection	32
DSAHP, pH=3.0 and 6.0	F	F(Ex=270, Em=437) nm	(0-10)$\times10^{-6}$ M	10^{-8} M	diluted hemodialysis solutions	33
salicylaldehyde carbohydrazone + surfactant(Triton: X-100)	FIA	F	1.1×10^{-7}-22.2×10^{-6} M	8.34×10^{-8} M	drinking water	34
salicylaldehyde-1-phthalazinohydrazone (SAPhH)	F	F(Ex=414, Em=475)nm	(3.7-37)$\times10^{-7}$ M	-	water, alloys	35
salicylidene-aminophenol	Solid-phase spectro-fluorometry	-	7.4×10^{-9}-5.2×10^{-7} M	7.4×10^{-10} M	natural-waters	36
2-hydroxy-3-sulfo-5-chloroaniline-N-salicylidene pH=6	FIA	F(Ex=420, Em=505)nm	1.85×10^{-7}-3.7×10^{-6} M	1.85×10^{-8} M	-	37
8-hydroxyquinoline-5-sulfonic	F	F(Ex=365,	-	3.7×10^{-8} M	Tap water, rain and snow	38

acid (HQS), pH=4.5		Em=490)nm				
8-hydroxyquinoline-5-sulfonic acid (HQS) pH=4	SIA	F	8.1×10^{-8}-11.1×10^{-6} M	3.4×10^{-8} M	commercial drinking and tap water	39
HQS+surfactant(CTMAB)	LC	F(Ex=410, Em=510)nm	7.4×10^{-7}-7.4×10^{-6} M	3.7×10^{-7} M	Water samples	40
8-HQS + surfactant(CTAB)	FIA (speciation)	F	(0-370.6) $\times10^{-6}$ M	3.33×10^{-8} M	waters	41
HQS + surfactant(CTAB) pH=5.15	FIA/LC	F	-	-	human serum	42
HQS + surfactant	MSFIA	F	3.7×10^{-7} -18.5×10^{-6} M	1.85×10^{-8} M	drinking water	43
8-hydroxyquinoline (8-HQ) pH=7.3-7.5 serum pH>4-8 urine	SE	F(Ex=380, Em=504) nm	7.4×10^{-8}-37×10^{-6} M	(2.6-7.4)$\times10^{-8}$ M	human biological fluids, Dialysis solutions, tap water	45
5-sulfo-8-quinolinol	F	F(Ex=367, Em=500) nm	(0-1060) $\times10^{-9}$ M	12×10^{-9} M	-	46
8-Q, pH=7	KD-HPLC	F(Ex=370, Em=504) nm	-	6.2×10^{-8} M	Gastric mucosa	47
1,2,4-trihydroxyanthraquinone pH=3.5	F	-	7.4×10^{-7}-2.4×10^{-6} M	10^{-8} M	blood-serum	48
alizarin red PS, pH=3	F	F(Ex=480, Em=564) nm	1.11×10^{-7}-3.7×10^{-6} M	3.33×10^{-8} M	silicate CRM	49
Mordant red 19	E	F(Ex=485, Em=549) nm	3.7×10^{-8}-1.11×10^{-6} M	9.3×10^{-9} M	Dialysis solutions	50
2,4,2'trihydroxyazobenzene 5'-sulfonicacid (Acid Alizarin Garnet R) pH=4.7	F	F(Ex=366, Em=570) nm	(0-7.4)$\times10^{-5}$ M	3.7×10^{-9} M	spinach leaves, river water	51
chromotropic acid pH=4.0±0.5	F	F(Ex=346, Em=370) nm	7.4×10^{-8}-3.7×10^{-6} M	3.7×10^{-8} M	tap, river and sea-water	52
chromotropic acid pH=4.1-4.7	F	F(Ex=360, Em=390) nm	3.7×10^{-8}-11.12×10^{-6} M	-	Environmental and biological samples	53
-	ETALEAF	-	2×10^{-9} M-1×10^{-6} M	1.85×10^{-10} M	seawater	54
Calcon pH=4.8, 1 h 60°C	F	F(Ex=565, Em=610) nm	(0-2.2) $\times10^{-6}$ M	1.1×10^{-7} M	silicon	55

DRAB , pH=8	F	F(Ex=477, Em=603) nm	4.4×10^{-9}-11.1×10^{-6} M	-	tap-water	56
CNDA	IEC	F	10^{-7}-2×10^{-5} M	1.11×10^{-5} M	tea drink	57
2,6-bis[(o-hydroxy)phenylimino-Methyl]-1-hydroxybenzene pH=5	F	-	3.7×10^{-8}-3.7×10^{-7} M	3.7×10^{-9} M	natural waters	58
panoic acid	-	F(Ex=379, Em=508) nm	$(0\text{-}6.3)\times10^{-4}$ M	7×10^{-7} M	-	60
1-hydroxy carboxyanthraquinone	-	-	(0-9.2) M	7.4×10^{-11} M	-	62
trimethoxykaempferol	-	F(Ex=366, Em=495) nm	$(0\text{-}1.2)\times10^{-7}$ M	$(0\text{-}5.1)\times10^{-9}$ M	Tin, sewage, natural underground waters	64
2,4-dihydroxybenzenaldehyde isonicotinoxyhydrazone	-	F(Ex378, Em=478) nm	-	1.8×10^{-8} M	Tap, river, lake waters	65
2-hydroxy-1-naphthaldehyde-4-methoxybenzoylhydrazone	K	F(Ex=420, Em=475) nm	$(0\text{-}10)\times10^{-6}$ M	0.02×10^{-6} M	-	66

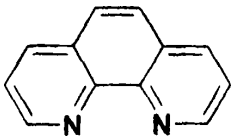

Figure 6.2. *Structure of 1,10-phenanathroline*

The most used reagents for the fluorescent detection of aluminum are: *Eriochrome Red B, Lumogallion, Morin, Salicylaldehyde Picolinoylhydrazone, 5-Bromo-Salicylaldehyde Salicyloylhydrazone, 8-Hydroxy-Quinoline-5-Sulphonic acid, Alizarin Red PS, Acid Alizarin Garnet R, Chromotropic Acid* and others.

Eriochrome Red B (ERB) (Figure 6.3) was first proposed as a fluorescent reagent for determining aluminum in 1968 [4].

Later, the method has been widely applied for the analysis of aluminum in water samples. Detection limit of 3.7×10^{-9} M, was reported [5].

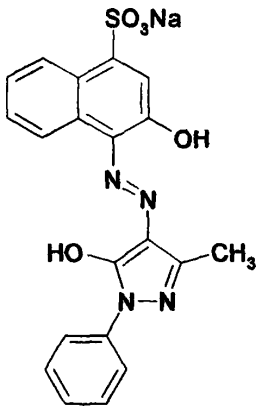

Figure 6.3 *Structure of Eriochrome Red B*

The traditional fluorometric determination of dissolved aluminum by the complex with *Lumogallion (LMG)* (Figure 6.4) is based on the exhibition of aluminum- lumogallion compound at an excitation wavelength of 465 nm and an emission wavelength of 555 nm. The method was first proposed by Nishikawa and co-workers in 1967 [7] and later modified by Hydes and Liss in 1976 [8].

The method was improved by Howard et al, who developed a sensitive fluorescence assay method of lumogallion for aluminum determination that exploits the 5-6-fold increase

in the fluorescence intensity of the aluminum-lumogallion complex in the presence of the non-ionic detergent Triton X-100. The procedure has a detection limit of 0.7×10^{-9} M [15].

Resing and Measures[17] applied the lumogallion method in flow injection analysis (FIA) with in-line pre-concentration onto a column of immobilized 8-hydroxyquinoline, and reported a detection limit of about 0.15×10^{-9} M.

Zang, et al. were developed a sensitive and selective extraction-fluorimetric method for the determination of traces amount of dissolved aluminum in natural waters. Aluminum-lumogallion is extracted into n-hexanol, and the fluorescence can be enhanced substantially up to 20-fold, with a detection limit of aluminum of 0.25×10^{-9} M[11].

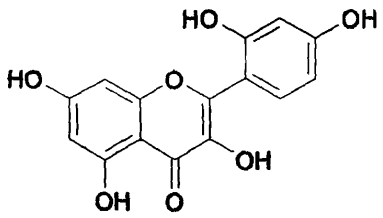

Figure 6.4 *Structure of Lumogallion*

Morin (3,5,7,2'-4' pentahydroxy flavone) (Figure 6.5) is a phenolic compound derived from hydroxyl substitution compound derived from hydroxyl substitution on the flavone chromophore.

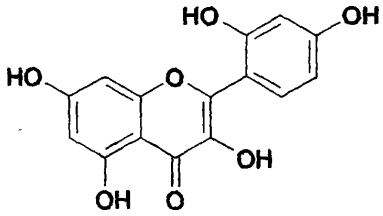

Figure 6.5 *Structure of Morin*

Morin is only weakly fluorescent in nature. However, when chelated with non-paramagnetic metal ions, especially aluminum(III) and beryllium(II), it forms highly fluorescent complexes. A property that has been explored in the identification and the determination of those metal ions[18]. The enhancement of the fluorescence upon chelating morin with the non-paramagnetic metal ions is related to the inhibition of the excited state intermolecular proton transfer [19].

The method was first proposed in 1961 by Will [20] and uses it for determination of aluminum in boiler water in the parts per billion ranges. Later, Morin has been widely used

for the determination of aluminum ions [21,22,23,24,25]. Detection limit of 2×10^{-9} M were reported [21].

It has been reported that the fluorescence of metal chelates is enhanced by the presence of short tailed non-ionic surfactant, such as Tween-20, with a detection limit of 1.1×10^{-7} M of aluminum [26]. The addition of hydrophobic surfactants such as hexadecyltrimethylammonium bromide (CTAB) or Triton-100 would lead to a quenching of the fluorescence due to the decomposition of the complex and enhanced of the blank [27].

Saarl and Seltz [28] have been proposed a spectrofluorometric method for aluminum determination, based on immobilized morin. Morin is immobilized on cellulose powder and attached to the end of a bifurcated fiber optic. When the immobilized morin is placed in a solution containing aluminum(III), fluorescence is observed from the aluminum(III)-morin complex. Detection limit of 10^{-6}M was reported.

Also, a method for the simultaneous determination of aluminum and beryllium in mixtures by first-derivative synchronous solid-phase spectrofluorimetry has been developed [22].Aluminum and beryllium reacted with morin to give fluorescent complexes which were fixed on a dextran-type resin. The method has a detection limit of 3.7×10^{-9} M.

Some authors have used *Salicylaldehyde Picolinoylhydrazone (SAPH)* (Figure 6.6) as fluorescent reagent for determination of aluminum. Detection limits at nanomolar levels were reported [29]

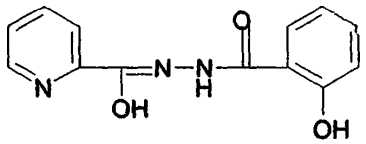

Figure 6.6 *Structure of SAPH*

Albendin et al. [30] applied the SAPH method in reverse flow-injection (r-FIA) manifold for the direct determination of aluminum in drinking water. It is based on a reagent-buffer injection into the flowing sample solution, where aluminum(III) forms a complex with SAPH in the reacting coil. The reverse flow-injection procedure allows determination of aluminum(III) at 10^{-8} M level (detection limit was 7×10^{-8} M).

A good detection limit of 3.7×10^{-8} M was reported for the stectrofluorimetric determination of trace amounts of aluminum with *5-Bromo-Salicylaldehyde Salicyloylhydrazone (5-Br-SAPH)* (Figure 6.7) [32].

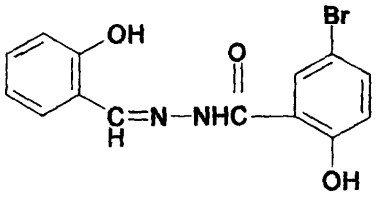

Figure 6.7 *Structure of 5-Br-SAPH*

The fluorescence properties of metal-*8-hydroxy-quinoline-5-sulphonic acid (HQS)* (Figure 6.8), a derivative of oxine, chelates have been exploited by several authors [38,39,40,41,42,43] and thus HQS has been selected as a fluorogenic ligand for spectrofluorimetric determination of aluminum by flow injection analysis FIA [41,42] or sequential injection analysis (SIA) [39].

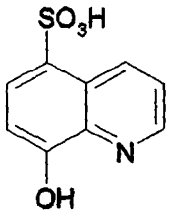

Figure 6.8 *Structure of HQS*

Zhang and Seitz[25] immobilized 8-hydroxyquinoline sulfonate (λ_{ex} = 366, λ_{em} = 510 nm) on an ion exchange resin, Amberlite CG-400, and placed the resin at the end of a trifurcated fiberoptic bundle. Al, Mg, Zn, and Cd could be detected at concentrations below 10^{-6} M after a 10-min reaction, but the response of the sensor was curvilinear.

In a kinetic determination of aluminum(III) with 8-hydroxyquinoline, Wilson and Ingle [44] showed that Zn or Au (100 ppm), Sn (10ppm), Hf (6ppm), Sn (5ppm), and Zr (1ppm) enhanced the rate of the reaction. From 1.5×10^{-8} M to 3.7×10^{-7} M of aluminum(III) was assayable.

The enhancement of the metal-HQS fluorescence by cationic micelles, especially *hexadecyltrimethylammonium ion* (Figure 6.9), has been reported by a number of researchers

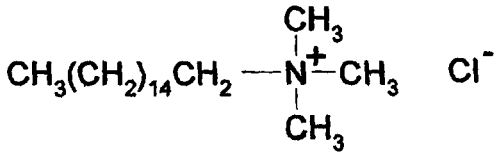

Figure 6.9 *Structure of hexadecyltrimethylammonium ion*

[40,41,42,43]. Cationic surfactants have been shown to be the most effective surfactant type for enhancing the fluorescence of aluminum-HQS, due presumably to the strong ion pairing effect likely to occur between the positive quaternary ammonium group and the negatively charged sulphonate group of HQS [27].

A time-based multisyringe flow injection procedure (MSFIA) for the spectrofluorimetric determination of aluminum in drinking water at low mineralization levels has been proposed [43].In order to enhance the luminescence, the reaction was carried out in micellar medium using hexadecyltrimethylammonium chloride as surfactant. Under the selected working conditions, a detection limit of 1.8×10^{-8} M was obtained.

Alizarin Red PS (1,2,4-trihydroxy 9,10-anthraquinone-3-sulfonic acid) (Figure 6.10) has been successfully used for sensitive fluorimetric determination of aluminum [49]. Limit of detection of 3.3×10^{-8} M was reported.

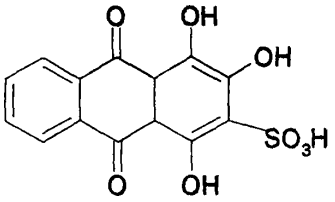

Figure 6.10 *Structure of Alizarin Red PS*

Campi and Ingle [51] were proposed a fluorometric reaction-rate method for determination of aluminum with *Acid Alizarin Garnet R* (2,4,2'-trihydroxyazobenzene-5'-sulfonic acid) (Figure 6.11). The rate of formation of the fluorescent aluminum chelate of 2,4,2'-trihydroxyazobenzene-5'- sulfonic acid is measured within 24 s after mixing with one reagent solution. The technique exhibits a detection limit of 3.7×10^{-9} M.

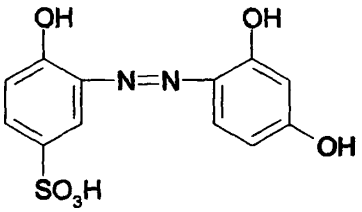

Figure 6.11 *Structure of Acid Alizarin Garnet R*

Chromotropic Acid (1,8-dihydroxynaphthlene-3,6-disulfonic acid) (Figure 6.12) was, also, proposed as a fluorescent reagent for aluminum determination [52,53]. Detection limit of 3.7×10^{-8} M was obtained [52].

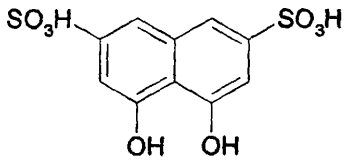

Figure 6.12 *Structure of Chromotropic Acid disodium salt dehydrate*

Bihan et al.[54] developed a very sensitive analytical method for the direct determination of ultra content of aluminum in seawater by electrothermal atomization-laser excited atomic fluorescence (ETA-LEAF) using a pulsed Nd:Yag laser associated with an optical parametric oscillator (OPO) and an intensified charge-coupled device (ICCD) camera with a detection limit of 1.8×10^{-10} M. The method was direct, did not require complex handling and further reactants could be avoided.

Complexes of aluminum with *salicylidene-o-aminophenol* [36], *salicylaldehyde carbohydrazone* [34], *salicylaldehyde-1- phthalazinohydrazone*

(SAPhH) [35], *2-hydroxy-3-sulfo-5- chloroaniline-N-salicylidene* [37], *2,6-bis[(o-hydroxy) phenylimino-Methyl]-1-hydroxybenzene* [58], *1,2,4 trihydroxyanthraqui-none* [48], *2,4,2'trihydroxyazobenzene* [51], *2, 2'-dihydroxyazobenzene (DRAB)* [56], *3-carboxy-2-napthylamine-N,N-diacetic acid (CNDA) (The method utilized CNDA* as a fluorescent post-column chelating reagent. Detection limit of 1.1×10^{-8} M was reported.) [57], *Mordant red 19* (The method suggested the extraction of the Aluminum complex in *isobutylmethylketone,* organic solvent. The limit of detection was 9.3×10^{-9} M) [50], *Calcon* [55], *8-hydroxylquinoline (8-HQ)* (The fluorescence intensity of the toluene-extracted metal chelate was measured, with detection limit of $(2.6\text{-}7.4)\times10^{-8}$ M) [45], *8-quinolinol (8-Q)* (The method involved a kinetic differentiation mode high-performance liquid chromatography with fluorimetric detection of the complex.) [47] have been also investigated. Detection limits not lower than 3.7×10^{-9} M have been reported.

The most useful was *5-bromo-2-(salicylidene-amino) phenol*, because of a low blank fluorescence and excellent sensitivity and reproducibility.

Garcia Sanchez et al. [59] described the simultaneous fluorometric assay of aluminum and beryllium in mixture by synchronous derivative fluorometry. The first and second

derivative spectra were recorded at 340 to 500 nm versus a reagent blank ($\Delta\lambda = 96$ nm), and a graphical model was used to measure derivative amplitudes. The method is based on the interference-free character of the isodifferential points in the derivative calibration graphs. The isodifferential points corresponding to the aluminum series is 446 nm, whereas that for the beryllium species is 422 nm. As little as 4.2×10^{-7} M of beryllium and 5.4×10^{-8} M of aluminum could be assayed.

Casassas et al. [60] used *2,2'-dihydroxy-3,3'-dicarboxy-1,1'-dinaphthylmethane (panoic acid*) as a reagent for Al (λ_{ex} = 379, λ_{em} = 508 nm). As little as 7×10^{-7} M is detectable with linearity to 6.3×10^{-4} M.

Calcon (Mordant Black 17) was used by Mansuet et al. [61]for assay of aluminum in food products (λ_{ex} = 546 ,λ_{em} = 635 nm)

Salinas et al. [62] proposed the use of *1-hydroxy-2-carboxyanthraquinone (1-hydroxy-9,10-dioxoanthracene-2-carboxylic acid)* for the assay of aluminum(III) in Portland cement and aluminum bronze. The detection limit is 7.4×10^{-11} M.

Deguchi et al. [63] described *2,4-dihydroxybenzenaldehyde semicarbazone* for assay of very small amounts (0.001 %) of aluminum in iron and steel.

Zel'tser et al. [64] described the use of *trimethoxykaempferol* [which complexes with $Al(OH)_2^+$] for the assay of aluminum (λ_{ex} = 366, λ_{em} = 495 nm). From 5.2 to 122.3 $\times10^{-9}$ M of aluminum is assayable in tin, sewage, and natural underground waters.

Vasilikiotis et al. [65] proposed *1-isonicotinoyl-2-(2',4'-dihydroxy) benzylidene hydrazine (2,4-dihydroxybenzenaldehyde isonicotinoxyhydrazone)* for the assay of aluminum. The excitation was at 378 nm, with emission at 478 nm and a detection limit of 1.8×10^{-8} M. Aluminum in tap, river, and lake waters was described.

Ioannou and Siskos [66] studied the kinetics of the reaction of *2-hydroxy-1-naphthaldehyde-4-methoxybenzoylhydrazone* with aluminum (λ_{ex} = 420, λ_{em} = 475 nm). With a measurement time of 1 min, 0.02-10×10^{-6} M aluminum can be determinate. Interferences from Sc and Ga were noted.

The fluorescence spectral characteristics of a number of metal chelates with *8-quinolinol* and its derivatives have been studied under various conditions by several authors. Nishikawa has reported on the fluorescence of the solid state chelates with the 8-quinolinol derivatives and the metals in groups I, II, III, and IV of the periodic system [67,68].

References:

1. Workman Jr. J., Koch M., Veltkamp D., *Process Analytical Chemistry review, Anal. Chem.* 77, 3789, 2005.
2. IUPAC, *Analytical methodology for the determination of aluminium fractions in natural fresh waters (Technical Report),* 1996
3. *Bio Ag Technologies International, Humic Acid Structure and Properties,* 1999.
4. Hocman G., Lacko G., Hedegus L., *Acta Fac. Rerum Nat. Comenianae Chim.,* 13:71, 1968.
5. Carrillo F., Perez C., Camara C., *Analytica Chimica Acta,* 243 (1): 121, 1991.
6. Carrillo F., Pérez C., *Analytica Chimica Acta,* 262: 91, 1992
7. Nishikawa Y., Hiraki K K., Morishige K., Shigematsu, *Japan Analyst* 16 692,1967.
8. Hydes D.J., Liss P.S., *Analyst* 101:922, 1976.
9. Sutheimer S.H., Cabaniss S.E., *Analytica Chimica Acta* 303: 211, 1995
10. Hoch R.L., *Analyst* 124 (5): 793,1999
11. Zang J., Xu H., Ren J.L., *Analytica Chimica Acta* 405 : 31, 2000
12. Zhou C.Y., Wu J., Chi H., Wong M.K., Koh L.L., Wee Y.C., *Talanta* 42 (3): 415, 1995
13. Fujita N., Kobayashi H., Enami T., Nagae N., Charleston N., *Bunseki Kagaku,* 53 (1): 17, 2004
14. Tamada T., *Bunseki Kagaku,* 53 (5): 435, 2004
15. Howard, Cohead A.J., Potter I.A., Watt A.P., *Analyst* (111): 1379, 1986
16. Takatsu A., Eyama S., Uchiumi A., *Chromatographia* 40 (3-4): 125, 1995
17. Resing J.A., Measures C.I., *Anal.Chem.* 66:4105, 1994.
18. Schulman S.G. (Ed.), Luminescence Spectroscopy: Methods and Applications. Part 1, Wiley, New York, pp. 438-439, 1985
19. Guitierrez A.C., Gehlen M.H., *Spoectrochim. Acta Part A* 58:83, 2002.
20. Will F., III, *Anal. Chem.*, 33, 1360, 1960.
21. Lian H.Z., Kang Y.F., Yasin A., Bi S.P., Shao D.L., Chen Y.J., Dai L.M., Tian L.C., *Journal of Chromatography A,* 993 (1-2): 179, 2003
22. Capitan F., Manzano E., Navalon A., Vilchez J.L., Capitanvallvey L.F., *Talanta* 39 (1): 21,1992
23. Lian H., Kang Y., Arkin Y., Bi S., Li D., Mei S., Wu X., Tao X., Chen Y., Dai L., Gan N., Tian L., *Analytica Chimica Acta* 511 : 25, 2004
24. Vitorello V.A., Haug A., *Plant Science* 122 (1): 35, 1997

25. Saarl L.A., Seltz W.R., *Anal. Chem.*, 55: 667, 1983
26. Al-Kindy S.M.Z., Suliman F.O., Salama S.B., *Microchemical Journal* 74 : 173, 2003
27. Sanz-Mendel A., Campa R.F., Alonso J.I., *Analyst* 112:493, 1987.
28. Zhang Z. and Seitz W.R., *Anal. Chim. Acta,* 171: 251, 1985.
29. Mánuel-Vez M.P., Moreno C., Gonzáles D.J., García-Vargas M., *Analytica Chimica Acta* 355 :157, 1997
30. Albendin G., Manuel-Vez M.P., Moreno C., Garcia-Vargas M., *Talanta* 60 (2-3): 425, 2003
31. Canizares P., Decastro M.D.L., Valcarcel M., *Analytical Letters*, 27 (2): 247, 1994
32. Jiang C., Tang B., Wang R., Yen J., *Talanta* 44: 197, 1997
33. Gunduz S.B., Kucukkolbasy S., Atakol O., Kylyc E., *Spectrochimica Acta Part A-Molecular and Biomolecular Spectroscopy*, 61(5): 913, 2005.
34. Rojas F.S., Alcaraz E.C., Pavon J.M.C., *Analyst* 119(6): 1221, 1994
35. Gallego M.C., Mochon M.C., Rodriguez M.T., Perez A.G., *Mikrochimica Acta* 109 (5-6): 301, 1992
36. Vilchez J.L., Navalon A., Avidad R., Garcialopez T., Capitanvallvey L.F., *Analyst* 118 (3): 303, 1993
37. Zenki M., Ineyama J., Watanabe J., Uyama Y., Toei K., *Bunseki Kagaku* 40 (7): 365, 1991
38. Kawakubo S., Yamamoto S., Iwatsuki M., Fukasawa T., *Bunseki Kagaku* 41 (5): T65, 1992
39. Brach-Papa C., Coulomb B., Boudenne J.L., Cerda V., Theraulaz F., *Analytica Chimica Acta*, 457 (2): 311, 2002
40. Memon N., Bhanger M.I., *Acta Chromatographica* 14 : 172, 2004
41. Fairman B., Sanzmedel A., *International Journal of Environmental Analytical Chemistry* 50 (3): 161, 1993
42. Kokot Z., Pawlaczyk J., *Chemia Analityczna*, 43 (2): 215, 1998
43. de Armas G., Miró M., Cladera A., Estela J.M., Cerdà V., *Analytica Chimica Acta,* 455 :149, 2002
44. Wilson R. L. and Ingle J. D., *Anal. Chim. Acta*, 82(2): 417, 1977.
45. Buratti M., Valla C., Pellegrino O., Rubino F.M., Colombi A., *Analytical Biochemistry*, 353 (1): 63, 1 2006
46. Vitense K., McGown L.B., *Analytica Chimica Acta* 193 : 119, 1987

47. Kashimura K., Mizushima Y., Hoshino E., Matsubara S., *Journal of Chromatography B-Analytical Technologies in the Biomedical and Life Sciences*, 791 (1-2): 13, 2003
48. Maties R., Arias J.J., Jimenez F., Roman M., *Analytical Letters* 25 (5): 851, 1992
49. dos Santos T.C.R., Aucelio R.Q., Campos R.C., *Microchimica Acta* , 142 (1-2): 63, 2003
50. Raggi M.A., Sabbioni C., Forti G.C., *Journal of Farmaceutical and Biomedical Analysis,* 21(6): 1191, 2000
51. Campi G.L., Ingle J.D., *Analytica Chimica Acta* 224: 363, 1989
52. Park C.I., Cha K.W., *Talanta* 51: 769, 2000
53. Baksi K., Pal B.K., *Talanta,* 41 (1): 81, 1994
54. Bihan A.L., Lijour Y., Giamarchi L., Burel-Deschamps L., Stephan L., *Spectrochimica Acta Part B,* 58 :15, 2003
55. Zini Q., *Fresenius Journal of Analytical Chemistry*, 344 (7-8): 322, 1992
56. Watanabe K., Iizuka T., Itagaki M., *Bunseki Kagaku* 51 (7): 545, 2002
57. Miyahara T., Kitamura H., Narita K., Toyo'oka T., *Biomedical Chromatography* 13 (1): 70, 1999
58. Capitan F., Avidad R., Navalon A., Capitanvallvey L.F., *Microchimica Acta* 107 (1-2): 65, 1992
59. Sanchez F.G., Gomez J.C.M., and Lopez M.H., *Analyst,* 112(5): 649, 1987.
60. Cassas E., Izquierdo-Ridorsa A., Garcia-Puignou L, and Dunach J., *Analytical Letters*, 18:2239, 1985.
61. Mansuet T. Le Clerc A.M., and Pallaget C., *Ann. Falsif. Expert. Chim.,* 72(779): 513, 1979.
62. Salinas F., Munoz de la Pena A., and Murillo J.A., *Analyst,* 109(9): 1135, 1984
63. Degruchi M., Masumoto T., Morisige K., and Okumura I., *Bunseki Kagaku*, 28(2): 127, 1979.
64. Zel'tser L.F., Arkhipova L.A., Talipov Sh.T., and Khikmatov Kh., *Zh. Anal. Khim.*, 38(5): 811, 1983.
65. Vasilikiotis G., Voulgaropoulos A., and Apostolopoulou C., *Microchemical Journal,* 34(2): 174-179, 1985.
66. Ioannou P.C., Siskos P.A., *Talanta,* 31(4): 253, 1984
67. Nishikawa, Y., *Journal of Chemical Society Japan* 79, 1003, 1958
68. Nishikawa, Y., *Journal of Chemical Society Japan* 79, 100

7. Statistics

7.1 Units for expressing concentration [1]

Concentration is a general measurement unit stating the amount of solute present in a known amount of solution

$$Concentration = \frac{amount.of.solute}{amount.of.solution} \qquad (7.1)$$

Although the terms 'solute' and 'solution' are often associated with liquid samples, they can be extended to gas-phase and solid-phase samples as well. The actual units for reporting concentration depend on how the amounts of solute and solution are measured.

Molarity (M) expresses concentration as moles per liter of solution.

$$(M) = \frac{moles.solute}{liters.of.solution} \qquad (7.2)$$

Molarity is the concentration of a particular chemical species in solution.

Formality (F) [2]

$$(F) = \frac{moles.undissolved.solute}{liters.of.solution} \qquad (7.3)$$

Formality is a substance's total concentration in solution without regard to its specific chemical form.

Normality (N) is the number of equivalent weights (EW) per unit volume.

$$(N) = \frac{equivalents.solute}{liters.of.solution} \qquad (7.4)$$

An equivalent weight is defined as the ratio of a chemical specie's formula weight (FW) to the number of its equivalents

$$EW = \frac{FW}{n} \qquad (7.5)$$

For acid-base reaction, 1 equivalent = 1 mole of hydrogen ions (or 1 mole of hydroxide ion) donated. For oxidation-reduction reaction, 1 equivalent = 1 mole of electrons. For determining electrolyte concentration, 1 equivalent = 1 mole of charge. Normality must be specified with respect to a define reaction.

Consequently, the following simple relationship exists between normality and molarity.

$$N = n \times M \quad (7.6)$$

Percent concentration (or parts per hundred) (%) can be expressed several ways:

a. Weight percent *(w/w)*:

$$Concentration_{(w/w)} = [weight\ solute\ (g)/weight\ solution\ (g)] \times 100\% \quad (7.7)$$

b. Volume percent *(v/v)*:

$$Concentration_{(v/v)} = [volume\ solute\ (mL)/volume\ solution\ (mL)] \times 100\% \quad (7.8)$$

c. Weight/Volume percent *(w/v)*:

$$Concentration_{(w/v)} = [weight\ solute\ (g)/volume\ solution\ (mL)] \times 100\% \quad (7.9)$$

Parts per thousand (‰):

The definition of *ppt* concentration is:

$$Concentration(‰) = [weight\ of\ substance(g)/weight\ of\ solution(g)] \times 1000\ ppt \quad (7.10)$$

Parts per million (ppm) [3]:

This unit of concentration may be expressed in a number of ways. It is often used to express the concentration of very dilute solutions. The 'technical' definition of parts per million is:

$$Concentration_{ppm} = [weight\ of\ substance(g)/weight\ of\ solution(g)] \times 10^6\ ppm \quad (7.11)$$

Note that for dilute, aqueous solutions, *1ppm = 1 mg/L* because *1L* approximately equals *1kilogram* of solution.

$$Concentration_{ppm} = [weight\ of\ substance(mg)/volume\ of\ solution(L)]\ ppm \quad (7.12)$$

$$Concentration_{ppm} = [weight\ of\ substance(mg)/\ weight\ of\ solution(kg)]\ ppm \quad (7.13)$$

Parts per billion (ppb)[3]:

This concentration unit is also used for very dilute solutions. The 'technical' definition is as follows:

$$Concentration_{ppb} = [weight\ of\ substance(g)/weight\ of\ solution(g)] \times 10^9\ ppb \quad (7.14)$$

Owing to the dilute nature of the solution, once again, the density of the solution will be about the same as the density of the solvent. Thus, we may also express parts per billion as:

$$Concentration_{ppb} = [weight\ of\ substance(\mu g)/volume\ of\ solution(L)]\ ppb \quad (7.15)$$

$$Concentration_{ppb} = [weight\ of\ substance(\mu g)/\ weight\ of\ solution(kg)]\ ppb \quad (7.16)$$

7.2 Elementary statistics relevant to Analytical Chemistry

Mean [4] The mean, $\overline{X}$ is the numerical average obtained by diving the sum of the individual measurements by the number of measurements

$$\overline{X} = \frac{\sum_{i=1}^{N} X_i}{N} \qquad (7.17)$$

Where X_i the i^{th} measurement and N is the number of independent measurements.

Median[4] The median, X_{med} is the middle value when data are ordered from the smallest to the largest value. When the data include an odd number of measurements, the median is the middle value. For an even number of measurements, the median is the average of the *N/2* and the *(N/2)+1* measurements, the number of measurements.

Standard Deviation [4] The standard deviation, *s*, is a statistical measure of the precision for a series of repetitive measurements. The average of using *s* to quote uncertainty in a result is that it has the same units as the mean value and is given as

$$s = \sqrt{\frac{\sum_{i=1}^{N}(X_i - \overline{X})^2}{N-1}} \qquad (7.18)$$

Where N is the number of measurements, X_i is each individual measurement, and $\overline{X}$ is the mean of all measurements. The quantity $(X_i - \overline{X})$ is called the 'residual' or the 'deviation from the mean' for each measurement. The quantity *(N-1)* is called the 'degree of freedom' for the measurement.

Standard error is given by:

$$s_m = \frac{s}{\sqrt{N}} \qquad (7.19)$$

And the *variance* (s^2) is given by:

$$\text{var}\,iance = s^2 = \frac{\sum_{i=1}^{N}(X_i - \overline{X})^2}{N-1} \qquad (7.20)$$

Relative Standard Deviation [4] The relative standard deviation *(RSD)* is useful for comparing the uncertainty between different measurements of varying absolute magnitude. The *RSD* is calculated from the standard deviation, *s*, and is commonly expressed as percentage *(%)*.

$$\%\text{- } RSD = \left(\frac{s}{\overline{X}}\right) \times 100\% \qquad (7.21)$$

The *%-RSD* is also called the 'coefficient of variance' or *CV*.

7.3 Performance characteristics of instruments

Signal to Noise Ratio

Signal/Noise ratio is a dimensionless measure of the relative strength of an analytical signal to the average strength of the background instrumental noise for a particular sample and is closely related to the detection level. The ratio is useful for determining the effect of the noise on the relative error of a measurement. The *Signal/Noise ratio* can be measured a variety of ways, but one convenient way to approximate the *Signal/Noise ratio* is to divide the arithmetic mean (average) of a series of replicates by the *standard deviation* of the replicate results [5].

Precision [4]:

Precision is a measure of spread of data about a central value and may be expressed as the range, the standard deviation, or the variance. Precision is commonly divided into two categories: repeatability and reproducibility. *Repeatability* is the precision obtained when all measurements are made by the same analyst during a single period of laboratory work, using the same solutions and equipment. *Reproducibility*, on the other hand, is the precision obtained under any other set of conditions, including that between analysts, or between laboratories sessions for a single analyst. Since reproducibility include additional sources of variability, the reproducibility of an analysis can be no better than its repeatability. Errors affecting the distribution of measurements around a central value are called indeterminate and are characterized by a random variation in both magnitude and direction. Indeterminate errors need not affect the accuracy of an analysis. Since indeterminate errors are randomly scattered around a central value, positive and negative errors tend to cancel, provided that enough measurements are made. In such situation the mean or median is largely unaffected by the precision of the analysis [6].

Accuracy: Accuracy is the nearness of a measurement or result to the true value. It is expressed in terms of error. The term accuracy generally refers to the difference between the mean, $\overline{X}$, of a set of results and the true or correct value for the quantity measured. According to IUPAC [7], accuracy relates to the difference between a result (or mean) and the true value.

For analytical methods, there are two possible ways of determining the accuracy *viz.* absolute method and comparative method.

Absolute method:

The test for accuracy of the method is carried out by taking varying amounts of the constituent and proceeding according to the specified instructions. The difference between the mean of an adequate number of results and the amount of constituent

$$\%\,Error = \frac{obtained.result - exp\,ected.result}{exp\,ected.result} \times 100 \qquad (7.22)$$

actually present, is usually expressed as parts per hundred *(%)* i.e. *% error*.

Comparative method:

In the analysis of steels, alloys, minerals, soil, biomaterials or synthetic mixtures (laboratory made) of desired composition, the content of the constituent sought is determined by two or more (proposed and standard/reported methods) supposedly 'accurate' methods. These methods, of essentially different character, can be accepted usually as indicating the absence of an appreciable determinate error. The general procedure for the determination of above samples either in the proposed or standard/reported methods comprises of various operations which include sampling, preparation of solutions, separation of interfering ions/substances, if any, and also proposing a method for quantitative determination [8] .

Sensitivity [9]:

The sensitivity of an instrument or a method is a measure of its ability to discriminate between small differences in analyte concentration. Two factors limit sensitivity: the slope of the calibration curve and the reproducibility or precision of the measuring device. If two methods that have equal precision, the one who has the steeper calibration curve will be the more sensitive. A corollary of this statement is that if two methods have calibration curve with equal slopes, the one that exhibits the better precision will be the more sensitive.

The quantitative definition of sensitivity that is accepted by the IUPAC is calibration sensitivity, which is the slope of the calibration curve at the concentration of interest. Most calibration curves that are used in analytical chemistry are linear and may be represented by the Equation

$$Y = mX + b \qquad (7.23)$$

where Y is the measured signal, X is the concentration of the analyte, b is the instrumental signal for a blank, and m is the slope of the straight line. The quantity b should

be the *Y-intercept* of the signal line. With such curves, the calibration sensitivity is depended of the concentration X and is equal to m. The calibration sensitivity as a figure of merit suffers from its failure to take into account the precision of individual measurements.

Selectivity of a method refers to the extent to which it can determine particular analyte(*s*) in a complex mixture without interference from the other components in the mixture. A method which is selective for an analyte or group of analytes is said to be *specific*. The applicability of the method should be studied using various samples, ranging from pure measurement standards to mixtures with complex matrices. In each case the recovery of the analyte(*s*) of interest should be determined and the influences of suspected interferences duly stated. Any restrictions in the applicability of the technique should be documented in the method [10].

Dynamic range [9]:Dynamic range extends from the lowest concentration at which quantitative measurements can be made (limit of quantitation, or *LOQ*) to the concentration at which the calibration curve departs from linearity (limit of linearity, or *LOL*). The lower limit of quantitative measurements is generally taken to be equal to ten times the standard deviation of repetitive measurements on a blank, or $10s_b$. At this point, the relative standard deviation is about 30% and decrease rapidly as concentration become larger. At the limit of detection, the relative standard deviation is *100%*. To be very useful, an analytical method should have a dynamic range of at least two orders of magnitude.

A method's *detection limit* [4] is the smallest amount or concentration of analyte that can be detected with statistical confidence. The International Union of Pure and Applied Chemistry (IUPAC) define the detection limit as the smallest concentration or absolute amount of analyte that has a signal significantly larger than the signal arising from a reagent blank. Mathematically, the analyte's signal at the detection limit, $(Y)_{DL}$, is

$$(Y)_{DL} = b + zs_b \qquad (7.24)$$

Where b is the signal for a reagent blank, s_b is the known standard deviation for the reagent blank's signal, and z is a factor of accounting for the desired confidence level.

The value for z depends on the desired significance level for reporting the detection limit. Typically, z is set to *3*. When s_b is unknown, the term zs_b may be replaced with ts_b, where t is the appropriate value from a t-table.

The American Chemical Society's Committee on Environmental Analytical Chemistry recommends the *limit of quantification*, $(Y)_{LOQ}$, which is defined as

$$(Y)_{LOQ} = b + 10s_b \qquad (7.25)$$

7.4 Calibration of instrumental methods:

Calibration curve:

To use the calibration curve (also called a working curve or an analytical curve) technique, several standards containing exactly known concentrations of the analyte are introduced into the instrument, and the instrument response is recorded. Ordinarily, this response is corrected for the instrument output obtained with a blank. Ideally, the blank contains all of the components of the original sample except for the analyte. The resulting data are then plotted to give a graph of corrected instrument response versus analyte concentration. Plots, that are linear over a significant concentration range (the dynamic range) are often obtained and are desirable because they are less subject to error than are nonlinear curves. Not uncommonly, however, nonlinear plots are observed, which require a large number of calibration data to establish accurately the relationship between the instrument response and concentration. Usually, an Equation is developed for the calibration curve by a least-squares technique so that sample concentrations can be computed directly. The success of the calibration curve method is critically dependent upon how accurately the analyte concentrations of the standards are known and how closely the matrix of the standards resembles that of the samples to be analyzed. Unfortunately, matching the matrix of complex samples is often difficult or impossible, and matrix effects lead to interference errors. To minimize matrix effects, it is often necessary to separate the analyte from the interferent before measuring the instrument response[9].

Method of least squares:

Least-squares regression analysis [11,12] used to describe the relationship between the response (Y) and concentration (X), can be represented by the general function:

$$Y = f(X, a, b_1, \text{- - - - - - - - -} b_m) \qquad (7.26)$$

where $a, b_1, \text{- - - - - - - - -} b_m$ are the parameters of the function.

The Equation for a linear calibration curve is

$$Y = b + mX \qquad (7.27)$$

where Y is the signal and X is the amount of analyte. The constants b and m are the true Y-intercept and the true slope, respectively. The goal of linear regression is to determine the best estimates for the slope, m, and y-intercept, b. This is accomplished by minimizing the residual error between the experimental values, Y_i, and those values $\hat{Y}_i$ predicted by Equation 7.27.

Correlation coefficient, r:

The correlation coefficient r is more helpful to indicate the relationship between the chosen scales. Correlation coefficient is calculated by the Equation,

$$r = \frac{\sum_i (X_i - \bar{X})(Y_i - \bar{Y})}{\sqrt{\sum_i (X_i - \bar{X})^2 \sum_i (Y_i - \bar{Y})^2}} \qquad (7.28)$$

The value of $r=1$ indicates the exact correlation between the true variables while $r=0$ indicates the complete independence of the variables. The $r > 0.99$ indicates excellent linearity.

Standard Addition Method [9] [13] :

A standard addition method can take several forms. One of the most common forms involves adding one or more increments of a standard solution to sample aliquots of the same size. This process is often called spiking the sample. Each solution is then diluted to a fixed volume before measurement. It should be noted that when the amount of sample is limited, standard addition can be carried out by successive introductions of increments of the standard to a single measured volume of the unknown. Measurements are made on the signal sample and on the sample plus the standard after each addition. In the most version of the standard addition method, the sample matrix is nearly identical after each addition, the only difference being the concentration of the analyte or, in cases involving the addition of an excess of an analytical reagent, the concentration of the reagent. All other constituents of the reaction mixture should be identical because the standards are prepared in aliquots of the sample.

Assume that the several identical aliquots V_X of the unknown solution with a concentration X_X are transferred to volumetric flask having a volume V_T. To each of these flasks is added a variable volume V_S mL of a standard solution of the analyte having a known concentration X_S. Suitable reagents are then added, and each solution is diluted to volume.

Instrumental measurements are then made on each of these solutions to yield an instrument response Y. If the instrument response is proportional to concentration, as it must be if the standard addition method is to be applicable, we may write:

$$Y = \frac{kV_S X_S}{V_T} + \frac{kV_X X_X}{V_T} \tag{7.29}$$

where k is a proportionality constant. A plot of Y as a function of V_S is a straight line of the form

$$Y = mV_S + b \tag{7.30}$$

where the slope m and the intercept b are given by

$$m = \frac{kX_S}{V_T} \tag{7.31}$$

and

$$b = \frac{kV_X X_X}{V_T} \tag{7.32}$$

A least-squares analysis can be used to determine m and b; X_X can then be obtained from the ratio of these two quantities and the known values of X_X, V_X, and V_S. Thus,

$$\frac{b}{m} = \frac{kV_X X_X / V_T}{kX_S / V_T} = \frac{V_X X_X}{X_S} \tag{7.33}$$

or

$$X_X = \frac{bX_S}{mV_X} \tag{7.34}$$

A value for the standard deviation in X_X can be obtained by assuming that the uncertainties in X_S, V_S, and V_T are negligible with respect to those in m and b. Then, the

relative variance of the result $(s_X/X_X)^2$ is assumed to be the sum of the relative variances of m and b. That is,

$$\left(\frac{s_X}{X_X}\right)^2 = \left(\frac{s_m}{m}\right)^2 + \left(\frac{s_b}{b}\right)^2 \qquad (7.35)$$

where s_m is the standard deviation of the slope and where s_b is the standard deviation of the intercept. Taking the square root of this Equation gives

$$s_X = c_X \sqrt{\left(\frac{s_m}{m}\right)^2 + \left(\frac{s_b}{b}\right)^2} \qquad (7.36)$$

Alternatively, a manual plot of the data may be constructed, and the linear portion of the plot may be extrapolated to the left of the origin. The difference between the volume of the standard added at the origin (zero) and the value of the volume at the intersection of the straight line with the *X-axis*, or the *X-intercept* $(V_X)_0$, is the volume of standard reagent equivalent to the amount of analyte in the sample. In addition, the *X-intercept* corresponds to zero instrument response, so that we may write

$$Y = \frac{kV_S X_S}{V_T} + \frac{kV_X X_X}{V_T} = 0 \qquad (7.37)$$

And we obtain

$$X_X = -\frac{(V_S)_0 X_S}{V_X} \qquad (7.38)$$

In the interest of saving time or sample, it is possible to perform a standard addition analysis by using only two increments of sample. Here, a single addition of V_S mL of standard would be added to one of the two samples, and we can write

$$Y_1 = \frac{kV_X X_X}{V_T} \qquad (7.39)$$

$$Y_2 = \frac{kV_X X_X}{V_T} + \frac{kV_S X_S}{V_T} \qquad (7.40)$$

were Y_1 and Y_2 are the analytical signal resulting from the diluted sample and the diluted sample plus standard, respectively. Dividing the second Equation by the first gives upon rearrangement

$$X_X = \frac{Y_1 X_S V_S}{(Y_2 - Y_1)V_X} \qquad (7.41)$$

7.5 Stoichiometry of Metal-Ligand complex

The stoichiometry for a metal-ligand complexation reaction of the following general form:

$$M + yL \leftrightarrow ML_y \qquad (7.42)$$

can be determinated by one of three methods: the method of continuous variation, the mole-ratio, and the slope-ratio method [14]

In the *mole-ratio method,* the method used in this work, the mole of reactant, usually the metal, are held constant, while the moles of the other reactant are varied [4]. A plot of absorbance versus mole ratio of the reactants is then prepared. If the formation constant is reasonably favourable, two straight lines of different slope that intersect at a mole ratio that corresponds to the combining ratio in the complex are obtained [9].

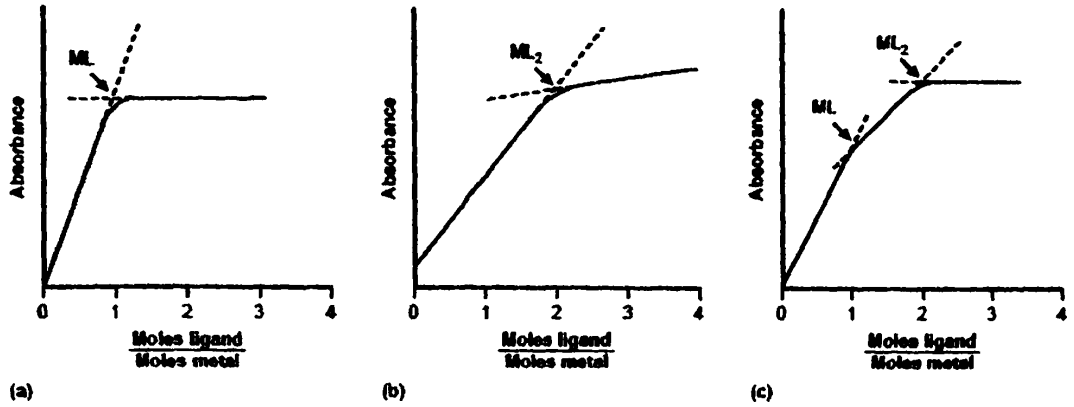

Figure.7.1 *Mole-ratio plots used to determine the stoichiometry of a metal-ligand complexation reaction*

Figure 7.1a shows a mole-ratio plot for the formation of a 1:1 complex in which the absorbance is monitored at a wavelength at which only the complex absorbs. Figure 7.1b shows a mole-ratio plot for a 1:2 complex in which the metal, the ligand, and the complex absorb at the selected wavelength. Unlike the method of continuous variations, the mole-ratio method can be used for complexation reactions that occur in a stepwise fashion, provided that the molar absorptivities of the metal–ligand complexes differ and the formation constants are sufficiently different. A typical mole-ratio plot for the stepwise formation of *ML* and ML_2 is shown in Figure 7.1c.

Both the method of continuous variations and the mole-ratio method rely on an extrapolation of absorbance data collected under conditions in which a linear relationship exists between absorbance and the relative amounts of metal and ligand[1].

References:

1. Gray, Analytical Chemistry Lecture Outline: Important Chemical Concept, Pack to Analytical Chemistry Menu.
2. http://en.wikipedia.org/wiki/Concentration
3. Ladon L., Concentration units, 2001.
4. Harvey D., Modern Analytical Chemistry, *McGraw-Hill Higher Education*, 2000.
5. Skoog D. A. and Leary J. J., Principles of Instrumental Analysis, *Fourth Edition, Saunders College Publishing*, 1992.
6. Guide for Use of Terms in Reporting Data, *Anal. Chem.*, 54, pp.157, 1982.
7. IUPAC, *Spectrochim. Acta*, 33 B, pp. 241, 1978.
8. D. L. Massart, B. G. M. Vandeginste, S. N. Deming, Y. Michotte and L. Kaufman, *Chemometrics*, Elsevier, Amsterdam, 1988.
9. Skoog D.A., Holler F.J., Nieman T.A., Principles of Instrumental Analysis, *fifth edition, Harcourt Brace & Company*, 1998
10. Guide to Quality in Analytical Chemistry, *CITAC & EURACHEM*, 2002.
11. M. D. Pattergill and D. E. Sands, *J. Chem. Edu.*, 58, pp. 244, 1979.
12. B. D. Robert, E. T. James and L. P. Harry, *Clin. Chem.*, 24, pp. 611, 1978.
13. Quevauviller Ph., Quality Assurance for water analysis, *John Wiley and Sons Technology & Industrial Ed*, 2002.
14. Burns D.T. et al., Use of the terms 'recovery' and 'apparent recovery' in analytical procedures, *IUPAC Recommendation* 2002.

8. Experimental part

8.1 Reagents and solutions used in the present study:

All experiments were performed with analytical-reagent grade chemicals and solvents. All solutions were prepared using distilled water from a borosilicate autostill (Jencons Ltd). All working standards were prepared by appropriate dilution of stock solutions with distilled water unless mentioned otherwise. All solutions were stored in plastic bottles at 4-6°C in dark. Cylindrical polyethylene test-tubs were used to prepare sample and standard solutions and a square polyethylene or silica cuvette was used for measurements. General-purpose polyethylene transferpipettes were used to fill and empty the test-tubes and cuvettes. Bottles and laboratory wares and cuvettes were periodically washed in 1+1 nitric acid-sulphuric acid. Normally, they were washed in soapy water, rinsed thoroughly with tap water, then with distilled water and finally dried in an oven at 80°C.

The following reagents and solutions were used in the present investigations:

Aluminum nitrate $[Al(NO_3)_3.9H_2O]$ of analytical-reagent grade, purchased from Merck, was used to prepare stock solutions. A stock solution of Al 10^{-3} M was prepared by dissolving 0.0376 g $Al(NO_3)_3.9H_2O$ in 100 mL nitric acid 0.1 N. More dilute solutions (working solutions) were prepared by diluting this solution with nitric acid 0.1 N and were daily prepared.

Also, standard stock solutions (10^{-3} M) were prepared by diluting a certified commercial standard (Merck; 1000 ppm aluminum) with nitric acid 0.1 N and stored in polyethylene bottles. Working solutions (10^{-5} and 10^{-6} M) were prepared by mixing appropriate volumes of the stock solution with nitric acid 0.1 N.

Buffer solutions were prepared by mixing sodium acetate (2 M) and acetic acid solutions (2 M) in the proportions required to give the desired pH.

Acid alizarin violet N was purchased from Aldrich. A stock solution of 10^{-3} M was prepared by dissolving 0.0366 g AVN in 100 mL distilled water. More dilute solutions (working solutions) were prepared by diluting this solution with distilled water and were daily prepared.

Acid Red 8 (AR8) was purchased from Aldrich. A stock solution of 10^{-3}M was prepared by dissolving 0.0480 g AR8 in 100mL distilled water.

A stock solution of *fluoride* (10^{-2} M) was prepared by dissolving 0.0420 g of NaF (Aldrich) in 100 mL distilled water.

A stock solution of *magnesium(II)* (10^{-2} M) was prepared by dissolving 0.2460 g of $MgSO_4.7H_2O$ (Aldrich) in 100 mL distilled water.

A stock solution of *nickel(II)* (10^{-3} M) was prepared by dissolving 0.0238 g of $NiCl_2.6H_2O$ (Aldrich) in 100 mL distilled water.

A stock solution of *manganese(II)* (10^{-3} M) was prepared by dissolving 0.0126 g of $MnCl_2$ (Aldrich) in 100 mL distilled water.

A stock solution of *barium(II)* (10^{-3} M) was prepared by dissolving 0.0244 g of $BaCl_2.2H_2O$ (Aldrich) in 100 mL distilled water.

A stock solution of *calcium(II)* (10^{-2} M) was prepared by dissolving 0.1110 g of $CaCl_2$ (Aldrich) in 100 mL distilled water.

A stock solution of *tin(II)* (10^{-3} M) was prepared by dissolving 0.0256 g of $SnCl_2.2H_2O$ (Aldrich) in 100 mL distilled water.

A stock solution of *chromium(III)* (10^{-3} M) was prepared by dissolving 0.0266 g of $CrCl_3.6H_2O$ (Aldrich) in 100 mL hydrochloric acid 0.1 N. More dilute solutions (working solutions) were prepared by diluting this solution with hydrochloric acid 0.1 N.

A stock solution of *beryllium(II)* (10^{-3} M) was prepared by dissolving 0.0177 g of $BeSO_4.4H_2O$ (Aldrich) in 100 mL distilled water.

A stock solution of *mercury(II)* (10^{-3} M) was prepared by dissolving 0.0297 g of $HgSO_4$ (Aldrich) in 100 mL hydrochloric acid 0.1 N at temperature.

A stock solution of *phosphate* (10^{-3} M) was prepared by dissolving 0.0174 g of K_2HPO_4 (Aldrich) in 100 mL distilled water.

A stock solution of *phosphate* (10^{-3} M) was prepared by dissolving 0.0136 g of KH_2PO_4 (Aldrich) in 100 mL distilled water.

A stock solution of *cobalt(II)* (10^{-3} M) was prepared by dissolving 0.0130 g of $CoCl_2$ (Aldrich) in 100 mL distilled water.

A stock solution of *iron(III)* (10^{-3} M) was prepared by dissolving 0.0404 g of $Fe(NO_3)_3.9H_2O$ (Aldrich) in 100 mL hydrochloric acid 0.1 N.

A stock solution of *copper(II)* (10^{-3} M) was prepared by dissolving 0.0242 g of $Cu(NO_3)_2.3H_2O$ (Aldrich) in 100 mL water.

A stock solution of *lead(II)* (10^{-3} M) was prepared by dissolving 0.0331 g of $Pb(NO_3)_2$ (Aldrich) in 100 mL water.

A stock solution of *sodium(I)* (10^{-2} M) was prepared by dissolving 0.0850 g of $NaNO_3$ (Aldrich) in 100 mL water.

A stock solution of *zinc(II)* (10^{-3} M) was prepared by dissolving 0.0298 g of $Zn(NO_3)_2.6H_2O$ (Aldrich) in 100 mL water.

A stock solution of *cadmium(II)* (10^{-3} M) was prepared by dissolving 0.0308 g of $Cd(NO_3)_2.4H_2O$ (Aldrich) in 100 mL water.

A stock solution of *strontium(II)* (10^{-3} M) was prepared by dissolving 0.0267 g of $SrCl_2.6H_2O$ (Aldrich) in 100 mL water.

A stock solution of *hydroxylamine hydrochloride* (0.15 M) was prepared by dissolving 1.0424 g of $NH_2OH.HCl$ (Fluka) in water.

A stock solution of *1, 10-pheanthroline* (5×10^{-3} M) was prepared by dissolving 0.0991 g of $C_{12}H_8N_2.H_2O$ in 100 mL water at temperature.

A working stock of *nitric acid* (0.1 N) was prepared by diluting 6.96 mL nitric acid concentrated with water, up to 1000 mL solution.

A working stock of *hydrochloric acid* (0.1 N) was prepared by diluting 8.28 mL hydrochloric acid concentrated with distilled water, up to 1000 mL solution.

Certified prawn (GBW 08572) was used to check the performance of the method.

Certified soft drinking water (UK) metals LGC 6011 (Laboratory of the Government Chemist, United Kingdom) was used to check the performance of the method.

Pharmaceutical antacid formulation was used to check the performance of the method.

8.2 Apparatus

Fluorescence measurements were performed with a *Cary Eclipse spectrophotometer*, as well as with a *Perkin-Elmer LS 3* and *Shimadzu RF-5301* one equipped with an R 928 photomultiplier tube, while absorbance measurements were made with a *Jasco V-530 UV-VIS spectrophotometer*, as well as with a *Hitachi 2000 UV-VIS spectrophotometer*. The *Crison GLP 21 pH-meter* with a glass-calomel electrode was used for pH measurements.

The Cary Eclipse fluorescence spectrophotometer is ideal for routine laboratory work and offers high performance and advanced design features. The instrument consists of two Czerny-Turner monochromators (excitation and emission), a Xenon light source, a range of fixed width selectable slits, selectable filters, attenuators and two photomultiplier tubes as detectors (Figure 8.1) [1].

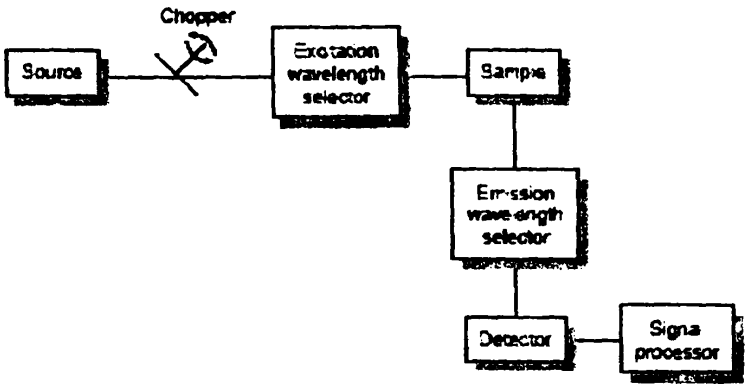

Figure 8.1. *Essential components of a fluorescence spectrometer* [2, pp 21-28]

Sources

Pulse xenon lamp, which operate at power of 15 W, provide short (pulse width 2-3 us) but very bright (60-75 kW) light pulse [1].

Excitation and emission monochromators

The exciting light is isolated by a grating monochromator with the possibility to select both the excitation and emission wavelengths. Such a fluorescence spectrometer is capable of recording both excitation and emission spectra and therefore makes full use of the analytical potential of the technique. If monochromators are employed, it should be possible to change the slit width of both the excitation and emission monochromators independently (Table 8.1 and Table 8.2). Many analyses will not require high resolution (essentially corresponding to high selectivity) and greater sensitivity will be obtained with wide slit widths. Conversely, to record the fine structure in the emission of, for example, polyaromatic hydrocarbons or to excite selectively one compound in the presence of another, narrow slit widths will be necessary, and sensitivity will be sacrificed [2, pp 21-28] .

Table 8.1 *Properties of the excitation monochromator* [1]

Type	Czerny–Turner
Dispersing method	Grating, 30 x 35 mm, 1200 lines/mm
Blaze angle	370 nm
Spectral bandwidths	1.5 nm 2.5 nm 5.0 nm 10 nm 20 nm 10 nm round

Filters	Selectable Open Closed 250 - 395 nm UG5 335 - 620 nm BG38 550 - 1100 nm OG550 695 - 1100 nm RG695 Auto
Reciprocated Linear dispersion	3 mm/mm
Wavelength range	190 to 900 nm
Accuracy	±1.0 nm, (±0.5 nm at 541.92 nm)
Wavelength repeatability	±0.2 nm
Wavelength drive	Software controlled motor drive. Non measurement phase stepping.
Maximum Slew rate	24,000 nm/min
Maximum Scan rate	24,000 nm/min

Table 8.2 *Properties of the emission monochromator* [1]

Type	Czerny–Turner
Dispersing method	Grating, 30 x 35 mm, 1200 lines/mm
Blaze angle	440 nm
Spectral bandwidths	Selectable fixed width at 1.5 nm 2.5 nm 5.0 nm 10 nm 20 nm and 10 nm round
Filters	Selectable Open Closed 250 - 395 nm UG5, 295 - 1100 nm WG295, 360 - 1100 nm 9086, 430 - 1100 nm GG435 550 - 1100 nm OG550 3%T attenuator Mesh (1.5 Abs) Auto.
Reciprocated Linear dispersion	3 mm/mm
Wavelength range	190 to 900 nm
Accuracy	±1.0 nm, (±0.5 nm at 541.92 nm)

Wavelength repeatability	±0.2 nm
Wavelength drive	Software controlled motor drive. Non measurement phase stepping.
Maximum Slew rate	24,000 nm/min
Maximum Scan rate	24,000 nm/min

Cells and cell compartments

Fluorescence cells are polished on all four faces, and are fabricated from plastics, glass or silica [3].

Detectors [2, pp. 21-28]

The fluorescence instrument uses photomultiplier tubes (×2) as detectors. The material from which the photocathode is made determines the spectral range of the photomultiplier and generally two tubes are required to cover the complete UV-visible range. The limit of sensitivity of a photomultiplier is normally governed by the level of dark current (which is the signal derived from the tube with no light falling on it). The dark current is caused by thermal activation and can usually be reduced by cooling the photomultiplier. Another method of minimizing dark current is to use a stroboscopic source since the ratio of dark current to fluorescence will be very small during each high intensity flash. During the periods between flashes when the dark current is relatively high, the photomultiplier output can be disconnected. The overall result is that the dark current no longer becomes the limitation to sensitivity.

The spectral response of photomultiplier varies with wavelength.

Read-out devices [2, pp 21-28]

The output from the detector is amplified and displayed on a readout device, a modern computer.

The crucial optical components (Table 8.3) in UV-visible spectrometry Jasco Model V-530/SPF UV/VIS double beam Spectrophotometer (Hitachi Model U-2010) (Figure 8.2) are the light source, the monochromator, and beam splitting system and the detector. In addition, the instrument includes mirrors or lens.

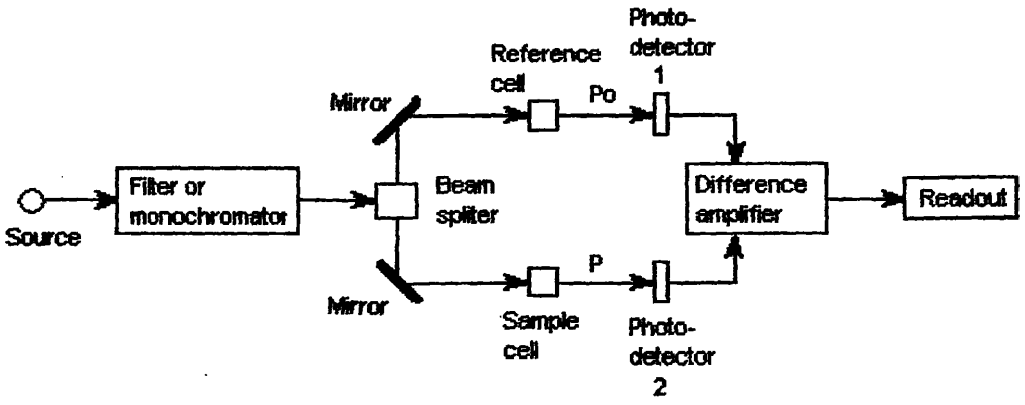

Figure 8.2. *Instrument design for double-beam spectrophotometer.*

Table 8.3. *Specifications of UV-visible spectrometry Jasco Model V-530/SPF UV/VIS double beam Spectrophotometer*

Optical system: Double beam, single monochromator with a 1200 grooves/mm concave grating and modified Rowland mount

Spectral bandwidth: 2 nm

Wavelength range: 190 – 1100 nm

Light sources: Deuterium lamp for UV range (190 – 350 nm)

Halogen lamp for VIS range (350 – 1100nm) (*automatic selected*)

Wavelength repeatability: ± 0.1 nm

Wavelength accuracy: ± 0.5 nm

Photometric mode: Abs, %T, %R

Photometric range: -2,3 Abs

Photometric reproducibility: ±0.001 Abs

Photometric accuracy: ±0.002 Abs (obtained using NIST SRM 930D)

Stray light: 0.04%T

Wavelength scan speed: 4000, 2000, 1000, 400, 200, 100, 40 nm/min

Wavelength slew speed: 8000 nm/min

Baseline stability: ± 0.001 Abs/hour

Baseline flatness: ± 0.001 Abs (within 200 – 1000 nm range)

Response time: Quick, Fast, Medium, and Slow

Detector: Silicon photo-diode (S1337)

Power requirement: 130 W

The light sources are the deuterium arc and the halogen lamps for lower and higher wavelength regions, respectively. A deuterium lamp produces a continuum spectrum in the ultraviolet region from 190 to 340 nm by electrical excitation of deuterium at low pressure. The mechanism by which a continuous spectrum is produced involves initial formation of an excited molecular deuterium followed by dissociation of the excited molecule to give two atomic species plus an ultraviolet photon. At higher wavelengths its intensity is rather feeble.

A halogen lamp becomes useful at about 340 nm and higher wavelengths. The lower limit is imposed by the absorption of radiation by the glass envelope that houses the filament.

A chopper controls the radiation's path, alternating it between the sample, the blank, and a shutter. The signal processor uses the chopper's known speed of rotation to resolve the signal reaching the detector into that due to the transmission of the blank (P_0) and the sample (P_T). By including an opaque surface as a shutter it is possible to continuously adjust the *0% T* response of the detector. The effective bandwidth of a double-beam spectrophotometer is controlled by means of adjustable slits at the entrance and exit of the monochromator. Effective bandwidths of are between 0.2 nm and 5.0 nm. A scanning monochromator allows for the automated recording of spectra.

The sample compartment for the instrument provides a light-tight environment that prevents the loss of radiation, as well as the addition of stray radiation. Samples are in the liquid or solution state and are placed in cells constructed with UV/VIS-transparent materials, such as quartz, glass, and plastic

Quartz or fused-silica cells are required when working at wavelengths of less than 300 nm where other materials show a significant absorption. The cell has a pathlength of 1cm. The highest quality cells are constructed in a rectangular shape, allowing the radiation to strike the cell at a 90° angle, where losses to reflection are minimal. These cells, which are usually available in matched pairs having identical optical properties, are the cells of choice for double-beam instruments.

The UV-visible instrument uses photomultiplier tube as detectors [3,4,5].

8.3 Certified reference materials

Prawn GBW (Guild Book Workers) 08572 was used as a certified reference material to check the performance of the method. The following report gives the certified and noncertified values for the metal existing in the prawn.

Certified Reference Material: GBW 08572 Prawn

Certified Elements, Values and Uncertainty

Element	***Value & Uncertainty***
K %	0.597 0.012
Na %	0.381 0.008
Ca %	0.304 0.006
Mg %	0.160 0.003
Al %	0.131 0.004
Cu μg/g	4.66 0.23
Zn μg/g	60.8 1.4
Mn μg/g	1.96 0.13
Fe μg/g	19.8 0.4
Sr μg/g	40.6 3.4
As μg/g	1.42 0.06
Se μg/g	1.52 0.04
Pb μg/g	0.298 0.019
Cd μg/g	0.023 0.004
Hg μg/g	0.201 0.004
Cr μg/g	0.24 0.06
Ba μg/g	4.29 0.72
N %	14.3 0.4
P %	0.845 0.012
F μg/g	5.31 0.39

Noncertified values

Element	***Noncertified Value***
Co μg/g	0.029
Ti μg/g	1.05
Br μg/g	13.5
S %	0.85

Soft drinking water (UK) metals, LGC 6011 (Laboratory of the Government Chemist, United Kingdom) was used as a certified reference material to check the performance of the method. The following report gives the certified values for the metal existing in the soft drinking water.

Certified Reference Material: LGC 6011

Soft drinking water (UK) – Metals

Certified values

Metal	***Content (μg/L)***
Aluminum	218
Silver	9.2
Barium	104
Chromium	48
Iron	194
Manganese	52
Nickel	51
Zinc	514
Lead	50
Calcium	28
Potassium	0.5
Magnesium	1.2
Sodium	4.5

Noncertified values

Metal	***Content (μg/L)***
Arsenic	51
Selenium	10
Antimony	11

8.4 Liquefaction of the biological sample

A sample of 0.21230 g of prawn accurately weighed was placed in a preweighed porcelain beaker. The sample was dried into an electric oven at 80°C for a minimum of 4-5 hours, and weighed after cooling to room temperature. The sample was repeatedly dried, cooled and weighed until a constant weigh of this was achieved. The loss was found to be around 8 % (the moisture content of the material).

Wet digestion HNO_3/H_2O_2

About 0.2 g of the prawn powder, reference material, accurately weighed, was quantitatively transferred into a clean beaker of 80 mL. Then, 2 mL of concentrated nitric acid (14.0 mol/L) was added to dissolve the resulted residue. The nitrate solution formed was warmed to about 90°C on an electric hot plate and under continuous magnetic stirring. Finally, an aqueous solution of H_2O_2 (30% v/v) was carefully added in 4.0 mL aliquots at intervals of 10 min, until all the black particles were digested and disappeared. The solution was evaporated to dryness and the resulting product was picked up with nitric acid 0.1 N,

transferred quantitatively into a 1000 mL volumetric flask, filled to volume with nitric acid 0.1 N and mixed well (stock solution of prawn). The final concentration of the prawn stock solution was 8.93×10^{-6} M.

8.5 Liquefaction of pharmaceutical formulation

To obtain a solution, 1 tablet of 1.2625 g containing 200 mg of $Al(OH)_3$ (nominated amount) was completely ground and homogenized. A weight of 15.6 mg of the powdered product, accurately weighed, was quantitatively placed into a clean porcelain crucible. Then, a volume of 0.5 mL of concentrated sulphuric acid was added and the system as a whole was slightly warmed to finish the neutralization reaction. The resulting product was picked up with distilled water, transferred into a 1000 mL volumetric flask, filled to volume with distilled water and mixed well (stock solution of pharmaceutical formulation). The final concentration of the standard solution was 31.683×10^{-6} M of aluminum(III).

8.6 Chemical structure and absorption spectrum of AVN

AVN (Figure 8.3) has two bulk moieties, the phenyl group and naphthyl group. Two hydroxyl groups are located in *ortho* positions to the azo group. The one attached to the phenyl moiety is the more acidic. The presence of negatively charged sulphonate moiety (attached to the phenyl moiety), located away from the coordinating site, allows solubilization of the ligand and its complexes in water [6].

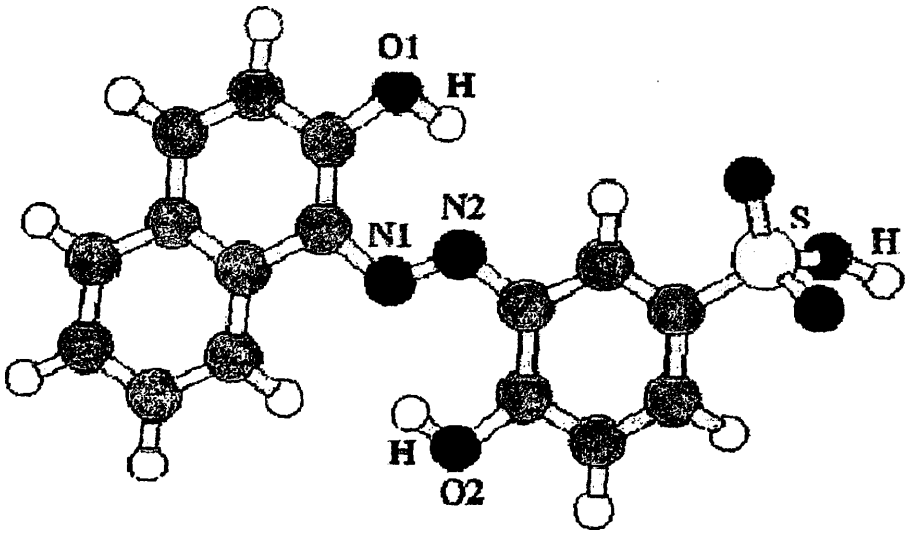

Figure 8.3. *Fully AM1 optimized geometry for the neutral AVN molecule in the gas phase.*

In o,o'-dihydroxy azo dye metal-ion indicators, one hydroxyl group is 10^4 times more acidic than the other. The location of the more acidic hydroxyl group has been established through different theories.

Special attention was focused on the study performed by Dakiky on acid alizarin violet N molecule. According to this work, in aqueous solution AVN can exist either in *azo*- or *hydrazo*-forms, each capable of forming three distinct species through stepwise proton ionizations (Figure 8.4). Additionally, monomer-dimer equilibrium exists at low pH. The third proton ionization, due to the naphthol proton, occurs only in very basic media, in which AVN is present mostly in the hydrazo form. In this form, the naphthol proton is located at the nitrogen of the azo group. Hydrazo protons are known to be very weakly acidic.

AVN can be represented as H_2In^-, in which the negative sign arises from the dissociation of the highly acidic sulphonate proton. Thus pK_2 and pK_3 refer to the following dissociation steps (Figure 8.4):

$$H_2In^- \leftrightarrow H^+ + HIn^{2-} \qquad (8.1)$$

$$HIn^{2-} \leftrightarrow H^+ + In^{3-} \qquad (8.2)$$

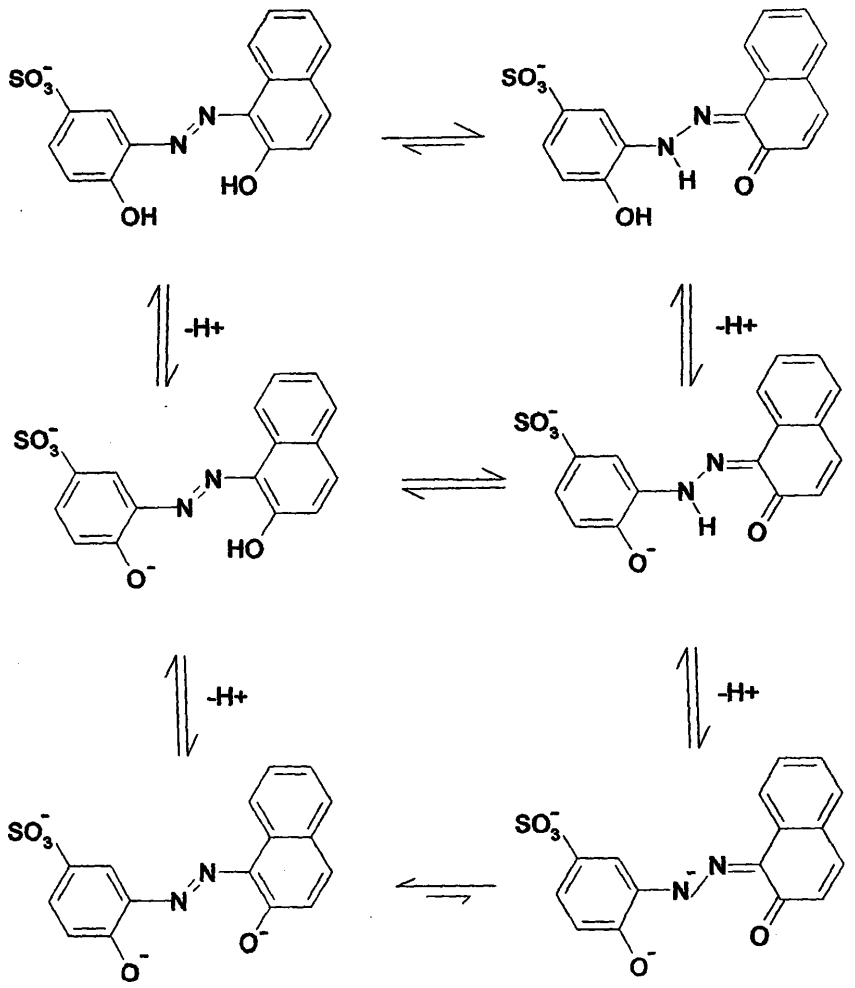

Figure 8.4. *Ionization steps of azo- and hydrazo-forms of AVN* [7].

On the other hand, based on the charge distribution for the two oxygen atoms of the two hydroxyl groups, derived from the theoretical calculation (*Hyperchem 6 software*), it is evident that the hydroxyl group attached to the phenyl moiety is more acidic than that one attached to the naphthyl moiety.

The trans geometries of the AVN molecule (neutral, mono-, di-, and tri-deprotonated) were optimized at AM1 level of the theory using *Hyperchem 6* [8] program. The structures of the AVN compounds were visualized with the *Hyperchem 6* program.

The structures of AVN compounds in trans conformations are shown in Figure 8.5. The charge distributions for the optimized geometries of AVN in trans conformations, in gas phase are shown in Table 8.4.

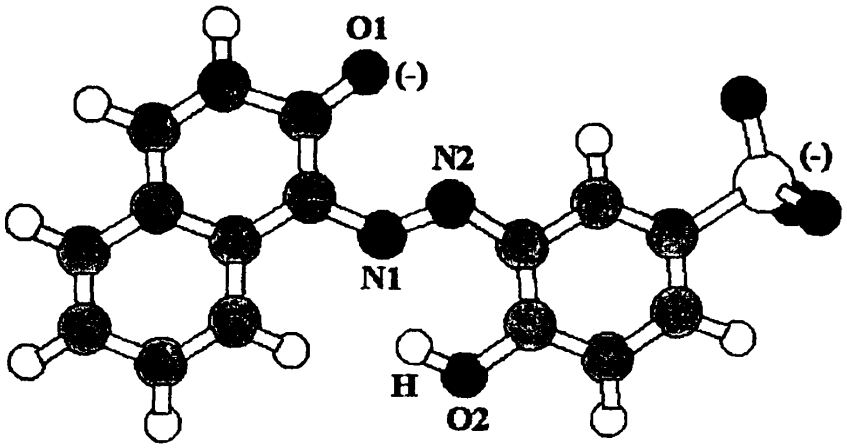

(a)

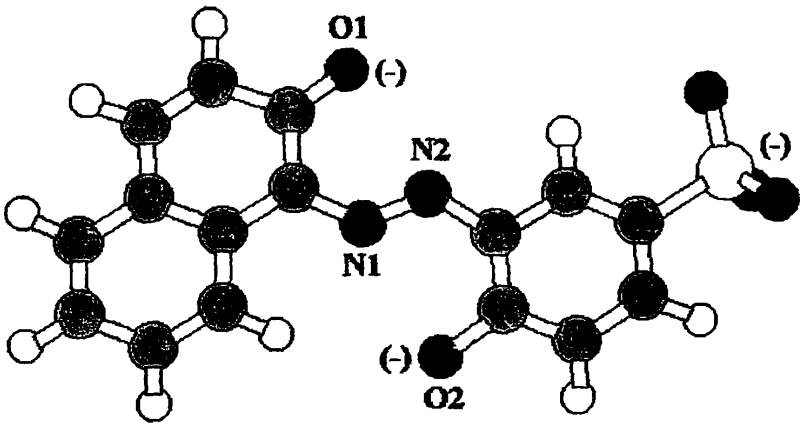

(b)

Figure 8.5. *Fully AM1 optimized geometry for (a) di-deprotonated AVN (which lack one hydrogen atom of the hydroxyl group to the sulphonic group and other hydrogen atom of the hydroxyl group attached to the naphthyl moiety) and (b) tri-deprotonated AVN (which lack one hydrogen atom of the hydroxyl group to the sulphonic group, one hydrogen atom of the hydroxyl group attached to the phenyl moiety and one hydrogen atom of the hydroxyl group attached to the naphthyl moiety), in trans conformations, in the gas phase.*

Table 8.4 *Charge distribution for the fully AM1 optimized geometry of the neutral, mono-deprotonated, di-deprotonated and tri-deprotonated AVN molecule.*

Atom	***Charge Neutral AVN***	***Charge Mono-deprotonated AVN***	***Charge Di-deprotonated AVN[a]***	***Charge Di-deprotonated AVN[b]***	***Charge Tri-deprotonated AVN***
O (phenyl)	*-0.239*	*-0.268*	*-0.422*	*-0.297*	*-0.524*
O (naphthyl)	*-0.242*	*-0.253*	*-0.292*	*-0.389*	*-0.474*
O (sulphonic)	*-0.766*	*-1.061*	*-1.085*	*-1.075*	*-1.107*
N (phenyl)	*-0.096*	*-0.089*	*-0.064*	*-0.089*	*-0.035*
N (naphthyl)	*-0.102*	*-0.130*	*-0.217*	*-0.121*	*-0.065*

mono-deprotonated AVN is AVN molecule which lacks one hydrogen atom of the hydroxyl group to the sulphonic moiety

di-deprotonated[a] AVN is AVN molecule which lack one hydrogen of the hydroxyl group to the sulphonic moiety and other hydrogen atom of the hydroxyl group attached to the phenyl moiety.

di-deprotonated[b] AVN is AVN molecule which lack one hydrogen atom of the hydroxyl group to the sulphonic group and other hydrogen atom of the hydroxyl group attached to the naphthyl moiety.

tri-deprotonated AVN is AVN molecule which lack one hydrogen atom of the hydroxyl group to the sulphonic group, one hydrogen atom of the hydroxyl group attached to the phenyl moiety and one hydrogen atom of the hydroxyl group attached to the naphthyl moiety

According to experimental data for neutral and mono-deprotonated AVN molecule, both oxygen atoms of the hydroxyl group attached to the phenyl and naphthyl moiety has almost the same acidity.

In the case of tri-deprotonated AVN molecule, the results show that the oxygen atom of the hydroxyl group attached to the phenyl moiety is more acidic than that of the hydroxyl group attached to the naphthyl moiety.

In all cases, it is evident that the most acidic oxygen atom is the one of the sulphonic moiety, while the nitrogen atom attached to the naphthyl moiety is more acidic than that of the hydroxyl group attached to the phenyl moiety.

Thus, probably AVN is complexed with Al through the oxygen atom of the naphthyl moiety and nitrogen atom of the phenyl moiety.

Based on the previous explanations and according to Martell, where it is found for the acid alizarin violet N *pK* values are 7.0 and 12.80, it can be supposed that the *pK* value of 7.0 corresponds to the hydroxyl group of the phenyl moiety, whereas the *pK* value of 12.80 to the hydroxyl group of naphthyl moiety.

Absorption spectra of AVN as a function of pH in aqueous solutions are shown in Figure 8.6. At pH≤9.0 absorbance maxima are observed at 500 and 560 nm. These can be assigned to H_2In^- and HIn^{2-}, respectively. A slightly distorted isosbestic point is located at 525 nm. H-NMR and spectrophotometric studies on similar polyprotic azo dyes have led to the conclusion that they exist predominantly as dimmers at pH<4[7]. Hydrogen bonding, electrostatic interactions, van der Waal's forces and hydrophobic interactions, are responsible for dye-dye self association (dimmers). Moreover, dissociation to monomers is typically accompanied by the appearance of shoulder at higher wavelength. The figure shows that, in addition to favoring the basic form, a rise in pH promotes dissociation to monomers as evidenced by a bathochromic acid band broadening.

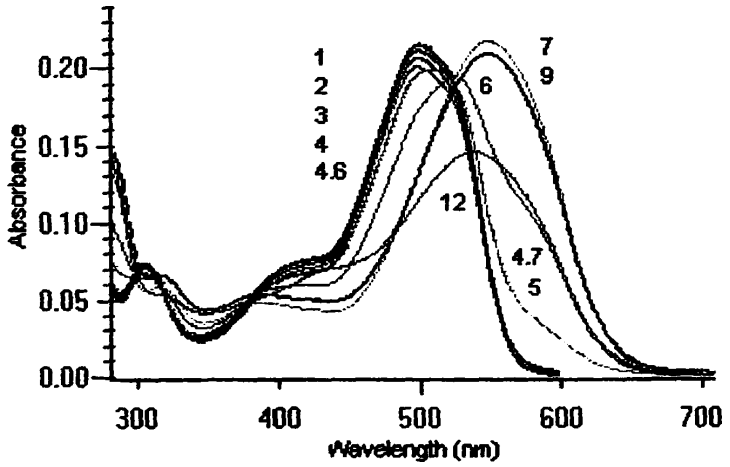

Fig. 8.6. *Absorption spectra of 2×10^{-5}M AVN as a function of pH. Numbers refer to pH values 1 (1.2), 2 (2.0), 3 (3.0), 4 (3.9), 4.6 (4.6), 4.7 (4.7), 5 (5.2), 6 (6.0), 7 (7.3), 9 (9.5) and 12 (12.4), respectively.*

Equilibrium stepwise reactions between AVN and a number of metal ions are also known [39,40,41], shown in Table 8.5:

Table 8.5 *Stability constants for the metal complexes (1:1, 1:2) of the ligand AVN.*

Complexation	*Al*	*Ca*	*Cu*	*Mg*	*Ni*	*Pb*	*Zn*	*Cd*	*Mn*
ML	18.4	6.6	21.8	8.6	15.9	12.5	13.5	11.47	10.96
ML 2	31.6	9.6	-	13.6	26.4	17.8	20.9	-	-

The excitation and emission fluorescence spectra of the ligand and Al(III)-AVN are shown in Figure 8.7. The excitation and emission signals of the Al(III)-AVN interaction increase substantially compared with those of the AVN alone, something which is explained by the fact that complexation of aluminum(III) with AVN restricts the rotational transitions of phenyl and naphthyl moieties. The observed difference between the excitation (a,a') and, mainly, the emission (b,b') spectra is a very important prerequisite support for the experimental application of this new analytical method. In order to avoid interferences the emission wavelength was optioned at 620 nm and throughout used, unless it is differently given for some experiments, while the excitation wavelength was selected at 520 nm.

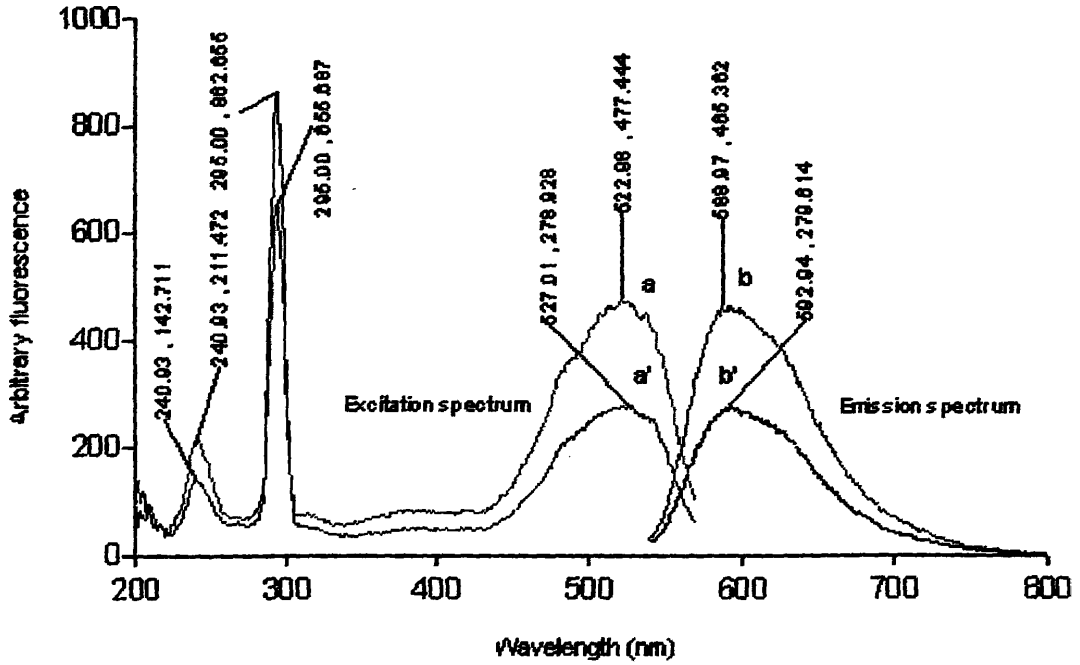

Figure 8.7. *Excitation and emission spectra of AVN in acetates buffer (pH=5.0), 1,10-phenantroline 5×10^{-5} M, $NH_2OH.HCl$ 0.015 M and AVN 1×10^{-5} M. (a,a') Excitation (λ_{em} 590*

nm); (b,b') Emission (λ_{ex} 520 nm); (a',b') No Al(III); (a,b) Al(III) 8×10^{-8} M. Instrumental parameters: high voltage, both excitation and emission slits were 10 nm.

Previous investigations on ligands of similar structures showed that the complexation of the metal ion occurs through the azo centre and the oxygen atoms in the ortho positions. [42]

However, the data of this thesis show that the o,o'-dihydroxy azo dye arrangement is an absolutely necessary presupposition to develop a fluorescence reaction for aluminum(III), or in other words the donor atoms for aluminum(III) are presumably the two oxygens of the ligand. It must also be noticed that this favourable interaction is probably the reason of the reaction kinetics (see paragraph of kinetics) qualifying the complexation of aluminum with reagents of the azo dye class.

For this purpose, a similar azo dye compound, the *acid red 8 (AR8),* which lacks one hydroxyl-group of the ligand (Figure 8.8), was tested in our laboratory to investigate if this compound gives a fluorescence reaction with aluminum(III).

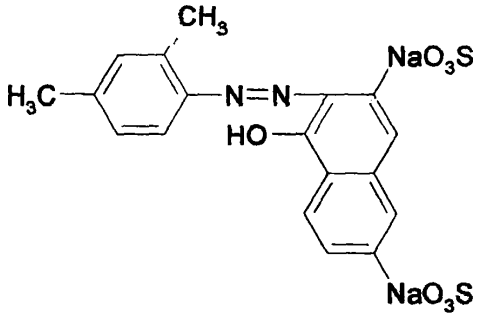

Figure 8.8. *Molecular structure of AR8*

The free compound was found to exhibit a maximum fluorescence at an emission of 606 nm (excitation at 504 nm) but its intensity was very low. Many solutions, of different pH values and after heating at 60°C for 30 min, containing various aluminum(III) and AR8 amounts, did not show a fluorescence reaction as shown in Figures 8.9. The behavior of this azo dye compound confirms that the presence of two hydroxyl groups in *ortho* position to the azo moiety is necessary for the complexation of aluminum(III), that is to say AVN is complexed to both oxygen atoms of the two hydroxyl groups at once and maybe it is also bound to nitrogen atom attached to the phenyl moiety, giving in this way a quite rigid complex with aluminum that is strongly fluorescent.

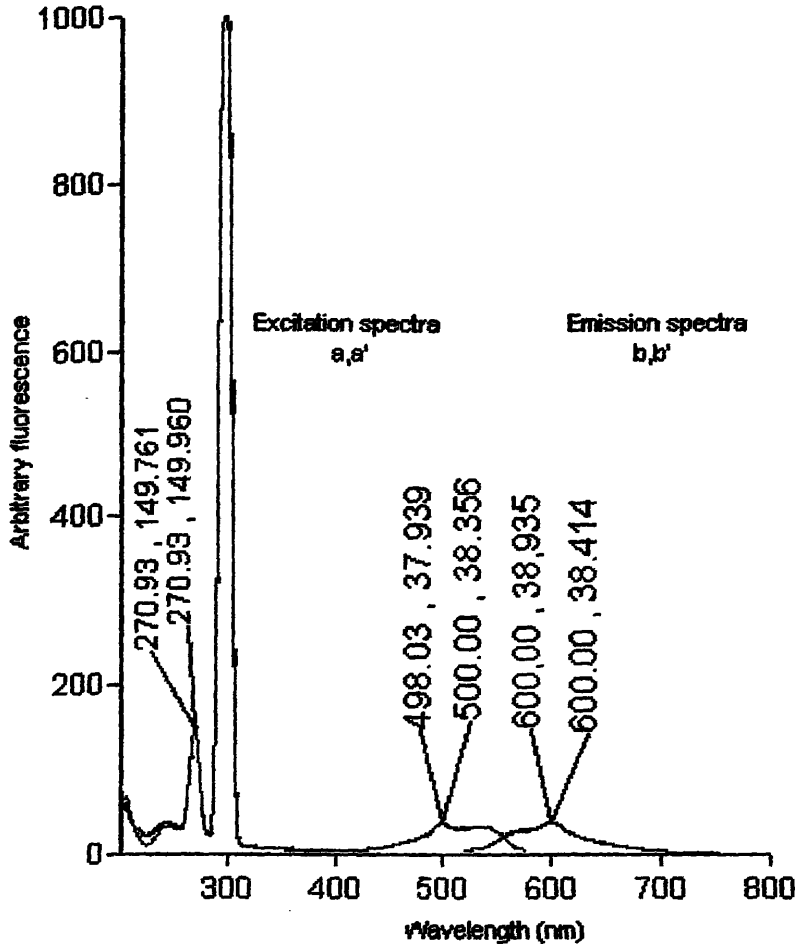

Figure 8.9 *Excitation and emission spectra of AR8 in acetates buffer (pH=5.0), AR8 1×10^{-5} M. (a,a') Excitation (λ_{em} 606 nm); (b,b') Emission (λ_{ex} 504 nm); (a',b') No Al(III); (a,b) Al(III) 1×10^{-5} M. Instrumental parameters: high voltage, both excitation and emission slits were 10 nm.*

The absorption spectra of AR8 and aluminum(III)-AR8 solutions, recorded at pH 5.0 and after heating for 30 min at 60°C, are shown in Figure 8.10. Maximum absorbance of the AR8 is observed at 508 nm, while addition of various aluminum(III) amounts does not change the absorbance spectrum of the free ligand. A small change is only observed at the near-UV region.

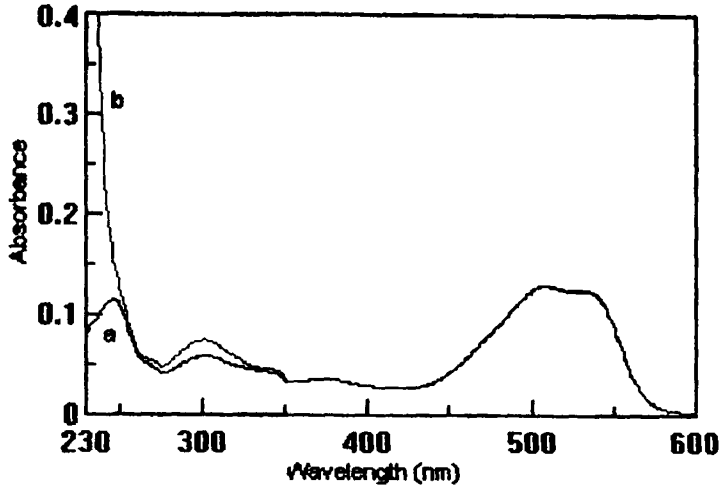

Figure 8.10. *Absorption spectra in acetates buffer (pH=5.0) and 1×10^{-5} M AR8 (a) no Al(III) and (b) 1×10^{-5} M Al(III).*

8.7 Determination of metals with AVN

Acid alizarin violet N, abbreviated *AVN, C.I. 15670 (4-Hydroxy-3-(2-hydroxynaphthylazo)- benzenesulphonic acid), known as well as eriochrome violet B, chrome fast violet B, solochrome violet RS, omega chrome dark violet D, pontachrome violet SW and palatinchromviolett,* is a weak diprotic acid with *pK* values equal to 7.0 and 12.80, respectively. AVN has been extensively used as a metal complexing agent for quantitative determination of different metal ions by various methods (Table 8.6).

The use of AVN for voltametric determination of aluminum has become well established since it was first reported by Willard and Dean in 1950 [9]. They found that in the presence of aluminum(III), the single polarographic reduction wave of AVN was split into two with the height of the wave at more negative potentials proportional to aluminum concentration. At pH 4.6 equilibrium of the aluminum-AVN solutions required over 4 h at room temperature and complex formation was most conveniently achieved by heating at 55-70°C for 5 min.

More recently, method based on cathodic stripping voltammetry of the Al-AVN complex at a hanging mercury drop electrode (HMDE) was reported by some authors [16,17,21,27,28,31,39].

A.c. oscillopolarography using AVN as complexing agent, was also employed in the determination of aluminum in natured water [18,19,20].

Johnson et al. reported determination of aluminum using AVN as a complexing agent, in pooled samples of cerebrospinal fluid by differential pulse polarography and also spectrophotometry [25].

Determination of iron by electrochemical stripping techniques has been performed using adsorption of organic ligand complex Fe-AVN on a mercury electrode followed by cathodic stripping [16,36,39].

The electrochemical detection of iron(III) coupled to ion interaction chromatography combines the high sensitivity of detection with the powerful selectivity capabilities of the separation system. This method enables the determination of iron(III) at 10^{-8} M levels [12]. Also, polarographic and coulometric determination of iron, have been reported [30].

It has also been showed that AVN can be employed in the determination of titanium(IV), by stripping voltametry [34,36], or by constant-current stripping voltammetry [23].

The levels of gallium can be, also, quantified by linear-sweep voltammetry after adsorptive preconcentration of the gallium/AVN chelate on the hanging mercury-drop electrode [33].

Also, low concentration of molybdenum, cadmium, vanadium [23], zirconium [35] and tin [38] can be determined following complexation with AVN, by adsorptive stripping voltammetry.

AVN has been employed, also, in the determination of gadolinium by cathode-ray polarography [29] and calcium by colorimetry [14].

For all these methods, limits of the metal detection were from 10^{-9} to 10^{-8} M.

Table 8.6 *Metal ions determination based on the formation of complexes with AVN*

Reagent	***Characteristics***	***Analytical method***	***Metal determined***	***Matrix sample***	***Ref.***
Acid alizarin violet N	Surfactants (CTAB, TX-100, SDS) pH=3.5; 7	-	-	-	[10]
Acid alizarin violet N	Surfactants (CTAB, TX-100, SDS)	-	-	-	[7]
Acid alizarin violet N	pH=5.5	Ion interaction chromatography coupled to electrochemical detection	Cu, Fe	Natural waters	[11]
Pontachrome violet SW	Substitution coordination for selective determination pH=5.5	Spectral correction technique	Cu	-	[12]
Pontachrome violet SW	Surfactant	colorimetry	Ca	Washing liquor	[13]
Pontachrome violet SW	Surfactant	-	Ca	-	[14]
Solohrome Violet RS	-	DPAdSV	Al, Fe	Dialysis fluids(peritoneal and hemodialysis fluids)	[15]
Solohrome Violet RS	Speciation, pH=5.2 and 8.5 10 min 70°C(or 50°C)	AdSV	Al	Natural waters	[16]
Solohrome Violet RS	Speciation, pH=5.2; 8.8	a.c. oscillopolarography	Al	Natural waters	[17]
Solohrome Violet RS	pH=8.8	a.c. oscillopolarography	Al	Real samples	[18]
Solohrome Violet RS	pH=5.2	a.c. oscillopolarography	Al	Real water samples	[19]
Solohrome Violet RS	-	Derivative adsorption chronopotentiometry	Al	Real water samples	[20]
Solohrome Violet RS	Surfactant (Triton X-100) pH=9.3, 30°C	Polarography	Y	Superconductor	[21]
Solohrome Violet RS	pH=4.5	Constant-current stripping potentiometry	Fe	Tap water and rain water samples	[22]
Solohrome Violet RS	pH=4.5	Constant-current stripping potentiometry	Ti, Fe	-	[23]
Solohrome Violet RS	pH=8.4	Differential pulse polarography	Al	Poole samples of cerebrospinal fluids	[24]
Solohrome Violet RS	-	Cathodic stripping voltametry	V, Mo, Cd	Sea and river waters	[25]

Solohrome Violet RS	pH=4.2	Adsorptive stripping voltametry	Al	Water, snow, medical aqueous preparations and lung tissue	[26]
Solohrome Violet RS	pH=8.8 (eliminate the heating and cooling step for reaction at pH=4.5)	Cathodic stripping voltammetry	Al	-	[27]
Solohrome Violet RS	pH=12.5; 15 min 70°C	Cathode-ray polarography	Gd	Medica cyclotron	[28]
Solohrome Violet RS	pH=4.7; 1 h 70°C	Polarography and coulometry	Fe	-	[29]
Solohrome Violet RS	pH=4.5; 10 min 90°C	Stripping voltammetry	Al	Snow samples	[30]
Solohrome Violet RS	pH=11	Adsorptive Stripping voltammetry	Y	-	[31]
Solohrome Violet RS	pH=4.8	Adsorptive Stripping voltammetry	Ga	Sea and rain waters	[32]
Solohrome Violet RS	pH=5.1	Stripping voltammetry	Ti	Sea, river and rain waters	[33]
Solohrome Violet RS	pH=4.6	Adsorptive Stripping voltammetry	Zr	Sea-water	[34]
Solohrome Violet RS	Speciation; pH=5.1	Adsorptive Stripping voltammetry	Fe, Ti, Ga	Natural waters	[35]
Solohrome Violet RS	pH=4.5	Constant-current stripping voltam.	Fe	Tap water	[36]
Solohrome Violet RS	-	Adsorptive Stripping voltammetry	Sn (IV)	-	[37]
Solochrome violet RS Palatine Chrome Black 6BN Chromazurol S Eriochrome Black T	Al; pH=4.5; 90°C Fe; pH=4.5; 90°C Al; pH=4.5; 50°C Fe; pH=7.0; 50°C Al; pH=7.0; 90°C Fe; pH=7.0; 50°C Al; pH=7.0; 30°C Fe; pH=7.0; 70°C	Adsorptive Stripping voltammetry	Al(III), Fe(II)	Dialysis fluids (peritoneal And Hemodialysis fluids)	[38]

8.8 Method fundamentals

8.8.1 PH optimization

The influence of the sample pH on the fluorescence of AVN and Al(III)-AVN system was investigated. The pH of sample is adjusted with hydrochloric acid for the acidic pH region and potassium hydroxide for the alkaline pH region. A first set of experiments was performed in order to study the behavior of AVN with pH, as follows:

Experiment: A set of nine polyethylene test-tubes was used. Into each tube 100 μL of 10^{-3} M AVN were placed. The pH into each polyethylene test-tube was adjusted using hydrochloric acid and potassium hydroxide solutions to cover a wide range from pH=1.1 to pH=12.4. The volume of each tube was made up to 5.0 mL with distilled water and was thoroughly mixed. The sample fluorescence intensities were recorded at the emission wavelength of 620 nm (excitation wavelength at 520 nm).

The fluorescence of the ligand was plotted against the sample pH, as shown in Figure 8.11. In the pH range from 1.4 to 6.0 a small fluctuation in fluorescence was observed. For pH values over than 6.0 the fluorescence intensity was insignificant. It is evident that the fluorescence is nearly related to the H_2In^- species of the ligand.

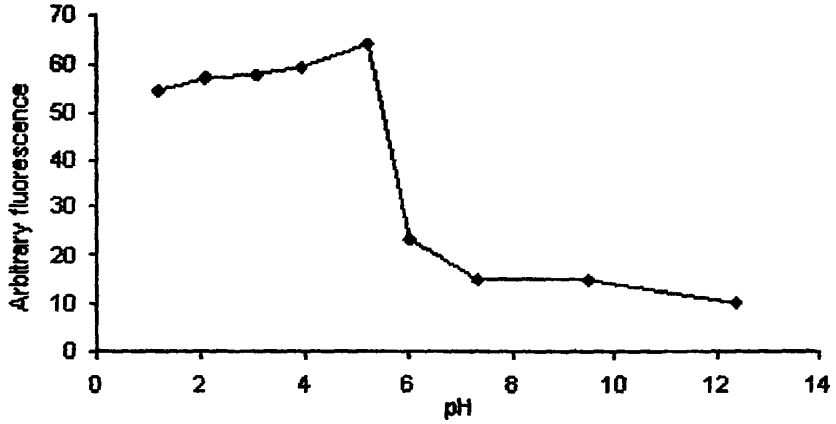

Figure 8.11. *Variation of fluorescence with pH. Concentration of AVN 2×10^{-5} M. Instrumental parameters: Excitation/Emission wavelength=520/620 nm, high voltage, both excitation and emission slits were 10 nm.*

According to the literature [43] the most stable AVN forms at pH value of 5.0 can be illustrated as follows:

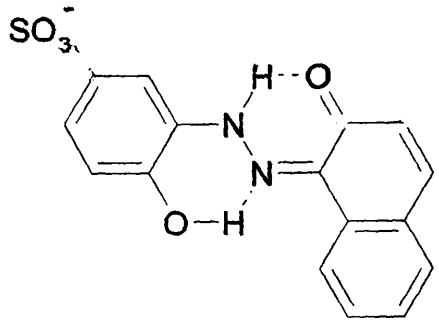

pH=5.0 (H_2In^-)

Figure 8.12.*The most stable AVN form at pH value of 5.0*

A second set of experiments was performed in order to evaluate the influence of pH on the fluorescence intensity of a known concentration of Al(III)-AVN complex in water. A set of tests was carried out by varying the pH using different concentrations of hydrochloric acid for the acidic pH region and potassium hydroxide for the alkaline pH region, covering the pH range from 2.4 to 10.0, as follows:

Experiment: A set of thirteen polyethylene test-tubes was used. Into each tube 100 μL of 10^{-3} M AVN and 50 μL of 10^{-4} M aluminum(III) were placed. The pH solution into each polyethylene test-tube was adjusted with hydrochloric acid and potassium hydroxide to cover a wide pH range from 2.4 to 10.0. The contents were well mixed, and then the volume of each tube was made up to 5 mL with distilled water and again was thoroughly mixed. The tubes were placed into a water bath, at 60°C, for 20 min, brought to room temperature and the sample fluorescence intensities were recorded at the emission wavelength of 620 nm (excitation wavelength at 520 nm).

The fluorescence intensity of the Al(III)-AVN system, depends dramatically on the pH of the solution, as shown in Figure 8.13. A pH between 4.0 and 5.0 allowed optimum formation of the Al(III)-AVN complex. Further increase or decrease in pH rapidly reduces the fluorescence intensity.

For pH values greater than 7.0, the reaction between the reactants is absent, owing to the fact that aluminum hydroxides are preferably formed. Conversely, for pH values lower than 2.0, the hydronium ions successfully compete with the hydrated aluminum ions and react with the coordinating groups of the ligand.

Based on the observed results, it is obvious that an acetates buffer solution of pH=5.0 provides adequate conditions for further analytical procedures.

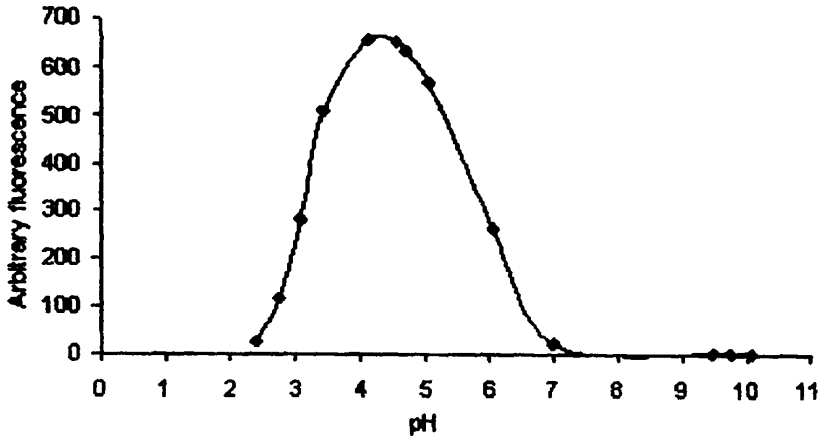

Figure 8.13 *Variation of fluorescence with pH. Concentrations: AVN 2×10^{-5} M and Al(III) 10^{-6} M. Instrumental parameters: Excitation/Emission wavelength= 540/590 nm, high voltage, both excitation and emission slits were 5 nm. (Shimadzu RF-5301 spectrophotometer)*

The optimal pH value obtained from our experiments is similar to that reported by Bergley and Barnard [44].

According to other works (Table 8.6), referred to aluminum(III) determination with AVN, two optimal regions useful for analysis exist around pH 5.0 and pH 8.0, respectively.

8.8.2 Kinetics and stability of the Al(III)-AVN complex

As for any given reaction, among other external factors, temperature also determines the rate at which this reaction takes place. Conducting a reaction at a higher temperature delivers more energy into the system and increases the reaction rate by causing more collisions between particles, as explained by collision theory. However the main reason why it increases the rate of the reaction is that more of the colliding particles will have the necessary activation energy resulting in more successful collisions-when bonds are formed between reactants.

Experiment: A set of five polyethylene test-tubes was used. Into each tube 0.5 mL of acetates buffer solution (pH=5.0), followed by 50 μL of 10^{-4} M AVN were placed. Further, a volume of 4.4 mL distilled water was added into each test-tube and the resulted mixtures were thoroughly stirred. Each test-tube was separately placed into a water bath and warmed at 40, 50, 60, 70 and 80°C, respectively, while the desired temperature was obtained. A volume of 50 μL of 10^{-4} M aluminum(III) was added, the content was well mixed, the temperature for

each test-tube was appropriately maintained constant and fluorescence measurements were made every 5 min at 620 nm (excitation at 520 nm).

It is again noticed that for equal concentrations of aluminum(III) and AVN the rate of their reaction was investigated for temperatures between 40 and 80°C in separate experiments.

Because AVN is a flexible molecule and may possess infinite number of configurations, this is probably the reason that the reaction proceeds slowly at low temperatures (room temperature or 40°C). From Figure 8.14, it is evident that an increase in temperature facilitates the complex formation. At 60°C, the fluorescence reaches the maximum after 45-50 min, and then tends to be stable at least 250 min. The lower fluorescence intensity at 60°C compared to that at 50°C, for any time where the reaction is completed or is near its completion, is assumed to be a consequence of the external conversion deactivation process of the excited molecules.

At 70 and 80°C, the fluorescence reached a maximum after 25 and 15 min, respectively, and then for a short time a small decrease was noticed after which the level of the fluorescence remained constant and lasted more than 4 hours.

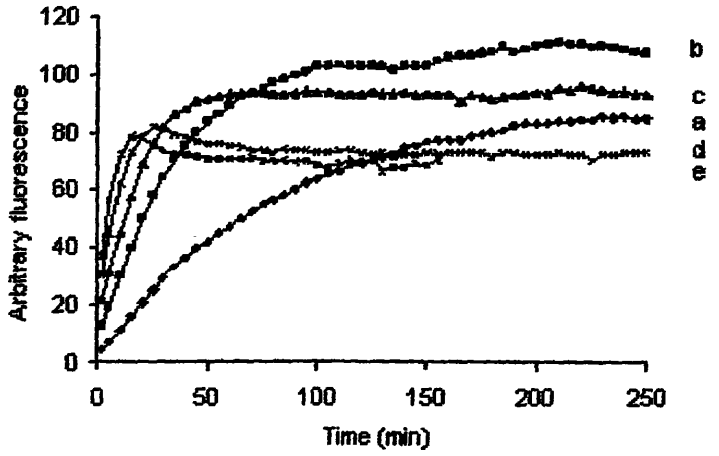

Figure 8.14. *Variation of fluorescence with time, for different temperatures ((a) 40, (b) 50, (c) 60, (d) 70 and (d) 80°C) in acetates buffer (pH=5.0), AVN 10^{-6} M and Al(III) 10^{-6} M. Instrumental parameters: Excitation/Emission wavelength=520/620 nm, high voltage, both excitation and emission slits were 5 nm.*

A ratio of aluminum(III):AVN equal to 1:20 was also investigated by measuring fluorescence intensity against time for temperatures between 23 and 60°C (Figure 8.15). At room temperature the rate is very slow and continues to be slow enough up to 50°C. The fluorescence, at 60°C, reaches the maximum after 20 min and then remains stable at least for 35-40 min.

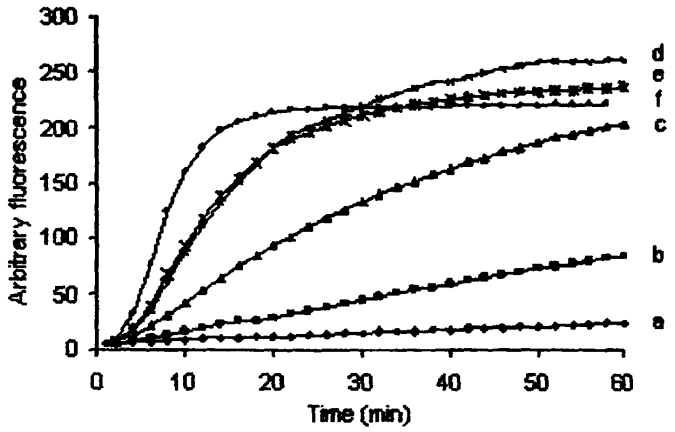

Figure 8.15. *Variation of fluorescence with time, for different temperatures ((a) 23, (b) 33, (c) 40, (d) 46, (e) 49 and (f) 60°C) in acetates buffer (pH=4.0), AVN 2×10^{-5} M and Al(III) 10^{-6} M. Instrumental parameters: Excitation/Emission wavelength= 518/570 nm, sensitivity factor F=10 (Perkin-Elmer LS 3 spectrophotometer).*

It is obvious that the AVN concentration substantially affects the rate of complexation and as a consequence, the time of the reaction completion. For this reason, at least a 10 times larger concentration of AVN in comparison to that of aluminum was decided for the experimental procedure.

The effect of the reaction time on the fluorescence of the Al(III)-AVN complex at different mole ratios (Al(III):AVN=1:10, 1:100, 1:1000) also was investigated, while the concentration of AVN was maintained constant. The next experiment was performed as an example.

Experiment: A set of three polyethylene test-tubes was used. Into each tube 0.5 mL of acetates buffer solution (pH=5.0), followed by 50 μL of 10^{-3} M AVN was placed. Then, volumes of 3950, 4400 and 4445 μL distilled water were added into the three test-tubes in turn and the contents were thoroughly stirred. The samples were placed into a water bath till the desired temperature of 60°C was achieved. Finally, volumes of 500, 50 and 5 μL of 10^{-5} M aluminum(III) were added into the test-tubes in turn, in order to obtain the following mole-

ratios: 1:10, 1:100, 1:1000 (Al(III):AVN). The temperature was maintained constant during the measurements. The fluorescence was measured every 5 min at 620 nm (excitation at 520 nm).

The experimental results (Figures 8.16 and 8.17a) show that the reaction is completed after 20 min. Then, the fluorescence tends to be stable for at least 30 min.

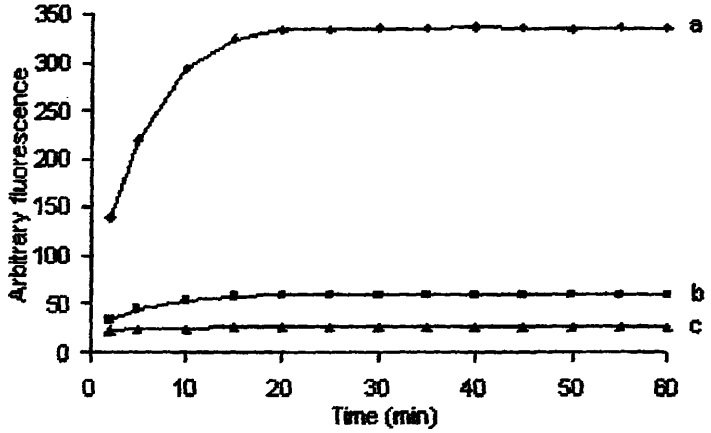

Figure 8.16 *Variation of fluorescence in acetates buffer of pH=5.0. (a) 10^{-6} M Al(III), 10^{-5} M AVN (1:10), (b) 10^{-7} M Al(III) , 10^{-5} M AVN (1:100) and (c) 10^{-8} M Al(III) , 10^{-5} M AVN (1:1000). Instrumental parameters: Excitation/Emission wavelength= 520/620 nm, high voltage, both excitation and emission slits were 5 nm.*

Henceforth, an experimental procedure was followed, where samples were heated for 30 min at 60°C, and then measurements were made at room temperature.

Stability of the complex Al(III):AVN 1:1000 was investigated by measuring to room temperature the fluorescence intensity against time, after heating the sample for 30 min at 60°C (Figure 8.17b). The fluorescence intensity significantly increases for a period of 20 min, till the room temperature was achieved, (at high temperature the rate of external conversion is high). It was found out that the system was stable for at least 80 min, after the system was cooling down to room temperature and changes in fluorescence were not more than 5 %.

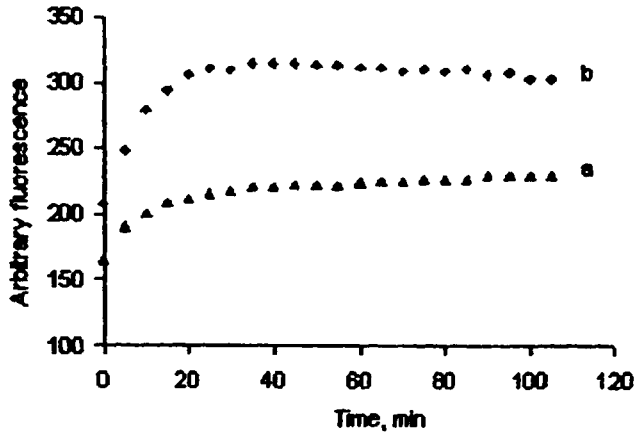

Figure 8.17 *Variation of fluorescence versus time in acetates buffer (pH=5.0), AVN 10^{-5} M and aluminum 10^{-8} M. (a) fluorescence versus time at 60°C and (b) fluorescence versus time after heating for 30 min at 60°C and cooling to room temperature. Instrumental parameters: Excitation/Emission wavelength= 520/620 nm, high voltage, both excitation and emission slits were 10 nm.*

8.8.3 Effect of AVN concentration

The effect of AVN concentration on complex formation was evaluated within the range 4×10^{-6} to 6×10^{-5} M. The experiments were performed for an aluminum(III) concentration of 10^{-6} M in acetates buffer of pH=5.0, as follows:

Experiment: Seven identical standard solutions of aluminum were directly prepared in a set of seven polyethylene test-tubes. Into each tube 0.5 mL of acetates buffer solution (pH=5.0), followed by 50 μL of 10^{-4} M aluminum(III) were placed. In each test-tube volumes of 15, 25, 50, 100, 150, 200 and 300 μL of the 10^{-3} M AVN solution were placed in turn. The contents were well mixed, and then the volume of each tube was made up to 5.0 mL with distilled water and again was thoroughly mixed. This procedure was steadily followed to avoid possible hydrolysis of aluminum. The tubes were placed into a water bath, at 60°C, for 20 min, brought to room temperature and finally the fluorescence was measured with a Perkin-Elmer LS 3 spectrophotometer at 570 nm (excitation at 518 nm).

It was observed that the fluorescence of the system containing 10^{-6} M aluminum(III) reaches a maximum when the concentration of AVN is 0.6-2×10^{-5} M; further increase in AVN concentration leads to a reduction in fluorescence (Figure 8.18).

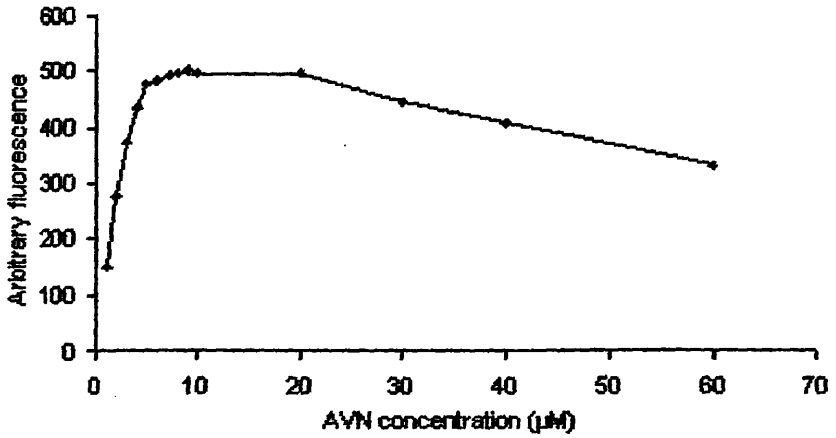

Figure 8.18 *Effect of concentration of AVN on the fluorescence of Al(III)-AVN in acetates buffer (pH=5.0) and Al(III) 10^{-6} M. Instrumental parameters: Excitation/Emission wavelength= 520/620 nm, high voltage, both excitation and emission slits were 5 nm.*

It is apparent that a ten-fold excess of AVN compared to that of aluminum is necessary to obtain a good sensitivity for the proposed method. Using higher concentrations of AVN, the fluorescence decreases because AVN and Al(III)-AVN absorb at the wavelength of emission or an inner filter effect is responsible for this. On the other hand, at smaller AVN concentration the complexation with aluminum is still far from its completion and as a consequence the sensitivity of the method would be inferior under these circumstances.

For further studies, a large enough excess of ligand was used, in order to improve the rate of the reaction, but a very large ligand excess was avoided, in order to secure the sensitivity of the method.

8.8.4 Stoichiometry between Al(III) and AVN

Equilibrium stepwise reactions between AVN and a number of metal ions are known [1,2]. For aluminum only two stepwise complexes have been addressed, although mole-ratio plots of fluorescence (Figures 8.19-24), show formation of more stepwise complexes. This conclusion is also evident from plots of fluorescence vs. time of reaction for various ratios of AVN to aluminum(III) (Figures 8.25-27).

Further studies on the interaction of aluminum(III) and AVN have been carried out for determining the stoichiometry of the plausible complexation by using mole-ratio method (Figures 8.19-24), as well as kinetics methods (Figures 8.25-27).

A study for developing the stoichiometry between aluminum(III) and AVN was fulfilled by the mole-ratio method. The principle underlying these experiments was based on keeping

the quantity of one reactant constant while varying the quantity of a second reactant. Therefore, two sets of experiments were prepared. In the first one, the concentration of AVN was maintained constant, while the concentration of the aluminum was varied (Figures 8.19-22). The second set of experiments was performed using a fixed concentration of aluminum(III) and a variable concentration of AVN (Figures 8.23-24).

In reality, the plots based on the mole ratio method are plots of fluorescence variation vs. the ratio of metal to ligand concentration. In our case the plots represent fluorescence variation vs. AVN concentration.

Experiment: An acetates buffer solution of pH=5.0 was prepared in a volumetric flask (according to the instructions of the *'Buffers for pH and metal ion control' D.D.Perrin, Boyd Dempsey*).

An AVN stock solution of 10^{-3} M was directly prepared in an acetates buffer solution of pH=5.0 and further a working stock AVN solution of 24×10^{-6} M was prepared in a volumetric flask of 250 mL by diluting 6 mL of the 10^{-3} M AVN solution with acetates buffer up to the volume.

An aluminum(III) stock solution 5×10^{-4} M was directly prepared in the working stock solution of 24×10^{-6} M AVN.

Appropriate volumes of aluminum(III) and AVN working solutions were placed into a set of 31 test-tubes as shown in Table 8.7. The contents were well mixed.

The tubes were placed into a water bath, at 60°C, for 30 min, brought to room temperature and finally the fluorescence was measured at 620 nm (excitation at 520 nm).

Table 8.7 *Al(III) and AVN working solutions to study their stoichiometry by the mole-ratio method in acetates buffer (pH=5.0). The concentration of AVN was 24×10^{-6} M, while that of Al(III) was between 0 and 15×10^{-6} M.*

No	*Aluminum 5×10^{-4}M in 24×10^{-6} M AVN solution*		*AVN 24×10^{-6}M in acetates buffer (pH=5.0)*
	μM	*μL*	*μL*
1	0	0	5000
2	0.5	5	4995
3	1	10	4990
4	1.5	15	4985
5	2	20	4980
6	2.5	25	4975
7	3	30	4970
8	3.5	35	4965
9	4	40	4960
10	4.5	45	4955
11	5	50	4950
12	5.5	55	4945
13	6	60	4940
14	6.5	65	4935
15	7	70	4930
16	7.5	75	4925
17	8	80	4920
18	8.5	85	4915
19	9	90	4910
20	9.5	95	4905
21	10	100	4900
22	10.5	105	4895
23	11	110	4890
24	11.5	115	4885
25	12	120	4880
26	12.5	125	4875
27	13	130	4870
28	13.5	135	4865
29	14	140	4860
30	14.5	145	4855
31	15	150	4850

The fluorescence response by combining incremental aluminum(III) concentrations (0-15×10^{-6} M) with a fixed concentration of AVN (24×10^{-6} M) was recorded. The straight-line portions are extrapolated to where they cross. At this point the ratio of metal to ligand determines the formula of a separate complex. From Figure 8.19 and Table 8.8 it is evident that metal to ligand complexes with ratios 1:2 and 1:3, exist.

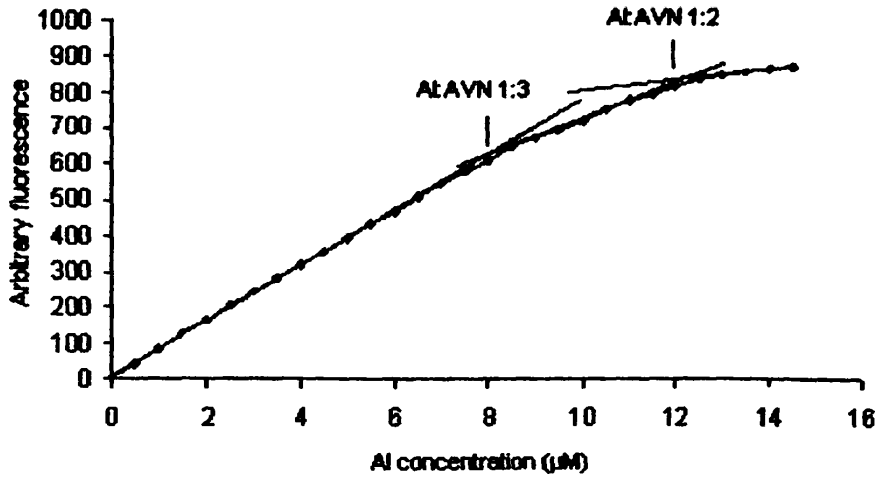

Figure 8.19 *Mole-ratio plots used to determine the stoichiometry of Al(III)-AVN complexation reaction in acetates buffer (pH=5.0) and AVN 24×10^{-6} M. Instrumental parameters: Excitation/Emission wavelength= 520/620 nm, high voltage, Slits: excitation 2.5 nm and emission 5 nm.*

Table 8.8. Linear ranges for Figure 8.19, from which different species can be detected in solution.

No	*Al(III) (μM)*	*Equation of the calibration curve*	*Correlation coefficient, r*
1	0-8	Y=76.44X+11.29	0.9995
2	8-12	Y=51.16X+214.43	0.9986
3	12-15	Y=19.49X+597.96	0.9989

Same conclusion also results from isosbestic points of the absorption spectra. The occurrence of an isosbestic point is often used as an indication (though not proof) of the presence of only two species, which are in equilibrium [45]. Figure 8.20 shows the absorption spectra of a constant concentration of AVN 24×10^{-6} M and different aluminum(III) concentrations from 0 to 15×10^{-6} M. This Figure macroscopically shows an ideal isosbestic point. However a zoom of the neighboring isosbestic point region shows two clear and different isosbestic points corresponding to Al-AVN complexes with ratios 1:2 and 1:3.

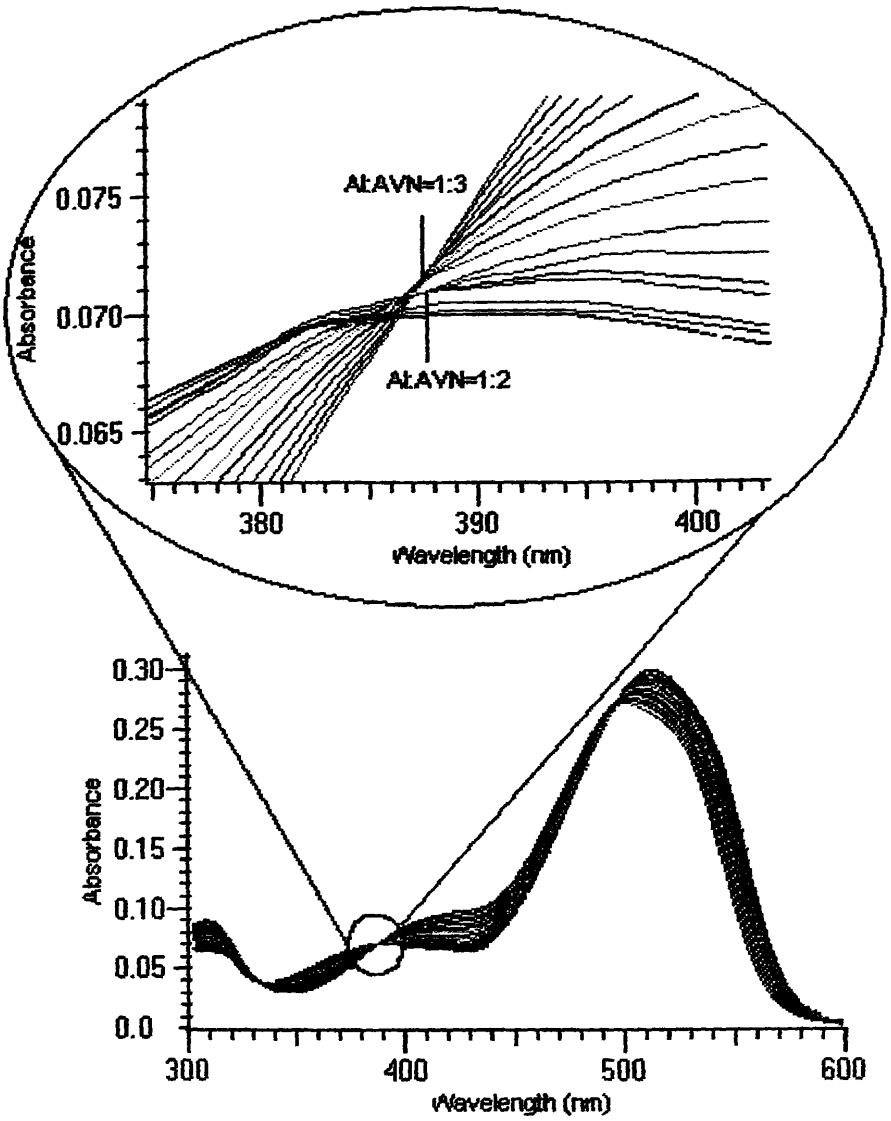

Figure 8.20 *Absorption spectra in acetates buffer (pH=5.0), 2.4×10^{-5}M AVN and Al(III) concentrations from 0 to 15×10^{-6}M.*

The existence of a complex Al:AVN 1:4 (Figure 8.21 and Table 8.9) was, also, proved. Therefore, an experiment was performed by adjusting a constant AVN concentration and varying that of aluminum(III).

Experiment: Aluminum(III) standard solutions were directly prepared in a set of 29 polyethylene test-tubes. Into each tube 0.5 mL of sodium acetate-acetic acid buffer solution (pH=5.0), followed by 100 μL of 10^{-3} M AVN were placed. Appropriate volumes of 10^{-3} M aluminum(III) standard solution were added into each of the test-tube. The contents were well mixed, then the volume of each tube was made up to 5.0 ml with distilled water and again were thoroughly mixed. This procedure was consistently followed to avoid possible hydrolysis of aluminum(III). The tubes were placed into a water bath, at 60°C, for 20 min,

brought to room temperature and finally the fluorescence was measured at 620 nm (excitation at 520 nm).

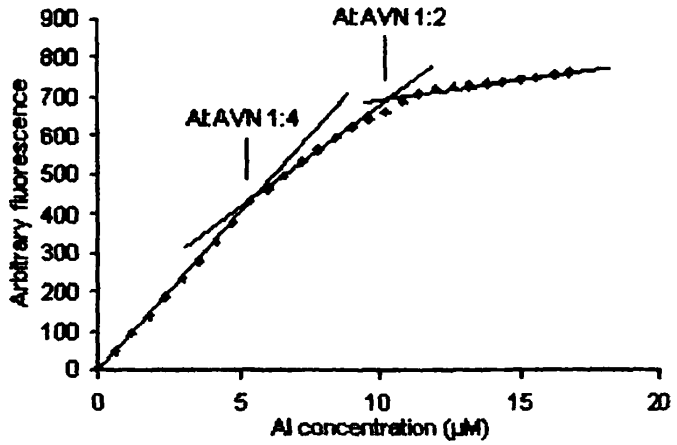

Figure 8.21 *Mole-ratio plots used to determine the stoichiometry of Al-AVN complexation reaction in acetates buffer (pH=5.0) and AVN 2×10^{-5} M. Instrumental parameters: Excitation/Emission wavelength= 520/620nm, high voltage, Slits: excitation 2.5 nm and emission 5 nm.*

Table 8.9 Linear ranges for Figure 8.21, from which different species can be detected in solution.

No	*Al(III) (μM)*	*Equation of the calibration curve*	*Correlation coefficient, r*
1	0-5	Y=77.261X+2.4659	0.9998
2	5-10	Y=53.883X+139.71	0.9985
3	10-16	Y=8.3783X+619.28	0.9985

The fluorescence response by adding incremental aluminum(III) concentrations (0-16.8×10^{-6} M) to a fixed concentration of AVN (20×10^{-6} M) was recorded. The mole ratio plots show the existence of Al-AVN complexes with ratios: 1:2 and 1:4.

The procedure followed bellow, to prove the existence of a complex Al-AVN 1:6 (Figure 8.22 and Table 8.10) was analogous to that already described in the above paragraph. The fluorescence response by adding incremental aluminum(III) concentration (0-7×10^{-6}M) to a fixed concentration of AVN (30×10^{-6} M) was recorded.

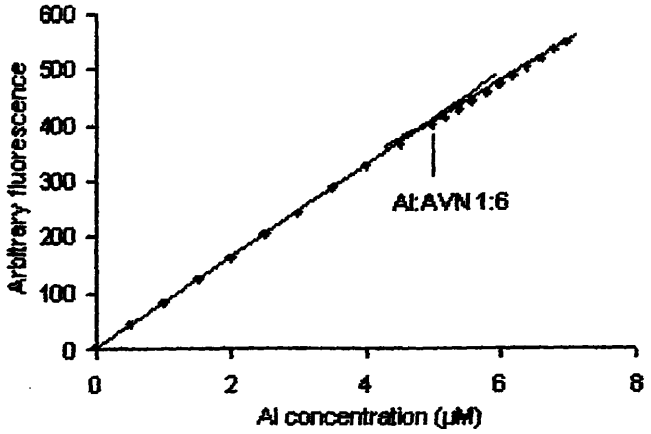

Figure 8.22 *Mole-ratio plots used to determine the stoichiometry of Al(III)-AVN complexation reaction in acetates buffer (pH=5.0) and AVN* 3×10^{-5} *M. Instrumental parameters: Excitation/Emission wavelength= 520/620 nm, high voltage, Slits: excitation 2.5 nm and emission 5 nm.*

Table 8.10 Linear ranges for Figure 8.22, from which different species can be detected in solution.

No	*Al(III) (μM)*	*Equation of the calibration curve*	*Correlation coefficient, r*
1	0-5	Y=80.192X+3.6215	0.9999
2	5-7	Y=75.646X+17.83	0.9997

Experiment: AVN standard solutions were directly prepared in a set of 34 polyethylene test-tubes. Into each tube was placed 0.5 mL of sodium acetate-acetic acid buffer solution (pH=5.0), followed by 30 μL of 10^{-3} M aluminum(III). Appropriate volumes of 10^{-3} M AVN standard solution were added in each of the test-tube. The contents were well mixed, then the volume of each tube was made up to 5.0 mL with distilled water and again were thoroughly mixed. This procedure was regularly followed to avoid possible hydrolysis of aluminum(III). The tubes were placed into a water bath, at 60°C, for 70 min, brought to room temperature and finally the fluorescence was measured at 620 nm (excitation at 520 nm).

The fluorescence response by combining incremental AVN concentrations ($0\text{-}20\times10^{-6}$ M) with a fixed aluminum(III) concentration (6×10^{-6} M) was recorded. Figure 8.23 and Table 8.11 prove the existence of Al-AVN complexes with ratios 1:1, 1:2 and 1:3.

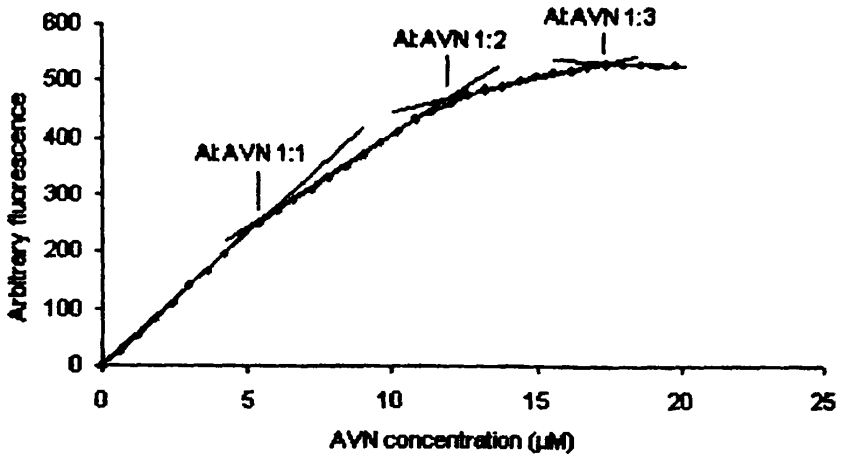

Figure 8.23 *Mole-ratio plots used to determine the stoichiometry of Al(III)-AVN complexation reaction in acetates buffer (pH=5.0) and Al(III) 6×10^{-6} M. Instrumental parameters: Excitation/Emission wavelength= 520/620 nm, high voltage, Slits: excitation 2.5 nm and emission 5 nm.*

Table 8.11 Linear ranges for Figure 8.23, from which different species can be detected in solution.

No	*AVN (μM)*	*Equation of the calibration curve*	*Correlation coefficient, r*
1	0-6	Y=42.857X-0.1214	0.9998
2	6-12	Y=32.37X+60.691	0.9998
3	12-18	Y=11.822X+309.06	0.996

The following procedure, to prove the existence of a complex Al-AVN 2:1 (Figure 8.24 and Table 8.12) was analogous to the one, already described. The fluorescence response by addition of incremental AVN concentrations (0-24×10^{-6} M) to a fixed concentration of aluminum(III) 24×10^{-6} M was recorded.

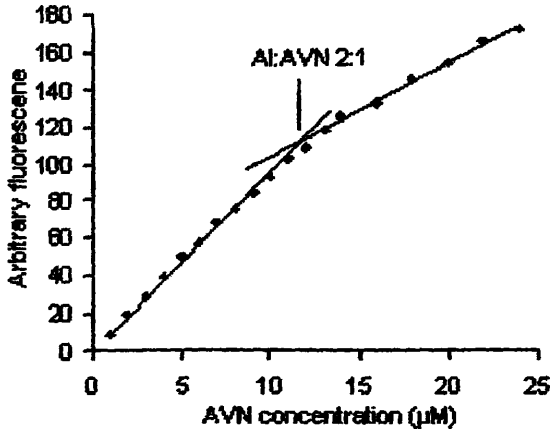

Figure 8.24 *Mole-ratio plots used to determine the stoichiometry of Al(III)-AVN complexation reaction in acetates buffer (pH=5.0) and Al(III) 24×10^{-6} M. Instrumental parameters: Excitation/Emission wavelength= 518/570 nm (Perkin-Elmer LS 3 spectrophotometer).*

Table 8.12 Linear ranges for Figure 8.24, from which different species can be detected in solution.

No	*AVN (μM)*	*Equation of the calibration curve*	*Correlation coefficient, r*
1	0-11	Y=9.2827x+1.1764	0.9992
2	13-24	Y=4.8788x+55.528	0.9978

The stoichiometry between aluminum(III) and AVN was, also, determined by the next procedure.

Experiment: A set of seven polyethylene test-tubes was used. Into each tube 0.5 mL of acetates buffer solution (pH=5.0), followed by 50 μL of 10^{-4} M aluminum(III) were placed. Then, in each test-tube volumes of 4450, 4400, 4350, 4300, 4250, 4200 and 4150 μL of distilled water were place in turn. The contents were well mixed, and then the samples were placed into a water bath till the desired temperature of 60°C was achieved and were well mixed. After that, in each test-tube volume of 0, 50, 100, 150, 200, 250, 300 μL of 1×10^{-4} M AVN were added in turn. The temperature was maintained constant at 60°C during the measurements. The fluorescence was measured every 5 min at 620 nm (excitation at 520 nm).

The stoichiometry between aluminum(III) and AVN was also examined by measuring fluorescence intensity vs. reaction time for various ratios of AVN to aluminum(III) at 60°C (Figures 8.25). Significant differences between the fluorescence of AVN and that of the

Al(III)-AVN mole ratios at any time where the reaction is completed, was assumed to be a consequence of existence of different Al(III):AVN complexes.

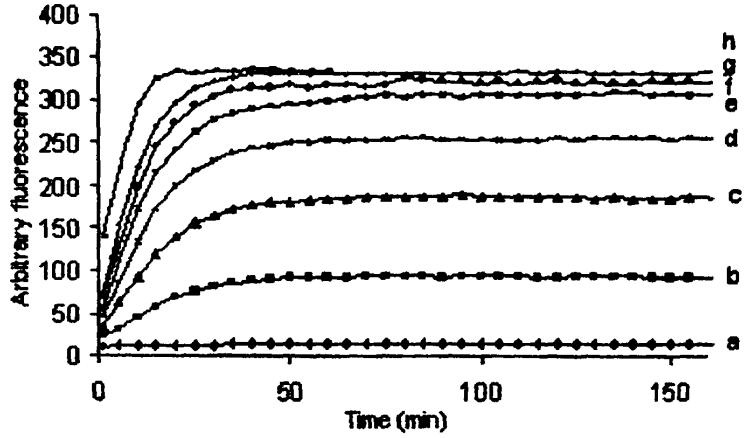

Figure 8.25 *Variation of fluorescence in acetates buffer (pH=5.0) of (a) AVN, (b) Al(AVN), (c) $Al(AVN)_2$, (d) $Al(AVN)_3$, (e) $Al(AVN)_4$, (f) $Al(AVN)_5$ (g) $Al(AVN)_6$ and (h) Al:AVN 1:10 at 60°C. Concentration: Aluminum 10^{-6} M, AVN 0, 1, 2, 3, 4, 5, 6 and 10×10^{-6} M, respectively. Instrumental parameters: Excitation/Emission wavelength= 520/620 nm, high voltage, both excitation and emission slits were 5 nm.*

This is also supported from the next experiment which shows variation of Al-AVN fluorescence versus AVN concentration for a constant concentration of aluminum (Figure 8.26). For a higher than 1:6 Al-AVN mole ratio the fluorescence intensity remains constant. This means that for lower than 1:6 Al-AVN mole ratios, formation of Al-AVN step-wise complexes takes place.

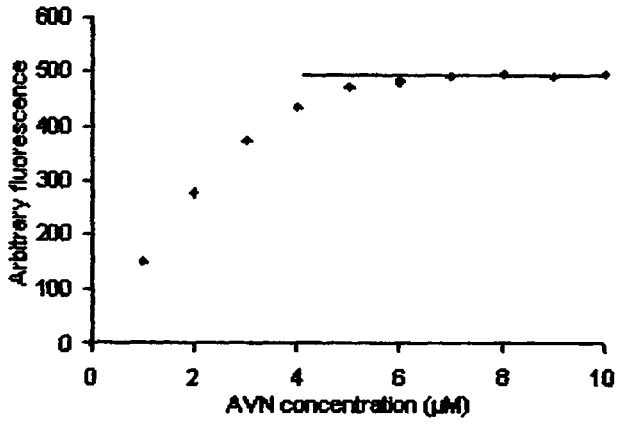

Figure 8.26 *Variation of fluorescence in acetates buffer (pH=5.0) after heating for 30 min at 60°C, Al(III) 10^{-6}M and AVN 0, 1, 2, 3, 4, 5, 6, 7, 8, 9 and 10×10^{-6}M. Instrumental parameters: Excitation/Emission wavelengths= 520/620 nm, high voltage, both excitation and emission slits were 5 nm.*

A part of the previous experiment was repeated at 40°C to emphasize that more than two complexes are possible between aluminum(III) and AVN. In this instance, criterion of existence of several Al(III)-AVN complexes was the time necessary to complete the reaction between these reagents.

According to the rate law the rate of a reaction increases as the concentration of one or more reactants becomes larger. Thus, as the AVN concentration increases, while the aluminum concentration is not varied, the time of the reaction completion would be decreased.

Figure 8.27 shows clearly, the effect of AVN concentration at constant concentration of aluminum(III) 1 μM in time of the reaction completion. The complex corresponding to concentration of 1 μM AVN is Al(AVN) (Figure 8.27a). As the concentration of AVN increases, Al(AVN) is converted to $Al(AVN)_2$, which is accompanied by an increase in the time of the reaction completion (Figure 8.27b). Furthermore, as the concentration of AVN increases, $Al(AVN)_2$ is converted to $Al(AVN)_3$ (Figure 8.27c), which is accompanied by an further increase in time of the reaction completion. This behavior can be explained if the gradual formation of compounds (stepwise complexation) of the type $Al(AVN)_x$ ($x>1$, $x\leq3$), is assumed to take place.

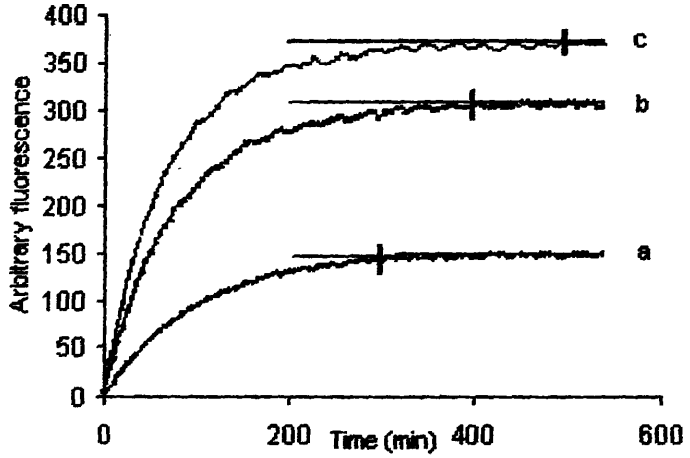

Figure 8.27 *Variation of fluorescence in acetates buffer (pH=5.0) of (a) Al(AVN), (b) $Al(AVN)_2$ and (c) $Al(AVN)_3$ at 40°C. Concentration: Al(III) 10^{-6} M, AVN 1, 2, and 3×10^{-6} M, respectively. Instrumental parameters: Excitation/Emission wavelength= 520/620 nm, high voltage, both excitation and emission slits were 5 nm.*

8.8.5 Effect of 1,10-phenanthroline concentration

The effect of 1,10-phenanthroline concentration within the range 10^{-6} to 10^{-4} M on the Al(III)-AVN complex was evaluated. The experiments were performed in an acetates buffer solution of pH=5.0 containing 4×10^{-7} M AVN, 5×10^{-8} M aluminum(III) and 0.015 M hydroxylamine hydrochloride. Under these conditions, the fluorescence intensity of Al(III)-AVN was found to be unchanged as shown in Figure 8.28. A final concentration of 5×10^{-5} M 1,10-phenanthroline was chosen for the experiments, unless it is differently given for some experiments.

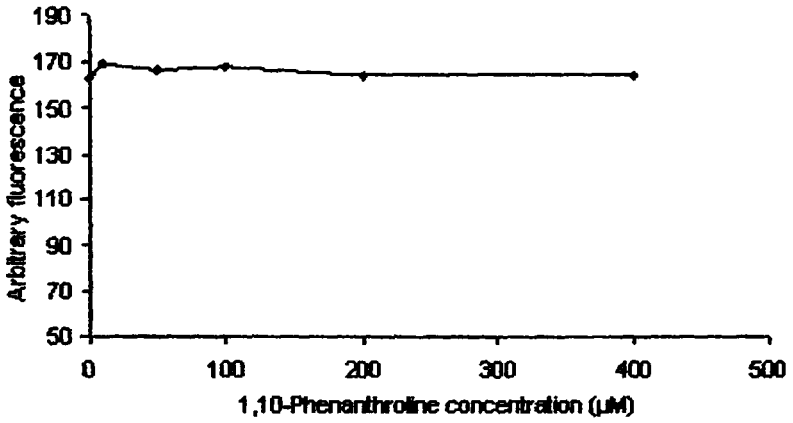

Figure 8.28. *Variation of fluorescence with concentration of 1,10-phenanthroline in acetates buffer (pH=5.0), 4×10^{-7} M AVN, 5×10^{-8} M Al(III) and 0.015 M $NH_2OH.HCl$. Instrumental parameters: Excitation/emission wavelength=540/620 nm, high voltage, both excitation and emission slits were 5 nm.*

8.8.6 Effect of HCl, HNO_3 and HCl:HNO_3(1:1) on the system stability

Initially, stock solutions (10^{-3} and 10^{-5} M) of aluminum(III) were prepared in water and stored in plastic bottles in a refrigerator at 4°C. Using for many days the same stock solution of aluminum(III), a systematic negative error of the method was noticed. Contrary, when the stock solution of aluminum(III) was freshly prepared, then errors were not seen anymore. So, it was assumed that the errors were originated from the fact that, aluminum forms insoluble $Al(OH)_3$ in distilled water, the pH of which is around 6.0, since it is known from the literature that between 5.2 and 8.8 $Al(OH)_3$ is the prevalent species of an aluminum salt.

For that reason, acid stock solutions of aluminium were further prepared and used.

Acids tested were hydrochloric acid (0.1 N), nitric acid (0.1 N) and a mixture of hydrochloric acid: nitric acid (1:1), as shown in Table 8.13. Calibration curves were

constructed for several concentration ranges of aluminium and the effect of the acids was examined. In the case of hydrochloric acid, the value of aluminum(III)-AVN fluorescence was observed, to be unsteady and a gradual decline of the slope of the working graph was noticed because of formation of possible Al-chloride complexes. Preparation of stock and working solutions of aluminum in nitric acid or hydrochloric acid: nitric acid (1:1) was proved to stabilize the fluorescence of aluminum(III)-AVN and was stable for at least 3 days. The calibration curve was reproducible for a period of 3 days, so it was not necessary to prepare fresh standards and working aluminum solutions within this period.

Table 8.13 *Effect of acids for Al(III) determination in acetates buffer (pH=5.0), 3×10^{-7} M AVN and 10^{-8}-10^{-7} M Al(III). Instrumental parameters: Excitation/Emission wavelength=520/620 nm, high voltage, Slits: excitation 10 nm and emission 20 nm.*

Acid, M	*Equation of the calibration curve*	*Correlation coefficient, r*	*Period, day*
HCl, 0.1M	Y=3202X+213.6	0.9917	0
	Y=2896.1X+194.8	0.9984	2
	Y=2689.6X+215.2	0.998	3
HNO_3, 0.1M	Y=2326.1X+258.9	0.9937	0
	Y=2352.2X+242.3	0.95	1
	Y=2354X+283.1	0.9955	3
0.1M HNO_3:0.1M HCl(1:1)	Y=2417.8X+212.9	0.9968	0
	Y=2491.3X+233.3	0.999	1
	Y=2321.5X+230.7	0.995	3

8.8.7 Performance characteristics

In common with all fluorescence methods, the sensitivity is largely determined by the choice of instrument and operating conditions, and the lowest determinable levels by reagent purity and handling conditions. In order to investigate the full potential of the system it becomes necessary to investigate in greater detail the source of the contamination and the instrumental performance. The sources of contamination from the blank values were eliminated by using analytical-reagent grade chemicals.

The experimental precision and sensitivity improvement were found to be dependent on the parameters of instrument, as photomultiplier and slit widths for excitation and emission (Tables 8.14 and 8.15). (Proper selection of bandwidths of excitation and emission monochromators as well as the photomultiplier voltage can lead to maximum signal.)

Table 8.14 *Effect of slit width combination on precision and detection of the method for 10^{-6} M AVN and Al(III) concentration from 10^{-8} M to 10^{-7} M, in an acetates buffer of pH=5.0, at room temperature. Instrumental parameter: Excitation/Emission wavelength=520/620 nm.*

No.	*Instrumental parameters*	*Equation of the calibration curve*	*Correlation coefficient, r*	*Standard deviation of blank*	*Relative Standard deviation*	***Limit of detection(M)*
1	^{1}H (20/5)	Y=768.8X+90.9	0.99844	0.272651	0.003	1.06×10^{-9}
2	H(10/10)	Y=1777.9X+210.4	0.99849	0.27289	0.0013	0.46×10^{-9}
3	^{2}M (20/5)	Y=56.5X+6.8	0.99819	0.023808	0.0035	1.26×10^{-9}
4	^{3}L (20/5)*	Y=4.9X+0.6	0.99779	0.007778	0.013	4.7×10^{-9}

^{1}H=high voltage, ^{2}M=medium voltage, ^{3}L=low voltage.

**Slits (excitation/emission) nm.*

*** Limit of detection calculated from the standard deviation of the blank.*

Stronger excitation conditions accompanied by higher quantum efficiencies, broader emission beams and larger voltages, ameliorate the sensitivity but calibration graph is limited because measurements go out of the instrument scale for higher aluminum concentrations.

Close investigation of the method performance reveals that better sensitivity involves lower relative standard deviations and lower detection limits, although they are susceptible to higher standard deviations. Deviation from this general conclusion is noticed for very low sensitivities where the magnitude of the signal begins to suffer from the instrument noise.

The average time of the lamp flash is related to the noise of the instrument and consequently has an effect on the limit of detection (Table 8.16). Estimating the pros and cons, 10-nm bandwidths for both excitation and emission monochromators, high voltage (gain) and 3 sec average time were finally selected.

Table 8.15 *Effect of slit width combination on precision of the method for 10^{-6} M AVN, 5×10^{-5} M 1,10-phenanthroline, 0.015 M $NH_2OH.HCl$ in an acetates buffer of pH=5.0, at room temperature. Instrumental parameter: Excitation/Emission wavelength=520/620 nm.*

	[1]H (1.5/20)*	H(2.5/20)	H(5/20)	H(10/20)	H(20/1.5)	H(20/2.5)	H(20/5)	H(20/10)
Stdev	0.055981	0.126337	0.264853	**0.670512**	0.01639	0.063997	0.273566	**0.701633**
RStdev	1.837	0.466	0.1911	**0.129**	1.014	0.469	0.345	**0.207**

	[2]M (1.5/20)	M(2.5/20)	M(5/20)	M(10/20)	M(20/1.5)	M(20/2.5)	M(20/5)	M(20/10)
Stdev	0.00643	0.015373	0.45519	**0.062662**	0.00506	0.008556	0.025219	**0.050018**
RStdev	2.575	0.767	0.443	**0.163**	3.76	0.83	0.423	**0.197**

	[3]L (1.5/20)	L(2.5/20)	L(5/20)	L(10/20)	L(20/1.5)	L(20/2.5)	L(20/5)	L(20/10)
Stdev	0.00478	0.008654	0.007349	**0.0074**	0.005322	0.004398	0.6222	**0.003528**
RStdev	11.17	12.78	3.177	**0.899**	29.4	11.19	15.83	**0.64**

	H(10/10)	M(10/10)	L(10/10)	H(5/5)	M(5/5)	L(5/5)	H(20/20)	M(20/20)	L(20/20)
Stdev	**0.443002**	0.0513	0.005122	**0.063676**	0.006408	0.011295	**0.365419**	0.258564	0.007777
RStdev	**0.243**	0.375	1.67	**0.393**	0.523	24.7	**0.0031**	0.266	0.378

[1]H=high voltage, [2]M=medium voltage, [3]L=low voltage.

** Slits (excitation/emission) nm.*

Table 8.16 *Effect of average time of the lamp flash on precision of the method for (1) 10^{-6} M and (2) 2×10^{-7} M AVN, 5×10^{-5} M 1,10-phenanthroline, 0.015 M $NH_2OH.HCl$ in an acetates buffer of pH=5.0, at room temperature. Instrumental parameter: Excitation/Emission wavelength=520/620 nm.*

1. Hight voltage Slits (excitation and emission) =10-20

Average time (seconds)	*1*	*2*	*3*	*4*	*5*
Stdev	4.581507	0.881831	**0.203689**	0.275698	0.244049
RStdev	0.09386	0.01843	**0.004255**	0.00563	0.00486

Hight voltage Slits (excitation and emission) =20-20

Average time (seconds)	*1*	*2*	*3*	*4*	*5*
Stdev	0.365419	0.424761	**0.345496**	0.45605	0.841474
RStdev	0.00313	0.00359	**0.002876**	0.003706	0.00664

2. Hight voltage Slits (excitation and emission) =10-20

Average time (seconds)	*1*	*2*	*3*	*4*	*5*
Stdev	0.288895	0.395664	**0.120656**	0.126846	0.091958
RStdev	0.0148	0.02035	**0.00619**	0.00646	0.00464

Hight voltage Slits (excitation and emission) =20-20

Average time (seconds)	*1*	*2*	*3*	*4*	*5*
Stdev	0.962018	0.309031	**0.189176**	0.126384	0.204262
RStdev	0.02015	0.00653	**0.003984**	0.002633	0.004204

8.9 Interferences

An interfering substance in analytical procedures is one that, at the given concentration, causes a systematic error in the analytical result. In the case of a quantitative determination this error has to be

a. greater than some arbitrarily-chosen percentage of the determinant concentration.

b. greater than a value given by the standard deviation of an unequivocally defined set of results obtained with the analytical procedure, multiplied by a numerical value which depends on the level of confidence desired (it is recommended to adopt a value of 3 for this numerical factor, which corresponds to a confidence level of 99.86% for a one-sided Gaussian distribution).

c. of any magnitude.[46]

A systematic study was performed in order to evaluate the effect of 16 inorganic species (cations and anions) in the determination of aluminum(III). For the study, aluminum(III) and AVN concentrations were fixed at 10^{-7} M and 10^{-6} M respectively, while different concentrations of cations or anions were tested. Cations were added as chloride, nitrate and sulfate salts and anions as sodium salts. When the signal between the analyte standard and the sample (containing the analyte in the presence of the interferent) was larger than ±5 %, the foreign ion was considered to be interfering with the determination of aluminum(III).

Experiment: Aluminum standard and sample solutions were directly prepared in a set of polyethylene test-tubes. Into each tube 0.5 mL of acetates buffer solution (pH=5.0), 50 μL of 10^{-4} M AVN, followed by 50 μL 10^{-5} M aluminum(III) were placed. Various working solutions (10^{-3} to 10^{-5} M) of foreign ions were used to study their interferences; each time an appropriate volume from one solution was transferred into a test-tube of the set. The contents were well mixed, then the volume of each tube was made up to 5.0 mL with distilled water and again were thoroughly mixed. The tubes were placed into a water bath, at 60°C, for 20 min, brought to room temperature and finally the fluorescence was measured at 620 nm (excitation at 520 nm).

The most critical interferences were found with iron(III), copper(II) and F^- (Table 8.17), but in the presence of masking agents, the interference effect of these ions was weakened to a considerable degree (Table 8.18).

Excess of chromium(III), nickel(II), strontium(II) and zinc(II) ions showed small modification on the aluminum(III)-AVN fluorescence intensity.

The obtained results indicated that the ions cobalt(II), manganese(II), barium(II), lead(II), cadmium(II), magnesium(II), calcium(II) beryllium(II) and PO_4^{3-} did not cause detectable changes in the fluorescence signal of the aluminum(III)-AVN system.

Table 8.17. *Errors in recovery of aluminum from 10^{-7}M solutions in acetates buffer (pH=5.0) and 10^{-6} M AVN in the presence of various concentration of 15 foreign ions. Instrumental parameters: Excitation/Emission wavelength =520/620 nm, high voltage, both excitation and emission slits were 10 nm.*

	Percentage of interference								
M:Al	**Sr(IV)**	**Be(II)***	**Fe(III)**	**Cu(II)**	**Zn(II)**	**F⁻**	**Cd(II)**	**Mg(II)****	**Ca(II)****
1	-3.32	-	-9.96	-57.27	+0.66	-4.98	+0.5	-0.66	+1.33
5	-2.3	-	-21.6	-100	-3.48	-9.96	-0.17	-2.4	-4.65
10	-4.98	-	-31.2	-100	-5.81	-17.9	+0.33	+0.33	-0.66
20	-7.3	-	-45	-100	-7.64	-33.2	+0.33	+2.16	+0.33
50	-9.13	-	-68.6	-100	-8.3	-58.7	-2.33	-2.16	-1.16
100	-9.8	-4.1	-87	-100	-8.8	-87.65	-3.32	-1.83	-4.8

	Percentage of interference					
M:Al	**Cr(III)**	**Ni(II)**	**Mn(II)**	**Ba(II)**	**Pb(II)**	**Co(II)**
0.1	-0.83	-3.15	+2.32	-4.98	-4	+3.32
0.5	+0.5	+1.16	+2.82	-3.5	-2.16	-3.65
1	-0.66	-4.15	+0.5	-4.15	-3.82	-3.65
2	-6.1	-5.98	+1.5	-3.5	-2	+0.5
5	-11.6	-8.47	+1.16	-3.82	-1.83	+2.66
10	-27.9	-15.94	+0.5	-5.6	-1.33	+2.16

* *M: Al: ten times higher than the ratios reported in the first column*

** *M: Al: one hundred times higher than the ratios reported in the first column*

Table 8.18. *Errors in recovery of alumiium from 10^{-7} M solutions in acetates buffer (pH=5.0), 10^{-6} M AVN 0.015 M $NH_2OH.HCl$, 5×10^{-5} M 1,10-phenanthroline and 10^{-4} M beryllium(II) in the presence of various concentration of 15 foreign ions. Instrumental parameters: Excitation/Emission wavelength =520/620 nm, high voltage, both excitation and emission slits were 10 nm.*

	Percentage of interference								
M:Al	**Sr(IV)**	**Be(II)***	**Fe(III)**	**Cu(II)**	**Zn(II)**	**F⁻**	**Cd(II)**	**Mg(II)****	**Ca(II)****
1	-2.82	-	-2.15	-2.66	+0.83	-0.66	-0.5	-1	-4.48
5	-1	-	+0.83	-6.8	+0.66	+2.82	-1.16	+2.82	-2
10	+1.66	-	+0.17	-15.6	+0.17	+1.16	-1.66	+0.33	-2.66
20	-0.17	-	-3.32	-29.05	+0.83	-4.6	-1.5	-0.33	-2.82
50	+3.8	-	-10.9	-62.7	-0.17	-14.94	-0.5	0	-4.3
100	+2	-4.1	-28.22	-100	+0.66	-30.21	-2.5	0	-4.8

	Percentage of interference					
M:Al	**Cr(III)**	**Ni(II)**	**Mn(II)**	**Ba(II)**	**Pb(II)**	**Co(II)**
0.1	-2.16	-0.33	-0.33	-0.33	+1.16	-1.5
0.5	0	+1.66	+1.66	+3.65	+0.66	+3.65
1	-3.8	-2.49	-0.5	+1.66	-0.5	-0.66
2	-5.81	+1.16	-0.5	+3.32	+1.82	+0.66
5	-16.1	-0.5	+2	+3.82	+1.5	+0.33
10	-31.4	0	-0.5	+3.15	+1.33	-4.3

* *M: Al: ten times higher than the ratios reported in the first column*

** *M: Al: one hundred times higher than the ratios reported in the first column*

8.9.1 Iron interference. Iron is known to interfere with the direct fluorimetric analysis of aluminum(III) in aqueous samples. In such an interference study three approaches deserve closer consideration:

a. Spectral interference is one source of errors. Several metal-AVN complexes absorb a part of the fluorescence (emission) light at the wavelength of measurement (620 nm) bringing about significant negative errors, as illustrated for iron(III) in Figure 8.29 and iron (II) in Figure 8.30.

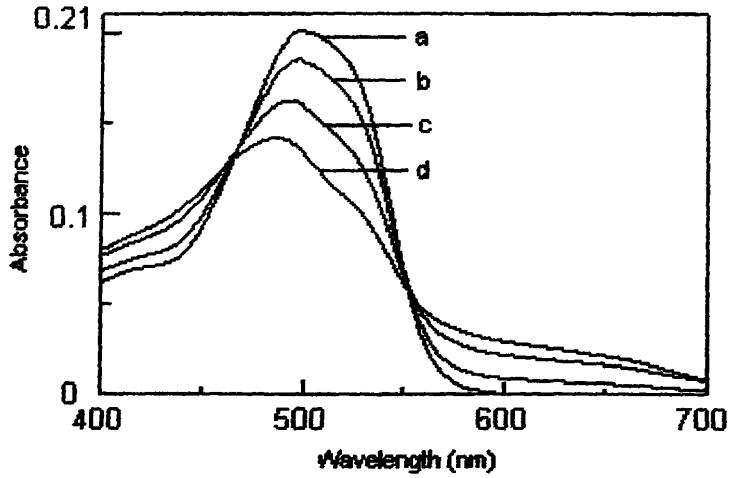

Figure 8.29. *Absorption spectra in acetates buffer (pH=5.0) and 2×10^{-5} M AVN. (a) No Fe(III); (b) Fe(III) 10^{-6} M; (c) Fe(III) 2×10^{-6} M and (d) Fe(III) 3×10^{-6} M.*

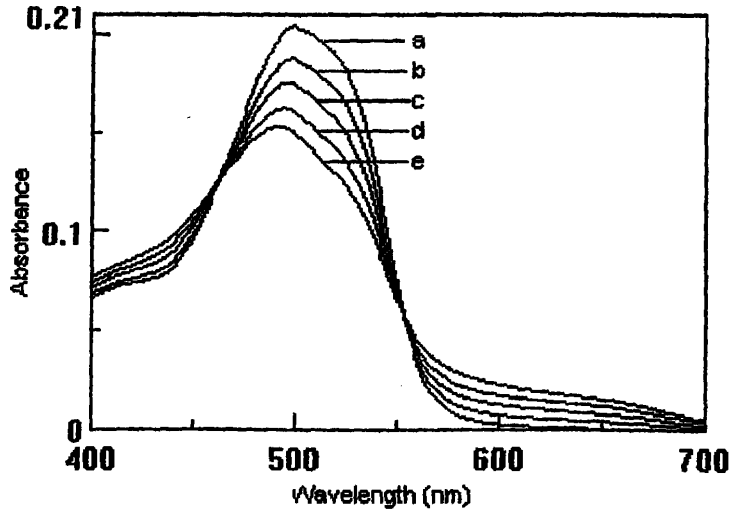

Figure 8.30. *Absorption spectra in acetates buffer (pH=5.0), 2×10^{-5} M AVN and $NH_2OH.HCl$ 0.015 M. (a) No Fe(III); (b) Fe(III) 10^{-6} M; (c) Fe (III) 2×10^{-6} M; (d) Fe(III) 3×10^{-6} M and (e) Fe(III) 4×10^{-6} M.*

Figure 8.29 and 8.30 show visible spectra of Fe(III)-AVN and Fe(II)-AVN systems in an acetates buffer solution of pH=5.0, where both absorbance maxima are observed at 499 nm , while the two isosbestic points of both iron(II) and iron(III) are observed at 468 and 554 nm. Addition of various concentrations of iron(III) and iron(II) causes a gradual slight hypsochromic shift of the 499 nm band to lower wavelength.

Fe(III)-AVN and Fe(II)-AVN (Figure 8.29 and 8.30) demonstrate a higher absorption than AVN alone at an emission wavelength of 620 nm, which dramatically reduces the photon flux of radiation at emission.

1,10-Phenanthroline is favorably known as reagent for iron(II) and other divalent cations (Table 8.19). The orange-red (maximum absorption at about 508 nm) 1,10-phenanthroline complex, $(C_{12}H_8N_2)_3Fe^{2+}$, can be formed quantitatively in the pH range 2.0-9.0.[47]

Equilibrium stepwise reactions between 1,10-phenanthroline and a number of metal ions are known and they are shown in Table 8.19:

Table 8.19. *Stability constants for some metal complexes (1:1, 1:2, 1:3) with 1,10-phenanthroline.* [48,49]

Complexation	***Ni(II)***	***Fe(II)***	***Fe(III)***	***Cu(II)***	***Cu(I)***	***Zn(II)***
ML	8.6	5.85	6.5	8.8	8.8	6.4
ML_2	16.7	11.15	11.4	15.3	15.3	12.2
ML_3	24.3	21.0	14.1	20.2	-	17.1

Complexation	***Hg(II)***	***Mn(II)***	***Co(II)***	***Sn(II)***	***Cd(II)***
ML	-	4.0	7.08	3.88	5.8
ML_2	19.65	7.3	13.72	-	10.6
ML_3	23.35	10.3	19.8	-	14.6

Thus, 1,10-phenanthroline was initially decided to serve as masking for iron and other foreign metals of the reference sample. However, errors continued to exist, since iron(III) prefers to coordinate AVN than 1,10-phenanthroline (Figure 8.31).

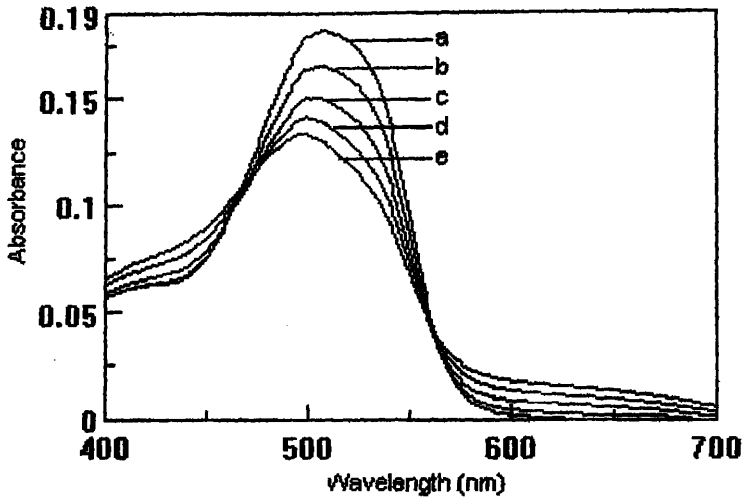

Figure 8.31. *Absorption spectra in acetates buffer (pH=5.0), 2×10^{-5} M AVN and 5×10^{-3} M 1,10-phenanthroline. (a) No Fe(III); (b) Fe(III) 10^{-6} M; (c) Fe(III) 2×10^{-6} M; (d) Fe(III) 3×10^{-6} M and (e) Fe(III) 4×10^{-6} M.*

The opposite goes for iron(II) and other divalent ions that are acceptably masked by 1,10- phenanthroline as shown in Figure 8.32 for iron(II) and tabulated in Table 8.19 for many other metal ions.

Addition of 1,10-phenanthroline in the system Fe(II)-AVN is accompanied by disappearance of the isosbestic points at 468 and 551.5 nm and the spectrum shows no absorption at the emission range over than 600 nm (Figures 8.32). It is evident that iron(II) prefers to coordinate 1,10- phenanthroline than AVN. Thus, errors due to spectral interferences are not more seen.

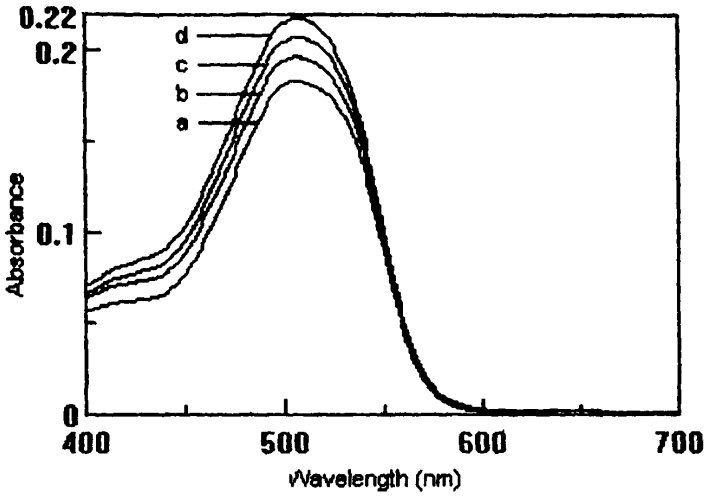

Figure 8.32. *Absorption spectra in acetates buffer (pH=5.0), 2×10^{-5}M AVN, 5×10^{-3} M 1,10-phenanthroline and 0.015 M $NH_2OH.HCl$ (in order to reduce Fe(III) to Fe(II)). (a) No Fe(III); (b) Fe(III) 10^{-6} M; (c) Fe(III) 2×10^{-6} M; and (d) Fe(III) 3×10^{-6} M.*

Thus, except 1,10-phenanthroline, hydroxylammonium chloride was also optioned as an essential agent to reduce some present trivalent ions in the sample and especially iron(III) to iron(II). As shown in Table 8.18, with a concentration of 5×10^{-5} M 1,10-phenanthroline and 0.015 M hydroxylammonium chloride, determination of aluminum(III) at a limiting concentration of 10^{-7} M, in acetates buffer (pH=5.0) and 10^{-6} M AVN, is successful and without errors even if iron(III) concentration is up to 2×10^{-6} M.

b. When AVN is not sufficient to obtain its maximum coordination to all metal ions of a sample (Al(III):AVN=1:3), then large negative errors result for aluminum in the presence of metal ions with stability constants greater than that of aluminum. In this particular case, even if weak complexes between AVN and some metal ions are formed, considerable errors for aluminum are again expected. This effect is shown in Figure 8.33 also for other ions.

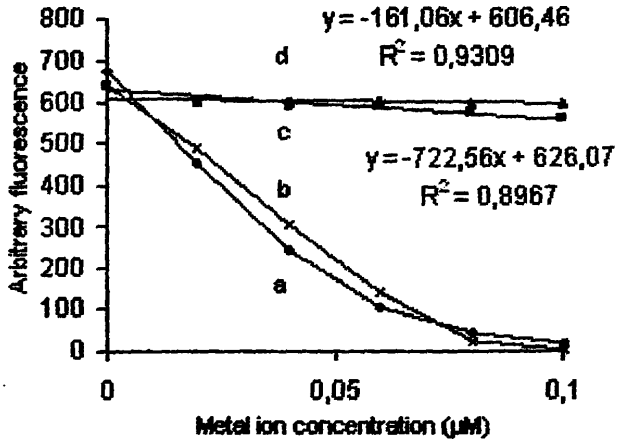

Figure 8.33 *Variation of fluorescence in acetates buffer (pH=5.0), AVN 1.8×10⁻⁶ M and Al(III) 6×10⁻⁶ M (a) Fe(III); (b) Cu(II); (c) Fe(III), and $NH_2OH.HCl$ 0.015 M and (d) Co(II). Instrumental parameters: Excitation/Emission wavelength =520/620 nm, high voltage, Slits: excitation 5 nm and emission 10 nm.*

For instance, the effect of iron(II) and iron(III) is also shown in Figure 8.33. Even, if small concentrations of iron(III) and iron(II) are added in a solution, a distribution of these metals and their species with AVN was observed. As a consequence iron(II) introduce, only, small errors for aluminum determination, while iron(III), having a stronger chemical affinity with AVN, gives very large errors.

c. If AVN is adequate to satisfy full complexation of each foreign metal ion, errors of those described above are absent, because no competition of the ions for the ligand exists and no replacement of aluminum occurs by ions giving more stable complexes. Despite this favourable behaviour, relatively small negative errors again appear due to fluorescence quenching of the coordinated AVN (which is a weakly fluorescent molecule) to foreign metal ions. By the way, Figure 8.34 shows the variation of fluorescence in the presence of iron(III).

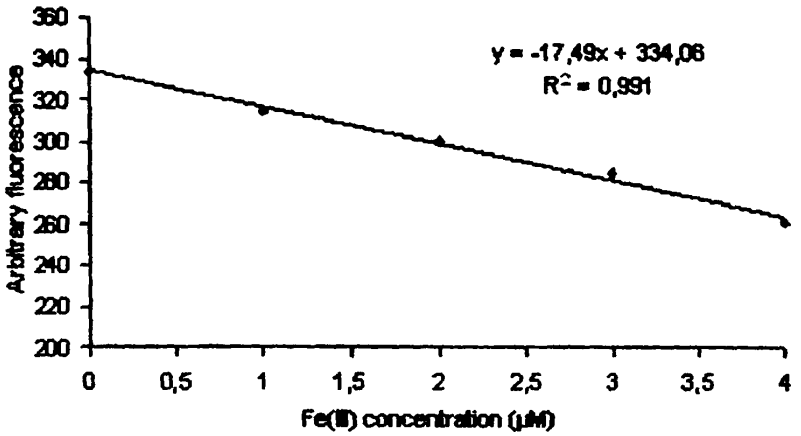

Figure 8.34. *Variation of fluorescence with concentration of Fe(III) in acetates buffer (pH=5.0) and 2×10^{-5} M AVN. Instrumental parameters: Excitation/Emission wavelength=520/620 nm, high voltage, both excitation and emission slits were 10 nm.*

Although an excess of AVN was decided to be used in this work, negative errors originating from absorption or quenching (first and third approach, respectively) would result if a convenient masking agent had not been utilized. Thus, 1,10- phenanthroline and hydroxylamine hydrochloride was decided to serve as masking system for iron and other foreign metals of the reference sample. Figure 8.35 shows the effect of iron(III) on the fluorometric determination of aluminum(III). It is clear that iron(III) in the presence of 1,10-phenanthroline and hydroxylamine hydrochloride does not essentially interfere. In contrast, iron(III) without hydroxylamine hydrochloride and 1,10- phenanthroline adds large errors in aluminum(III) determination.

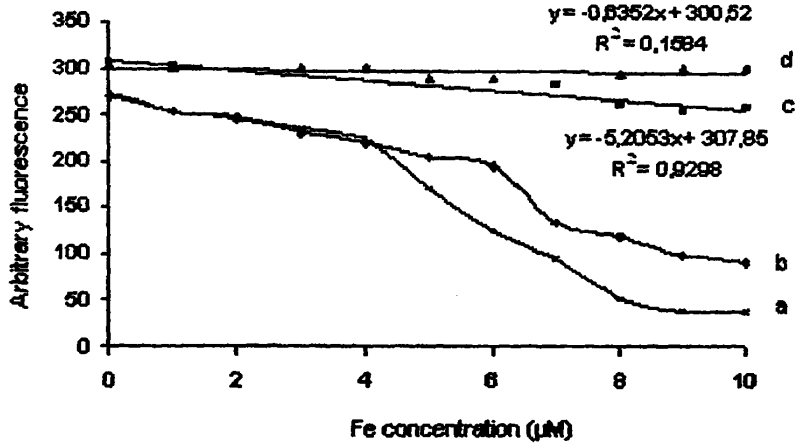

Figure 8.35. *Variation of fluorescence with Fe(III) in acetates buffer (pH=5.0) and AVN 2×10^{-5} M. (a) Fe(III) alone; (b) Fe(III) and 1,10-Phenanthroline 5×10^{-5} M ; (c) Fe(III) and*

$NH_2OH.HCl$ 0.015 M (d) Fe(III) , 1,10-Phenanthroline 5×10^{-5} M and $NH_2OH.HCl$ 0.015 M. Instrumental parameters: Excitation/Emission wavelength =520/620nm, high voltage, both excitation and emission slits were 10 nm.

8.9.2 Copper interference. The results shown in Table 8.17, also, indicate strong interference in the presence of copper(II).

a. Figure 8.36 shows visible spectra of Cu(II)-AVN system in an acetates buffer solution of pH=5.0. Absorbance maximum is observed at 499 nm. An isosbestic point is located at 502 nm. Addition of various copper(II) concentrations causes a gradual slight bathochromic shift to 512 nm. Cu(II)-AVN complex absorbs light at the wavelength of measurement (620 nm); while by adding masking system (1,10-phenanthroline and hydroxylamine hydrochloride), errors due to spectral interferences are not seen anymore.

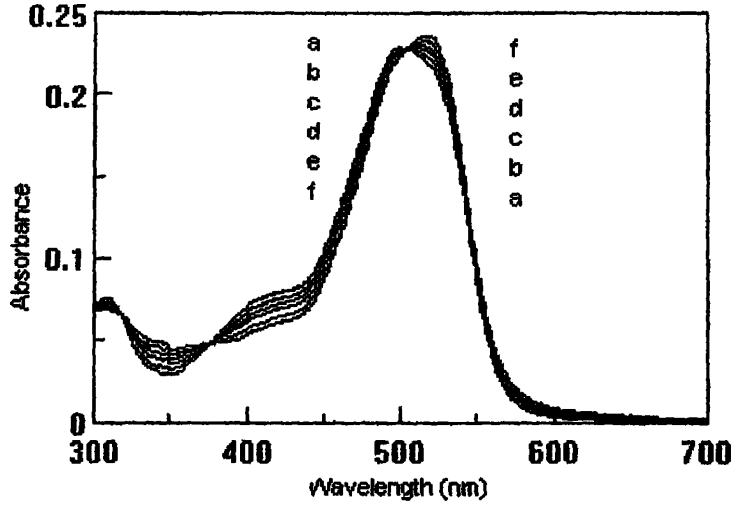

Figure 8.36 *Absorption spectra in acetates buffer (pH=5.0) and 2.4×10^{-5} M AVN. (a) No Cu(II); (b) Cu(II) 10^{-6} M; (c) Cu(II) 2×10^{-6} M (d) Cu(II) 3×10^{-6} M (e) Cu(II) 4×10^{-6} M and (f) Cu(II) 5×10^{-6} M.*

Addition of hydroxylamine hydrochloride and 1,10-phenanthroline in the system of Cu(II)-AVN is accompanied by disappearance of the isobestic point at 502 nm and entire coincidence of the AVN and Cu(II)-AVN spectra (Figure 8.37).

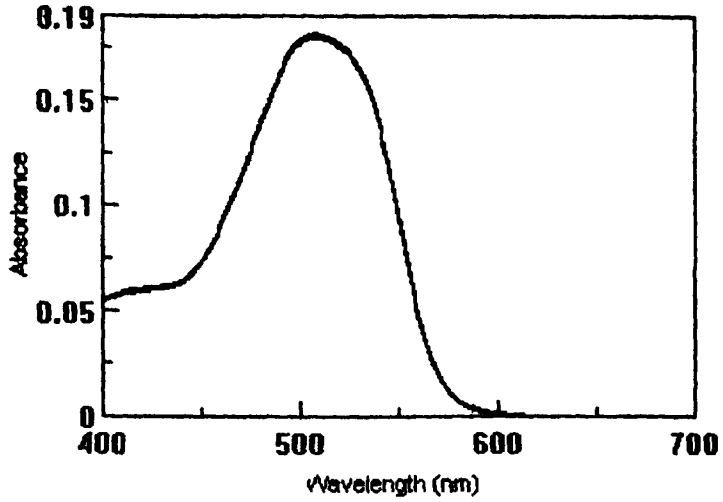

Figure 8.37 *Absorption spectra in acetates buffer (pH=5.0), 2×10^{-5} M AVN, 5×10^{-3} M 1,10-phenanthroline, $NH_2OH.HCl$ 0.015 M and Cu(II) 0,1,2,3,4$\times10^{-6}$ M.*

b. Large negative errors result for aluminum in the presence of copper(II) when AVN is not sufficient to obtain its maximum coordination to all metal ions of a sample (Al(III):AVN=1:3). This is a consequence of the overall stability constant of copper(II) with AVN which is greater than that of aluminum(III), as in the case of iron(III). The strong chemical affinity of copper(II) with AVN gives very large errors in fluorometric determination of aluminum(III), an effect that is well evident from Figure 8.38.

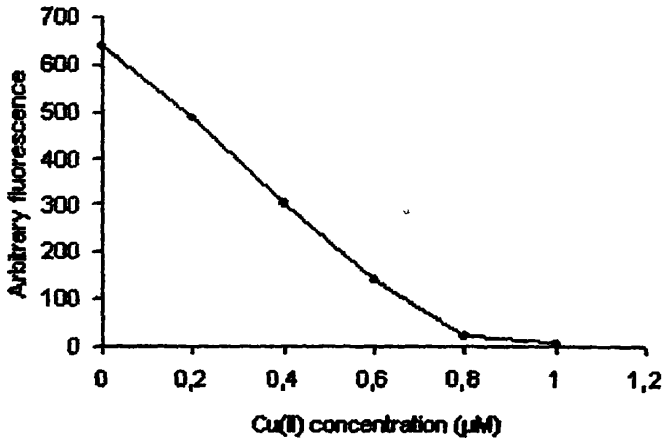

Figure 8.38. *Variation of fluorescence with Cu(II) in acetates buffer (pH=5.0), AVN 1.8×10^{-6} M and Al(III) 6×10^{-7} M. Instrumental parameters: Excitation/Emission wavelength =520/620 nm, high voltage, Slits: excitation 5nm and emission 10 nm.*

c. Interferences in the presence of copper(II) result, also, from the fact that copper(II) reacts with AVN in excess forming non-fluorescent complexes, that is to say errors come into the presence due to fluorescence quenching of the coordinated AVN in excess, which is a weakly fluorescent molecule. This interfering effect of copper(II) was prevented by adding hydroxylamine hydrochloride and 1,10-phenanathroline (Figure 8.39 and Table 8.18).

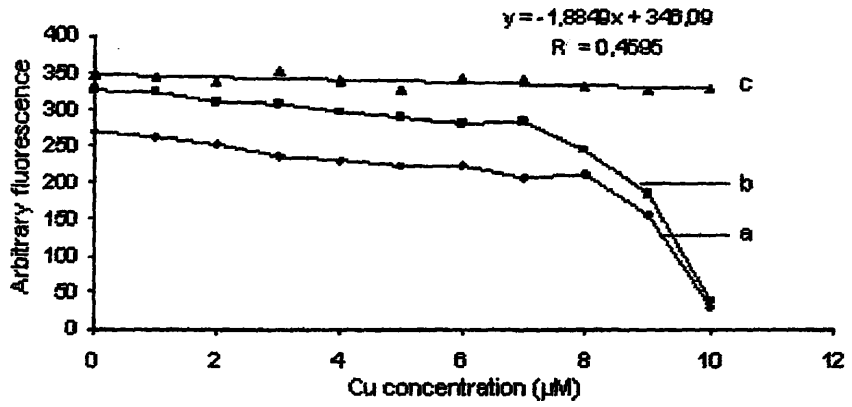

Figure 8.39. *Variation of fluorescence with Cu(II) in acetates buffer (pH=5.0) and AVN 2×10^{-5} M. (a) Cu(II) alone; (b) Cu(II) and $NH_2OH.HCl$ 0.015 M (c) Cu(II), 1,10-Phenanthroline 5×10^{-5} M and $NH_2OH.HCl$ 0.015 M. Instrumental parameters: Excitation/Emission wavelength =520/620 nm, high voltage, both excitation and emission slits were 10 nm.*

Thus, with a concentration of 5×10^{-5} M of 1,10-phenanthroline and 0.015 M hydroxylamine hydrochloride, determination of aluminum(III) can be accomplished with small errors from the presence of copper(II), even though the concentration of the metal is up to 10^{-6} M, for 10^{-6} M AVN and 10^{-7} M aluminum(III) in acetates buffer (pH=5.0) (Table 8.18).

8.9.3 Cobalt interference. At high concentration of cobalt(II) could be a potential interferent. Figure 8.40 shows visible spectra of Co(II)-AVN system in an acetates buffer solution of pH=5.0. Absorbance maximum is observed at 499 nm, while an isobestic point is located at 539 nm. Addition of various cobalt(II) concentrations causes a gradual slight bathochromic shift .

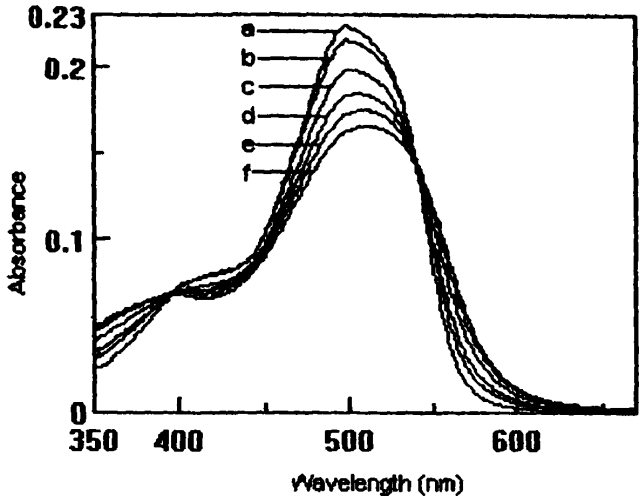

Figure 8.40. *Absorption spectra in acetates buffer (pH=5.0) and 2.4×10^{-5} M AVN. (a) No Co(II); (b) Co(II) 10^{-6} M; (c) Co(II) 2×10^{-6} M; (d) Co(II) 4×10^{-6} M; (e) Co(II) 6×10^{-6} M and (f) Co(II) 8×10^{-6} M.*

Co(II)-AVN complexes absorb a part of the fluorescence (emission) light of the Al(III)-AVN system at the wavelength of measurement (620 nm), bringing significant negative errors, as illustrated in Figure 8.40.

The absorption spectrum of AVN and those with various cobalt(II) concentrations in the presence of masking agents are shown in Figure 8.41. It is evident, that under these conditions the spectral interferences are not seen anymore at 620nm, where fluorescence measurements are made for aluminum(III) determination.

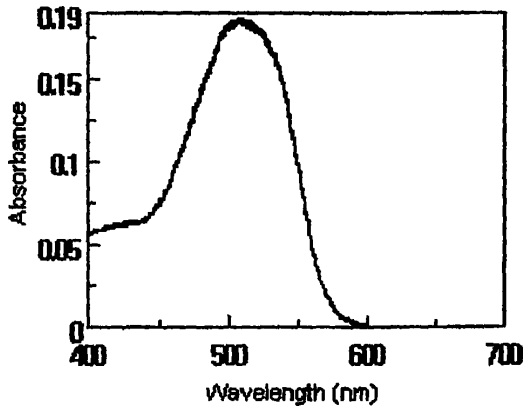

Figure 8.41. *Absorption spectra in acetates buffer (pH=5.0), 10^{-4} M AVN, 5×10^{-3} M 1, 10-phenanthroline and $NH_2OH.HCl$ 0.015 M. (a) No Co(II); (b) Co(II) 2×10^{-6} M and (c) Co(II) 3×10^{-6} M.*

Also, relative small negative errors again appear due to fluorescence quenching of the coordinated AVN in excess, as shown in Figure 8.42.

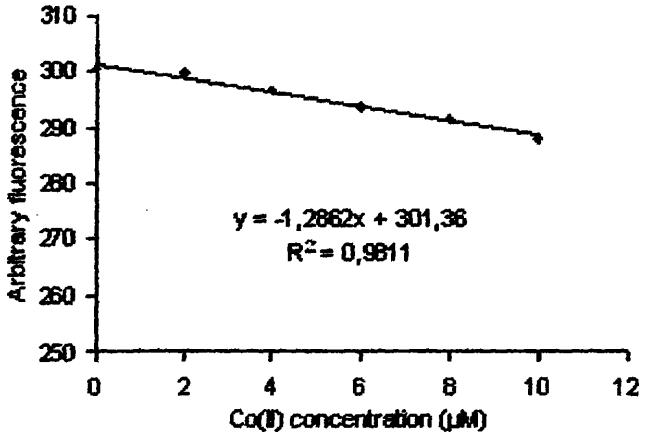

Figure 8.42. *Variation of fluorescence with Co(II) in acetates buffer (pH=5.0), AVN 2×10^{-5} M. Instrumental parameters: Excitation wavelength/Emission wavelength =520/620 nm, High voltage, both excitation and emission slits were 10 nm.*

The masking capacity of various reagents was tried, to restrain undesirable interference from cobalt(II), as follows: 1.7×10^{-2} M KSCN, 0.02 M glycine, 3 % H_2O_2 and 0.5 M NaF. The interference from cobalt(II) on the determination of aluminum can not be reduced in the presence of the above masking agents.

However, cobalt(II) ions have a limited only interfering effect in the fluorometric determination of aluminum(III) (Table 8.17) for concentration Co(II):Al(III) ratios up to 10.

8.9.4 Chromium interference The results shown in Table 8.17, also, indicate interference in the presence of chromium(III). Interferences in the presence of chromium(III) result from the fact that chromium(III) reacts with AVN forming non-fluorescent complexes, that is to say errors come about because of fluorescence quenching of the coordinated AVN, which is a weakly fluorescent molecule, as shown in Figure 8.43a. Interference of this type exists even if the masking agents are added (Figure 8.43b).

Thus, the proposed method for aluminum determination is convenient if the samples for analysis are characterized by a low content in chromium(III). However, chromium(III) ions have a limited only interfering effect in the fluorimetric determination of aluminum(III) (Table 8.17) for Cr(III):Al(III) concentration ratios up to 2.

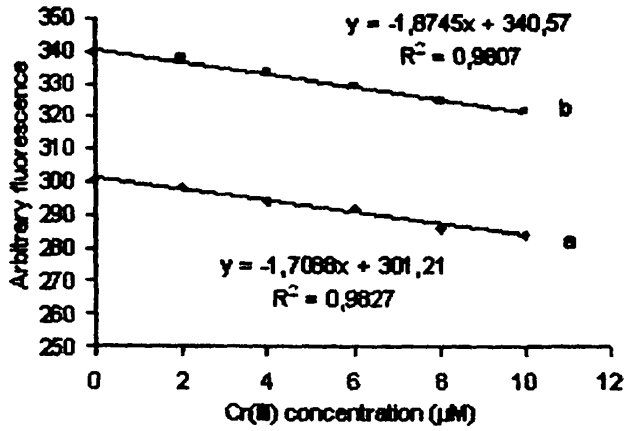

Figure 8.43. *Variation of fluorescence with Cr(III) in acetates buffer (pH=5.0), AVN 2×10^{-5} M; (a) Cr(III), (b) Cr(III) 1,10-Phenanthroline 5×10^{-5} M and $NH_2OH.HCl$ 0.015 M. Instrumental parameters: Excitation/Emission wavelength =520/620 nm, high voltage, both excitation and emission slits were 10 nm.*

8.9.5 Fluoride interference. Addition of fluorides in Al(III)-AVN system (Figure 8.44) is accompanied by disappearance of the isosbestic point at 502nm and entire coincidence of the AVN and Al(III)-AVN spectra (Figure 8.45).

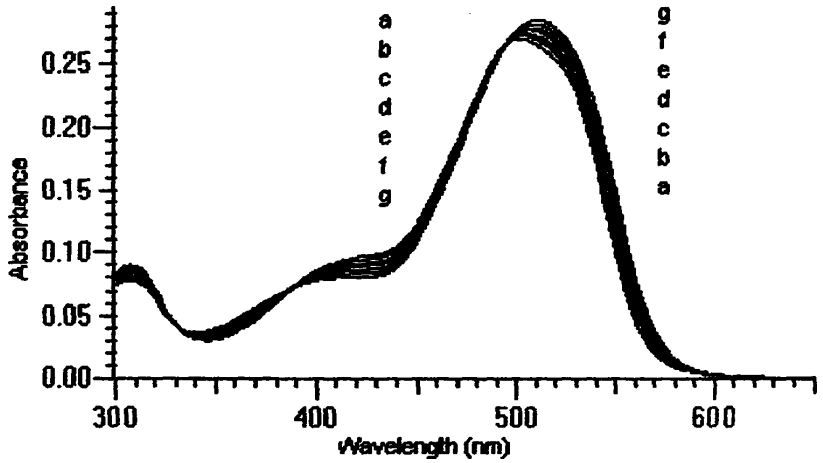

Figure 8.44. *Absorption spectra in acetates buffer (pH=5.0) and 2.4×10^{-5} M AVN. (a) No Al(III); (b) Al(III) 10^{-6} M; (c) Al(III) 2×10^{-6} M; (d) Al(III) 3×10^{-6} M; (e) Al(III) 4×10^{-6} M; (f) Al(III) 5×10^{-6} M; and (g) Al(III) 6×10^{-6} M.*

Figure 8.44 shows visible spectra of Al(III)-AVN system in an acetates buffer solution of pH=5.0, where the absorbance maximum is observed at 500 nm. An isosbestic point is

located at 499 nm. Addition of various concentrations of aluminum(III) causes a gradual slight bathochromic shift to 510 nm.

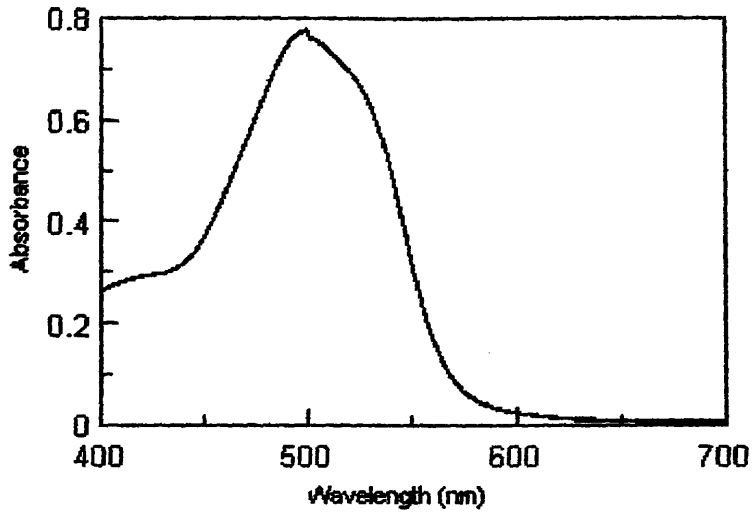

Figure 8.45 *Absorption spectra in acetates buffer (pH=5.0), 10^{-4} M AVN, 0, 2.5, 5, 10×10^{-6} M Al(III) and 0.5 M NaF.*

The presence of fluorides interfere with the determination of aluminum(III) due to the fact that this anion strongly reacts with aluminum(III) giving complexes of the type $AlF_x^{-(x-3)}$ (x:1-6).

Aluminum(III) is not necessarily released from $AlF_x^{-(x-3)}$ and for this reason negative errors are expected in a sample analysis for aluminum determination. The same effect also, was noticed for iron(III). The influence of fluorides can be anticipated by addition in the sample of a salt of beryllium(II) that has a good affinity with fluorides to release aluminum(III) from $AlF_x^{-(x-3)}$[50]. When beryllium(II) is introduced into a sample, the interference of fluorides can be largely reduced. For example by addition of 10^{-4} M of beryllium(II), the error in aluminum determination is less than 5 % for a fluoride concentration 20-fold larger, compared to that of aluminum(III).The reaction of beryllium(II) and fluorides is fast and the products are stable in analytical procedure.

8.9.6 Phosphate interference. It is known from literature that phosphates interfere with determination of aluminum(III) by forming such stable complexes that the formation of the complex with a chromogenic reagent is prevented. The stability of the aluminum phosphate species is highly pH-dependent. The lowest solubility of the aluminum phosphates is at a pH around 6.0, while it is about 10 000 times more soluble at pH 4.0 [51]. In the method

proposed, however, determination of aluminum(III) is successful and without error even if phosphates concentration is up to 4×10^{-4} M for 10^{-6} M AVN and 10^{-7} M aluminum(III), in acetates buffer solution of pH=5.0.

8.9.7 Organic compounds interference. Both low-molecular-weight organic acids and high-molecular-weight humic compounds form complexes with aluminum. The stabilities of these organo-aluminum complexes are highly variable, and the magnitude of these interferences is therefore difficult to predict. However, methods for the determination of aluminum in biological materials involve a digestion procedure to remove the organic compounds [52], or a speciation procedure where the organic aluminum complexes are separated from the inorganic species of aluminum[53]. No efforts were made to evaluate these possible interferences.

References:

1 *Carry Eclipse online help*, specification

2 Perkin Elmer Inc, *An introduction to Fluorescence Spectroscopy*, 2000.

3 Clark B.J., Frost T. Russell M.A., *Techniques in visible and ultraviolet spectrometry. UV Spectroscopy. Techniques, instrumentation, data handing*, vol. 4, Chapman & Hall, London, pp. 32, 1993

4 Harvey D., Modern Analytical Chemistry, McGraw-Hill Higher Education, pp. 388-390, 2000

5 D. A. Skoog, F. J. Holler, T. A. Nieman, Principles of instrumental analysis, fifth edition, pp. 312-316, 1998

6 Lindstrom F., Womble A.E., Locating the more acidic hydroxyl group on dihydroxy compounds, o,o'-dihydroxyazo-dye metal-ion indicators, Tal., 20:589, 1972

7 Dakiky M., Manassra A., Kareem M.A., Jumean F., Khamis M., *Dyes and Pigments*, 63:101,2004

8 Hyperchem 6 software

9 Willard H.H., Dean J.A., Anal.Chem., 22:1264, 1950

10 Khamis M., Bulos B., Jumean F., Manassra A., Dakiky M., *Dyes and Pigments*, 66 (3): 179, 2005

11 Sarzanini C., Abollino O., Bruzzoniti M.C., Mentasti E., *Journal of Chromatography A*, 804 (1-2): 241, 1998

12 Gao H.W., Hu N.L., *Journal of the Chinese Chemical Society*, 49 (6): 965, 2002

13 Satsuki T., Nagoh Y., Yoshimura H., *Tenside Surfactants Detergents*, 35 (1): 60, 1998

14 Satsuki T., Nagoh Y., Yoshimura H., *Tenside Surfactants Detergents*, 35 (2): 112, 1998

15 Locatelli C., *Electroanalysis*, 15 (17): 1397, 2003

16 Wang X.L., Lei J.P., Bi S.P., Gan N., Wei Z.B., *Anal. Chim. Acta*, 449 (1-2): 35, 2001

17 Gan N., Tan Y.X., Wang X.L., Lei J.P., Bi S.P., *Chinesse Journal of Inorganic Chemistry*, 17 (5): 718, 2001

18 Gan N., Tan Y.X., Wang X.L., Lei J.P., Bi S.P., *Chinesse Journal of Inorganic Chemistry*, 29 (2): 212, 2001

19 Bi S.P., Liu F., Dai L.M., Cao M., Chen Y.J., Lian H.Z., *Chemical Papers-Chemicke Zvesti* 53 (2): 93, 1999

20 Bi S.P., Song M.J., Xu D., *Anal. Let.* , 31 (11): 1937, 1998

21 Lanza P., *Anal. Chim. Acta* 341 (1): 91, 1997

22 Jagner D., Renman L., Stefansdottir S.H., *Anal. Chim. Acta* 281 (2): 305, 1993

23 Jagner D., Renman L., Stefansdottir S.H., *Anal. Chim. Acta* 281 (2): 315, 1993

24 Johnson K.E., Treble R.G., *Canadian Journal of Chemistry-revue Canadienne de Chimie*, 71 (6): 824, 1993

25 Farias P.A.M., Takase I., *Electroanalysis*, 4 (8): 823, 1992

26 Stryjewska E., Rubel S., Kusmierczyk K., *Chemia Analityczna*, 37 (1): 43, 1992

27 Downard A.J., Powell H.K.J., Xu S.H., *Anal. Chim. Acta*, 262 (2): 339, 1992

28 Short Communication , *Talanta* 21:771, 1974

29 Fogg A.C., Lewis J.E., *Talanta* 25:461,1985

30 Wang J., Farias P.A.M., Mahmoud J.S., *Anal. Chim. Acta*, 172:57, 1985

31 Wang J., Zadeii J.M., *Talanta*, 33: 321, 1986

32 Wang J., Zadeii J.M., *Anal. Chim. Acta*, 185: 229, 1986

33 Wang J., Mahoud J.S., *J. Electroanal. Chem.*, 208: 383, 1986

34 Wang J., Tuzhi P., Varughese K., *Talanta* 34 :561, 1986

35 Wang J., Tuzhi P., Martinez T., *Anal. Chim. Acta*, 201:43, 1987

36 Hua C., Jagner D., Renman L., *Talanta* 35(8) : 597, 1988

37 Wang J., Taha Z., *Anal. Chim. Acta*, 215 : 29, 1988

38 Locatelli C., *Electroanalysis*, 15(17):1397, 2003

39 E. Bishop (Ed.), Indicators, Pergamon Press, Oxford, pp.262, 1972.

40 Martell, A. E.; Smith, R. M.; Critical Stability Constants; Plenum Press, New York, 1991.

41 Abollino O., Sarzanini C., Mentasti E., Evaluation of stability constants of metal complexes with sulphonated azo-ligands, Talanta 41(2):1107, 1994

42 Abollino O., Sarzanini C., Mentasti E. Liberatori A., Trace metal preconcentration with sulphonated azo-dyes and ICP/AES determination, Spectrochimica Acta , 49A(9):1411, 1993

43 Ma M., Johnson K.E., *J. Electroanal. Chem.*, 355:97, 1993.

44 Bergley I.S., Barnard C.L.R., Anal. Proc. (London), 29:56, 1992

45 de Levie R., Principles of quantitative chemical analysis, ed. McGraw-Hill, 1997, pp. 492.

46 Van Linden W.E., Definition and classification of interferences in analytical procedures, Pure&Appl. Chem., IUPAC, 61(1):91-95, 1989,

47 Onishi H., Photometric determination of traces of metals, Wiley-Interscience Publication, John Wiley & Sons, Fourth Edition, 1986

48 Stability constants supplement no.1, Special publication 25, The Chemical Society London, Alden Press London, pp.906, 1971

49 Smith M., Critical Stability Constants, volume 5: First Supplement, Plenum Press, New York, pp. 254, 1982

50 Zang J., Xu H., Ren J.L., Fluorimetric determination of dissolved aluminum in natural waters after liquid-liquid extraction into n-hexanol, *Anal. Chim. Acta,* 405:31-42, 2000

51 Royset O., Comparison of four chromogenic reagents for the flow-injection determination of aluminum in water, *Anal. Chim. Acta*, 178:223-230, 1985

52 G. Ogner, A. Haugen, M. Opem, G. Sjotveit and B. Sorlie, The Chemical Analysis program at The Norwegian Forest Research Institute, 1984, Norwegian Forest Res. Inst., 1432 Aas-NLH (1984).

53 C. T. Driscoll, Ph.D. Thesis, Cornell University (1980); Int. *J. Environ. Anal. Chem.,* 16 (1984) 267.

9. Calibration methods for aluminum determination

The fluorescence reaction between aluminum(III) and AVN was directly proportional in a range of aluminum(III) concentrations from 2×10^{-9} to 5×10^{-6} M. The two out of three most common calibration methods, those of the calibration curve and the standard addition one, were used in this work to determine aluminum(III) in soft drinking water, prawn and a pharmaceutical formulation. To obtain a determination, three concentration ranges for aluminum(III) standard solutions, that bracket the concentration expected for the samples, were employed. The ranges used were 10^{-9} to 10^{-8} M, 10^{-8} to 10^{-7} M and 10^{-7} to 10^{-6} M.

9.1a Calibration curve method, certified prawn, 10^{-9} to 10^{-8} M range for standard aluminum(III) solutions.

Experiment: Aluminum standard solutions in triplicate and six identical sample solutions were directly prepared in a set of twenty-four test-tubes. Into each tube 0.5 mL of sodium acetate-acetic acid buffer solution (pH=5.0), 50 μL of 5×10^{-3} M 1,10-phenanthroline, 0.5 mL of 0.15 M hydroxylammonium chloride and 0.1 mL of 5×10^{-3} M beryllium sulphate, followed by 50 μL of 10^{-3} M AVN were placed. In each set of three test-tubes (first eighteen tubes) volumes of 0, 10, 20, 30, 40 and 50 μL of the 10^{-6} M aluminum(III) standard solution were dispensed in turn. In each of the remaining six test-tubes 40 μL of a ten times diluted in 0.1 N nitric acid prawn stock solution, were placed. The contents were well mixed, then the volume of each tube was made up to 5.0 mL with distilled water and again were thoroughly mixed. This procedure was consistently followed to avoid possible hydrolysis of aluminum(III). The tubes were placed into a water bath, at 60°C, for 30 min, brought to room temperature and finally the fluorescence was measured at 620 nm (excitation at 520 nm).

In this range of aluminum(III) concentrations a dispersion of the measurements was observed. This effect was confronted by repeated measurements of the standard and unknown solutions or/and by preparing and measuring several identical solutions for each standard and unknown. Deviations in the calibration graph for the determination of aluminum(III) are shown in Table 9.1. The relative standard deviation of the slope for this curve was 2.9 %, corresponding to confidence limits of 6405±517, at the 95 % level. The correlation coefficient

was 0.9983. The values were calculated by the method of least squares using Equation 9.1, with b = 157.5±3.13.

$$Y = b + mX \qquad (9.1)$$

where b is the intercept, m the slope and X the concentration.

Table 9.1. *Accuracy of the spectrofluorimetric determination of Al(III) in an acetates buffer solution of pH 5.0, 0.015 M $NH_2OH.HCl$, 5×10^{-4} M 1,10-phenanthroline, 10^{-4}M beryllium sulphate and 10^{-5} M AVN.*

Aluminum concentration (μM)		*Deviation (%)*
x^a	x_i^b	*[100(x_i-x)/x]*
0	0	0
0.002	0.001763	-11.8
0.004	0.003783	-5.4
0.006	0.005962	-0.63
0.008	0.008211	+2.64
0.01	0.00999	-0.1

[a] *Prepared values.*

[b] *Mean values of triplicate solutions calculated from the fluorescence using Equation 9.1.*

Two cases for defining the detection and quantitation limits have been developed:

a. In the first case, the limits of detection and quantitation, calculated from the regression line [1], were found to be 7.3×10^{-10} M and 2.4×10^{-9} M, respectively. The standard deviation ($S_{y/x}$), based on the fluorescence values of all solutions of the calibration graph, was found to be $S_{y/x}$=1.56.

b. In the second case, the limits of detection and quantitation, calculated from the standard deviation (s_b) of the blank [2, pp307], were found to be 2.28×10^{-10} M and 7.6×10^{-10} M, respectively. Here, the standard deviation, evaluated by making 20 replicate fluorescence measurements of the blank in exactly the same way, was found to be s_b=0.46.

Since the standard deviations have been found, the limit of detection (LD) is evaluated as $LD=3S_{y/x}/m$ (first case) or $LD=3s_b/m$ (second case) and the limit of quantitation (LQ) as $LQ=10S_{y/x}/m$ (first case) or $LQ=10s_b/m$ (second case), where b is the slope of the calibration graph.

The aluminum(III) concentrations of the six prawn solutions (test-tubes 19-24) were calculated from Equation 9.1 (*Y=157+6405X*) and then were referred to the initial reference material. The relative standard deviation (R.S.D.) of the aluminum(III) content of the reference sample of prawn (GBW 08572) was 6.76 %, corresponding to confidence limits of 0.128±0.008 %, at the 95 % level. This content, found by means of the present method, lies very close to the certified value (0.131±0.004 %) of the reference material.

9.1b Standard addition method, certified prawn, 10^{-9} to 10^{-8} M range for standard aluminum(III) solutions.

In order to evaluate overall recovery of the procedure, calibration plots were built up by preparing and adding increments of a standard aluminum(III) solution (increments in the 2×10^{-9}-10^{-8} M range) in a number of test-tubes including only blank (group a), as well as in another number of test-tubes (group b) containing blank and prawn aliquots of the same size (40 μL of a ten times diluted prawn stock solution). The reaction of aluminum(III) and AVN in group A is considered to be complete, that is to say a 100 % recovery of aluminum(III) is obtained. Comparison of the slopes of the two working curves referred to groups a and b, respectively, can be used to estimate the effect caused by matrix concomitants on the recovery of added aluminum(III). In the absence of the matrix effect the ratio between the slopes of the two curves is equal to 1 and this condition ensures full aluminum(III) recovery. For this experiment, however, the ratio of the two slopes (shown in Figure 9.1) was found to be 0.80. Although this result is not promising a 100 % recovery of aluminum(III), next experiments show that the procedure of the standard additions does not suffer from effects caused by matrix concomitants.

Experiment: A set of eighteen polyethylene test-tubes was used to prepare solutions needed for aluminum determination in prawn by the method of standard additions. Into each test-tube 0.5 mL of sodium acetate-acetic acid buffer solution (pH=5.0), 50 μL of 5×10^{-3} M 1,10-phenanthroline, 0.5 mL of 0.15 M hydroxylammonium chloride, 0.1 mL of 5×10^{-3} M beryllium sulphate, 50 μL of 10^{-3} M AVN, followed by 40 μL of a ten times diluted in 0.1 N nitric acid stock solution of the certified prawn were placed. In each set of three test-tubes volumes of 0, 10, 20, 30, 40 and 50 μL of the 10^{-6} M aluminum(III) standard solution were dispensed in turn. The contents were well mixed, then the volume of each tube was made up to 5.0 mL with distilled water and again were thoroughly mixed. This procedure was consistently followed to avoid possible hydrolysis of aluminum(III). The test-tubes were

placed into a water bath at 60°C for 30 min, brought to room temperature and finally the fluorescence was measured at 620 nm (excitation at 520 nm). The plot of fluorescence versus aluminum concentration is shown in Figure 9.1b. A second experiment, without adding prawn sample was carried out in exactly the same way and used to prove possible effects of the matrix concomitants. The results of this second experiment are shown in Figure 9.1a.

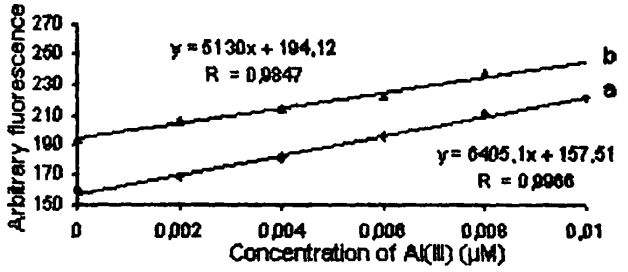

Figure 9.1. *Method of standard additions of aluminum(III) (volumes of 0, 10, 20, 30, 40 and 50 μL of 10^{-6} M Al(III)). in (a) only blank and (b) blank plus prawn. Chemical composition: acetates buffer (pH=5.0), 0.015 M $NH_2OH.HCl$, 5×10^{-4} M 1,10-phenanthroline, 10^{-4}M beryllium sulphate and 10^{-5} M AVN. Instrumental parameters: Excitation/Emission wavelength=520/620 nm, high voltage, both excitation and emission slits were 10 nm.*

The method of standard additions is applicable only if instrument response (Y) versus concentration (X) of standard solutions is a straight line and passes through the origin, namely the straight line represents a first degree equation of the form $Y=mX$, containing no intercept. In this study the curve 9.1.a shows a large value of intercept which was calculated from Equation 9.1. Therefore, the curve 9.1b, prepared by the method of standard addition, could not be directly used for aluminum determination in prawn, but only after subtracting the blank value from the fluorescence of each solution used to prepare the curve 9.1b. Thus, a potent analytical curve resulted and the aluminum(III) of the prawn aliquots (40 μL of the stock solution) was calculated from Equations 9.2 or 9.3 [2].

$$X_X = \frac{bX_S}{mV_X} \qquad (9.2)$$

$$X_X = -\frac{(V_S)_0 X_S}{V_X} \qquad (9.3)$$

The value of the aluminum(III) concentration was referred to the initial certified prawn sample and its content (0.1074±0.006 %) found to lie close enough to the certified value (0.131±0.004 %).

9.2a Calibration curve method, certified prawn, 10^{-8} to 10^{-7} M range for standard aluminum(III) solutions.

The procedure followed here, in order to determine aluminum(III) in prawn (40 μL of the reference prawn stock solution), was analogous to that already described in paragraph 9.1a.

Deviations in the calibration graph for the determination of aluminum(III) are shown in Table 9.2. The relative standard deviation of the slope for this curve was 1.18 %, corresponding to confidence limits of 4998±164, at the 95% level. The correlation coefficient was 0.9997. The values were calculated by the method of least squares using Equation 9.1, with b = 161.96±9.94.

Table 9.2 *Accuracy of the spectrofluorimetric determination of Al(III) in an acetates buffer solution of pH 5.0, 0.015 M $NH_2OH.HCl$, 5×10^{-4} M 1,10-phenanthroline, 10^{-4}M beryllium sulphate and 10^{-5} M AVN.*

Aluminum concentration (μM)		***Deviation (%)***
x^a	x_i^b	$[100(x_i-x)/x]$
0	0	0
0.02	0.01992	-0.4
0.04	0.04154	+3.85
0.06	0.05995	-0.1
0.08	0.07897	-1.28
0.1	0.10025	+0.25

[a] *Prepared values.*

[b] *Mean values of triplicate solutions calculated from the fluorescence using Equation 9.1.*

Here, also two cases for defining the detection and quantitation limits have been developed:

a. In the first case, the limits of detection and quantitation, calculated from the regression line [1], were found to be 2.9×10^{-9} M and 9.9×10^{-9} M, respectively. The standard deviation ($S_{y/x}$) was found to be $S_{y/x}$=4.95.

b. In the second case, the limits of detection and quantitation, calculated from the standard deviation (s_b) of the blank [2, pp307], were found to be 3.9×10^{-10} M and 1.3×10^{-9} M, respectively. Here, the standard deviation was found to be s_b=0.65[3].

The aluminum(III) concentrations of six prawn solutions were calculated from Equation 9.1 (Y=161+4998X) and then were referred to the initial reference material. The relative standard deviation (R.S.D.) of the aluminum(III) content of the reference sample of prawn (GBW 08572) was 4.40 %, corresponding to confidence limits of 0.1309±0.0058 %, at the 95% level. This content, found by means of the present method, was about the same to the certified value (0.131±0.004 %) of the reference material.

9.2b Calibration curve method, certified soft drinking water, 10^{-8} to 10^{-7} M range for standard aluminum(III) solutions.

In this experiment, aluminum(III) determination in soft drinking water (50 μL of the reference soft drinking water), was performed by a procedure analogous to that already described in paragraph 9.1a. Deviations in the calibration graph (Figure 9.2) for the determination of aluminum(III) are shown in Table 9.3. The relative standard deviation of the slope for this curve was 2.6 %, corresponding to confidence limits of 6832± 418, at the 95 % level. The correlation coefficient was 0.9976. The values were calculated by the method of least squares using Equation (9.1), with b =383.08± 23.54.

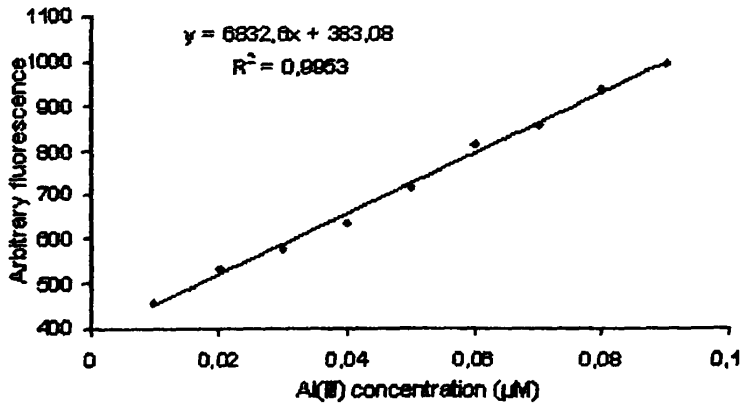

Figure 9.2. *Variation of fluorescence with concentration of aluminum(III) in an acetates buffer solution of pH=5.0, 0.015 M $NH_2OH.HCl$, 5×10^{-4} M 1,10-phenanthroline and 10^{-6} M AVN, Instrumental parameters: Excitation/Emission wavelength=520/620 nm, high voltage, Slits: excitation 10nm and emission 20 nm.*

Table 9.3. *Accuracy of the spectrofluorimetric determination of aluminum(III) in an acetates buffer solution of pH 5.0, 0.015 M $NH_2OH.HCl$, 5×10^{-4} M 1,10-phenanthroline and 10^{-6} M AVN.*

Aluminum concentration (μM)		*Deviation (%)*
x^a	x_i^b	*[100(x_i-x)/x]*
0.01	0.0108	+8
0.02	0.022217	+11.1
0.03	0.028501	-5
0.04	0.036771	+8.1
0.05	0.048692	-2.6
0.06	0.062732	+4.6
0.07	0.069727	-0.4
0.08	0.08079	+1
0.09	0.089767	-0.3

[a] *Prepared values.*

[b] *Mean values of duplicate solutions calculated from the fluorescence using Equation 9.1.*

Here, also two cases for defining the detection and quantitation limits have been developed:

a. In the first case, the limits of detection and quantitation, calculated from the regression line [1], were found to be 6×10^{-9} M and 2×10^{-8} M, respectively. The standard deviation ($S_{y/x}$), based on the fluorescence values of all solutions of the calibration graph was found to be $S_{y/x}$=13.70.

b. In the second case, the limits of detection and quantitation, calculated from the standard deviation (s_b) of the blank [2, pp307], were found to be 4.4×10^{-10} M and 1.5×10^{-9} M, respectively. Here, the standard deviation was found to be s_b=1.08[3].

The aluminum(III) concentrations of six soft drinking water samples were calculated from Equation 9.1 (Y=383+6832X) and then were referred to the initial reference material.

The relative standard deviation (R.S.D.) of the aluminum(III) content of the reference sample of soft drinking water (LGC 6011) was 5.32 %, corresponding to confidence limits of 206± 11.0 μg/L, at the 95 % level. This content, found by means of the present method, lies close to the certified value (218±8 μg/L) of the reference material.

9.2c Standard addition method, certified prawn, 10^{-8} to 10^{-7} M range for standard aluminum(III) solutions.

The procedure followed here, in order to determine aluminum(III) in prawn by standard addition method, was analogous to that already described in paragraph 9.1b. Thus, the calibration plots were built up by preparing and adding increments of a standard aluminum(III) solution (increments in the 2×10^{-8}-10^{-7} M range) in a number of test-tubes including only blank (group a), as well as in another number of test-tubes (group b) containing blank and prawn aliquots of the same size (20 μL of the reference prawn stock solution). In this case, the ratio between the slopes of the two curves (shown in Figure 9.3) was found to be 1.01. This result shows that the procedure of the standard additions does not suffer from any effect caused by matrix concomitants.

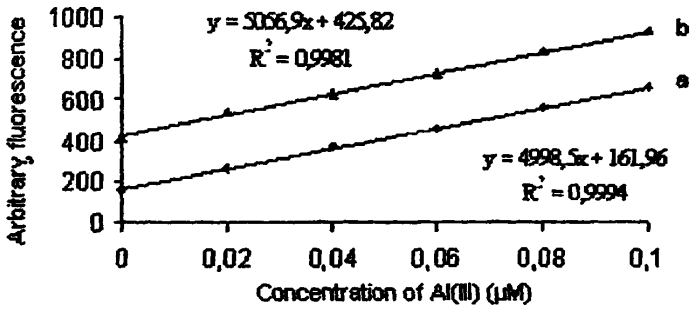

Figure 9.3 *Method of standard additions of aluminum(III) (volumes of 0, 10, 20, 30, 40 and 50 μL of 10^{-5} M Al(III)) in (a) blank and (b) 20 μL of a prawn stock solution. Chemical composition: Acetates buffer (pH=5.0), 0.015 M $NH_2OH.HCl$, 5×10^{-4} M 1,10-phenanthroline, 10^{-4}M beryllium sulphate and 10^{-5} M AVN. Instrumental parameters: Excitation/Emission wavelength=520/620 nm, high voltage, both excitation and emission slits were 10 nm.*

The aluminum(III) concentration of the prawn solution were calculated from Equation 9.1, after subtracting the blank value from the fluorescence of each solution used to prepare the curve 9.3b. The value of the aluminum(III) concentration was referred to the initial

certified prawn sample and its content (0.125±0.008 %) was found to lie close to the certified value (0.131±0.004 %).

9.2d Standard addition method, certified soft drinking water, 10^{-8} to 10^{-7} M range for standard aluminum(III) solutions.

A calibration plot (Figure 9.4.a) was build up by preparing and adding increments of a standard aluminum solution (increments in the 2×10^{-8}-10^{-7} M range) in a number of test-tubs containing blank and prawn aliquots of the same size (25 μL of the reference soft drinking water). In order to determine aluminum(III) concentration in soft drinking water by standard addition method, a new calibration plot (Figure 9.4.b) was build up by subtracting the blank value from the fluorescence of each solution used to prepare the curve 9.4.a.

Thereafter, the aluminum(III) concentration of the soft drinking water was calculated from Equation 9.1. The value of the aluminum(III) concentration was referred to the initial certified soft drinking water and its content (222.3±5.5 μg/L) was found to lie very close to the certified value (218±8 μg/L).

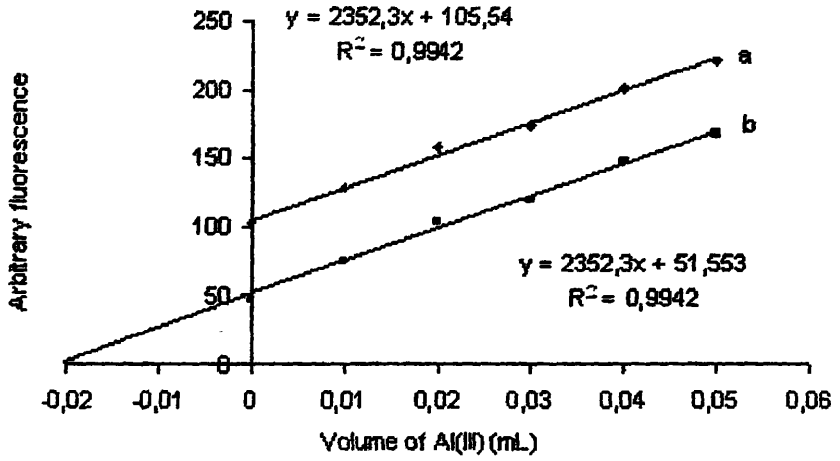

Figure 9.4. *(a) Method of standard additions of aluminum(III) (volumes of 0, 10, 20, 30, 40 and 50 μL of 10^{-5} M Al(III)) in blank plus soft drinking water (25 μL sample aliquots). (b) Graph after subtracting the blank value from the fluorescence of each solution used to prepare the graph a . Chemical composition: Acetates buffer (pH=5.0), 0.015 M $NH_2OH.HCl$, 5×10^{-4} M 1,10-phenanthroline and 10^{-6} M AVN. Instrumental parameters: Excitation/Emission wavelength = 520/620 nm, high voltage, slits of excitation 10 nm and emission 5 nm.*

9.3 Calibration curve method, pharmaceutical formulation Maalox sample, 10^{-7} to 10^{-6} M range for standard aluminum(III) solutions.

The procedure followed here, in order to determine aluminum(III) in pharmaceutical formulation Maalox (500 μL of the pharmaceutical antacid formulation stock solution in an acetates buffer of pH=4.0), was analogous to that already described in paragraph 9.1a.

Deviations in the calibration graph (Figure 9.5) for the determination of aluminum(III) are shown in Table 9.4. The relative standard deviation of the slope for this curve was 3.5 %, corresponding to confidence limits of 571±56, at the 95 % level. The correlation coefficient was 0.9975. The values were calculated by the method of least squares using Equation 9.1, with b=105.96±33.68.

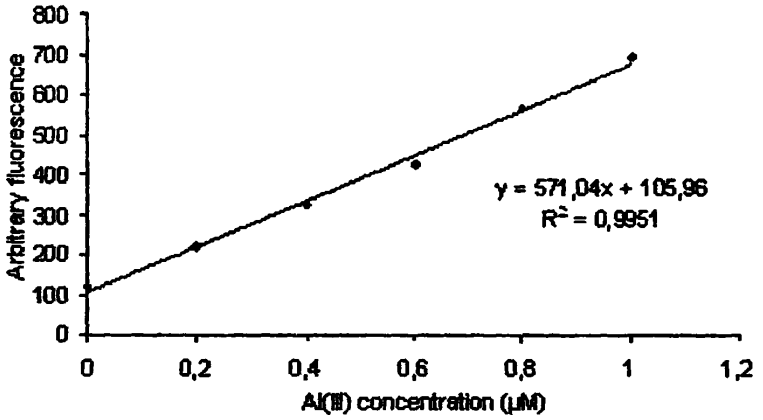

Figure 9.5. *Variation of fluorescence with concentration of aluminum in acetates buffer solution of pH=4.0, and 2×10^{-5} M AVN, Instrumental parameters: Excitation/Emission wavelength=520/590 nm, high voltage, both excitation and emission slits were 5 nm.*

Table 9.4. *Accuracy of the spectrofluorimetric determination of aluminum in an acetates buffer solution of pH 4.0, and 2×10^{-5} M AVN.*

Aluminum concentration (μM)		***Deviation (%)***
x^a	x_i^b	$[100(x_i-x)/x]$
0	0.022135	0
0.2	0.20531	+2.66
0.4	0.382705	-4.3
0.6	0.556598	-7.2
0.8	0.806844	+0.9
1	1.026443	+2.6

[a] *Prepared values.*

[b] *Mean values of triplicate solutions calculated from the fluorescence using Equation 9.1.*

The limits of detection and quantitation, calculated from the regression line [1], were found to be 8.8×10^{-8} M and 2.9×10^{-7} M, respectively. The standard deviation ($S_{y/x}$), based on their fluorescence values of all solutions of the calibration graph was found to be $S_{y/x}$=16.76.

The aluminum(III) concentrations of six pharmaceutical samples were calculated from Equation 9.1 (Y=105.96+571X) and then were referred to the initial reference material. The relative standard deviation (R.S.D.) of the aluminum(III) content of the reference sample of pharmaceutical antacid formulation was 2.5 %, corresponding to confidence limits of 192.1 ± 4.86 mg, at the 95 % level. This content, found by means of the present method, lies close to the certified value (200 mg) of the reference material.

References:

1 J.C. Miller, J.N. Miller, Statistics for Analytical Chemistry, 2nd ed., Wiley, New York, 1988, pp. 101–117.

2 Skoog D.A., Holler F.J., Nieman T.A., Principles of Instrumental Analysis, fifth Edition, Harcourt Brace & Company, pp.307, 1998.

3 He R., Wang J., Novel catalytic spectrophotometric procedure for the determination of trace-level aluminum, Analytica Chimica Acta, 412:241-245, 2000

Conclusions

1. Aluminum traces were determined with AVN in a couple of reference materials by spectro- fluorimetry.
2. Aqueous solutions were used throughout.
3. The accuracy and precise of the method was more reliable if stock aluminum solutions in 0.1N nitric acid were used.
4. No separation or preconcentration steeps were involved during the preparation and measurement of the samples. Instead, appropriate masking agents were utilized as a consequence of a careful study.
5. The choice of the experimental conditions and the method process were a result of the following: (a) Nature of the sample. (b) Absorption spectra of species between interfering elements and AVN. (c) Emission fluorescence spectra of aluminum and AVN species. (d) pH effect. (e) Temperature effect. (f) Time of reaction completion depending upon the concentration of AVN.
6. Species of various stoichiometry between aluminum and AVN were verified.
7. In the absence of masking agents large errors were found, due to replacement of aluminum in its complex with AVN by other ions or fluorescence quenching of the coordinated AVN to other metal ions. Spectral errors were also found if fluorescence measurements made at wavelengths shorter than 620 nm.
8. The limits of detection and quantitation were found to be considerably lower in the event that the standard deviation of the method was calculated from the blank and not from every point of the calibration graph.
9. To the best of our knowledge the present method is superior compared to others appearing in the literature. This method is highly sensitive, simple, relative fast, inexpensive from a point of view of reagents cost and well selective.
10. Aluminum determination based on the method of standard additions demonstrated no interaction between analyte and sample constituents, namely no matrix effect. Thus, for samples related to the reference materials studied the facile method of the calibration curve must be optioned.

Perspective

Further, application of the method for aluminum determination in a great deal of waters, environmental, biological and victuals samples, pharmaceutical and industrial products is possible, provided a safe investigation related to matrices of the samples will be made.

Summary

For over 20 years the problems related to aluminum overload in the human body are well known. Aluminum accumulation may increase the risk of neurological and bone diseases, e.g., Alzheimer's disease, Lou Gehrig's and Parkinson's diseases, encephalopathy, and osteomalacia.

The large quantity of aluminum in nature and its many uses make exposure to aluminum unavoidable. This exposure is mainly through oral intake, and the major sources are drinking water (from the use of aluminum in municipal water treatment), residues in food, cooking utensils, food and beverage packing, and aluminum-containing medications (e.g., antacids, buffered aspirins, anti-ulcerative medication or kaolin-based anti-diarrhea medication). Other routes of potential exposure to aluminum are via inhalation of atmospheric dust and through the skin (e.g., via use of antiperspirants). Occupational exposure to aluminum occurs in the refining of the primary metal and in secondary industries that use aluminum products, such as aircrafts, automotives, and metal products. Greater exposure to aluminum is possible for persons living in the vicinity of industrial emission sources and hazardous waste sites.

Therefore, the determination of aluminum levels in drinking water, food, pharmaceutical formulations, biological and other samples is necessary for prevention of aluminum overload and has attracted considerable attention. For this purpose, several instrumental techniques have been employed, such as electrothermal atomic-absorption spectrometry (ETAAS), instrumental neutron activation analysis (INAA), spectrophotometry (SP), high-performance liquid chromatography (HPLC), ion chromatography (IC), voltametry (V), potentiometry (P) and fluorimetry (F) which was utilized in our laboratory.

Our efforts were indeed proved fruitful by choosing acid alizarin violet N (AVN) as a potent coordination reagent, that gives a very strong fluorescence reaction with aluminum(III). Some method essentials including concentration of ligand, reaction pH, temperature, time required for completion of the reaction, relative chemical affinity between metals and ligand, absorption and fluorescence spectra, average time of the lamp flash, monochromators bandwidth and photomultiplier voltage, were investigated in detail to establish the optimum conditions for the method.

The o,o'-dihydroxy arrangement to the azo group of the dye is an absolutely necessary presupposition to develop a fluorescence reaction for aluminum(III), that is to say AVN is undoubtedly complexed to both oxygen of the two hydroxyl groups at once, giving in this way a quite rigid complex with aluminum(III) that is strongly fluorescent. This is supported from the fact that similar azo dye compound which lacks one hydroxyl-group of the ligand does not give any fluorescence reaction with aluminum(III).

The most appropriate pH range, where the fluorescence reaction of aluminum(III) and AVN was investigated, was found to be between 4.0 and 5.0. Both acid and alkaline solutions were studied and the results showed that below pH 3.0 and above pH 6.0 a fluorescence reaction between aluminum(III) and AVN does not exist. Thus an acetates buffer solution of pH 5.0 was used throughout, to prevent undesirable deviations of measurements, because a fluorescence plateau does not cover a relatively wide size of pH range.

As for any given reaction, among other external factors temperature also determines the rate at witch this reaction takes place. Because AVN is a flexible molecule and may posses infinite number of configurations, this probably is the reason that the reaction proceeds slowly. Thus, an experimental procedure was followed, where samples were heated for 30 min at 60°C and then measurements were made at room temperature. The stability of the aluminum(III)-AVN complex was also investigated. It was found out that after heating and cooling at room temperature the system was stable for at least 80 min.

Experimental data show that both AVN and aluminum(III) concentration substantially affects the time of the reaction completion. For this reason, a short enough and about the same time for the reaction completion was conditioned to perform quantitative and other measurements by using a 10 times larger AVN concentration in comparison to that of aluminum.

The time of the reaction completion as well as the mole ratio method were efficiently used to determine formation of different species between aluminum(III) and AVN. Experimental data prove the existence of seven complexes with metal (M) to ligand (L) ratios as follows: ML, ML_2, ML_3, ML_4, ML_5, ML_6 and M_2L.

Foreign ions, usually found in several samples, interfere with the determination of aluminum and errors due to (a) displacement of the coordinated aluminum(III), (b) fluorescence quenching of the coordinated AVN to these ions and (c) absorption of the fluorescence light by the complexes of the foreign ions with AVN, result. Thus, a potent

masking system consisting from 1,10-phenanthroline, hydroxyl-ammonium chloride and beryllium sulphate was finally optioned and utilized to prevent interference effects.

Stock and working aluminum(III) solutions were prepared in 0.1N nitric acid to avoid hydrolysis and probable formation of metal-chloride complexes. In this case, a sufficient convergence of repeated fluorescence measurements for standards was noticed and separate calibration curves of similar features, unchanged for about one week, were drown by using the same working aluminum solution.

Estimating the pros and cons of the experimental process, proper instrumental conditions were optioned, that ameliorate the dynamic range of the calibration curve and fundamental statistical parameters such as standard deviation and sensitivity, which finally mark out the detection and quantitation limit of the method.

By means of the calibration curve and standard addition method and applying least squares, the variation of fluorescence versus concentration of aluminum(III) was utilized to determine the metal in several reference samples and prove the applicability of the finding of this thesis. Dynamic ranges of regression lines were obtained for aluminum(III) standard solutions between $10^{-9}$and 10^{-6} M, while low detection and quantitation limits of the analyte such as 2.28×10^{-10} and 7.6×10^{-10} M, respectively, calculated from the standard deviation of the blank, were found.

Περίληψη

Το πρόβλημα συσσώρευσης του αργιλίου στον ανθρώπινο οργανισμό είναι γνωστό για περισσότερο από 20 χρόνια. Η συσσώρευση του αργιλίου στον ανθρώπινο οργανισμό έχει ως αποτέλεσμα αυξημένες πιθανότητες εμφάνισης νευρολογικών παθήσεων ή ασθενειών των οστών όπως Alzheimer, Lou Gehrig, Parkinson, εγκεφαλοπάθειες και οστεομαλάκυνση.

Η έκθεση του ανθρώπου στο αργίλιο είναι αναπόφευκτη αφενός λόγω της παρουσίας του σε μεγάλα ποσά στην φύση και αφετέρου λόγω των πολλαπλών χρήσεων του. Η πρόσληψη αυτή είναι κυρίως στοματική και οι κύριες πηγές είναι το πόσιμο νερό (από τη χρήση αλουμινίου στην κατεργασία του νερού στα συστήματα ύδρευσης), τρόφιμα, μαγειρικά σκεύη, συσκευασίες τροφίμων καθώς και φάρμακα (π.χ αντιόξινα, ασπιρίνες, καθώς και φάρμακα κατά του έλκους και της διάρροιας με βάση την καολίνη). Επιπλέον, η έκθεση σε αργίλιο πιθανόν να προέρχεται από την εισπνοή αιρουμένων σωματιδίων της ατμόσφαιρας ή από το δέρμα (π.χ με τη χρήση ανθιδρωτικών μέσων). Έκθεση σε αργίλιο συμβαίνει επίσης στην βιομηχανία τόσο κατά την πρωτογενή κατεργασία του υλικού όσο και σε Βιομηχανίες που χρησιμοποιούν προϊόντα αλουμινίου, όπως στην κατασκευή αεροσκαφών, αυτοκινήτων και μεταλλικών προϊόντων. Αυξημένη έκθεση επίσης έχει παρατηρηθεί σε ανθρώπους που ζουν σε περιοχές με εκπομπή βιομηχανικών ρύπων και περιοχές απόθεσης τοξικών αποβλήτων.

Για τους παραπάνω λόγους, ο προσδιορισμός της συγκέντρωσης του αργιλίου στο πόσιμο νερό, στα τρόφιμα, σε φαρμακευτικά προϊόντα και σε βιολογικά δείγματα, είναι απαραίτητος για αποφυγή της συσσώρευσης του μετάλλου και ήδη έχει προσελκύσει μεγάλο ενδιαφέρον. Για το σκοπό αυτό είχαν εφαρμοστεί διάφορες τεχνικές ενόργανης ανάλυσης, όπως ηλεκτροθερμική φασματομετρία ατομικής απορρόφησης (ETAAS), ενόργανη ανάλυση ενεργοποίησης νετρονίων (INAA), φασματοφωτομετρία (SP), υγρή χρωματογραφία υψηλής απόδοσης (HPLC), ιοντική χρωματογραφία (IC), βολταμετρία (V), ποτενσιομετρία (P) και φθορισμομετρία (F), η οποία και χρησιμοποιήθηκε στο εργαστήριο μας .

Στην κατεύθυνση αυτή, η επιλογή του acid alizarin violet N (AVN) ως αντιδραστηρίου σύζευξης, έδωσε πολύ ισχυρή αντίδραση φθορισμού με αργίλιο(III). Οι παράμετροι που μελετήθηκαν για βελτιστοποίηση της μεθόδου ήταν η συγκέντρωση του υποκατάστατη, το pH, ο χρόνος και η θερμοκρασία της αντίδρασης, η σχετική χημική συγγένεια μεταξύ των

μετάλλων και του υποκατάστατη, το φάσμα απορρόφησης και φθορισμού, ο μέσος χρόνος λειτουργίας του λαμπτήρα, η τάση του φωτοπολλαπλασιαστή και το εύρος μονοχρωματικής δέσμης.

Η ο,ο-διυδροξυ διάταξη της αζω-ομάδας της χρωστικής είναι απαραίτητη προϋπόθεση για την εμφάνιση αντίδρασης φθορισμού για το αργίλιο (III), ώστε μπορούμε να ισχυριστούμε ότι το AVN συνδέεται χωρίς αμφιβολία και με τα δύο άτομα οξυγόνου των δυο υδροξυλομάδων, δίνοντας με αυτό τον τρόπο ένα σταθερό σύμπλοκο με το αργίλιο (III) το οποίο φθορίζει έντονα. Η υπόθεση αυτή ενισχύεται από το γεγονός ότι παρόμοιες χρωστικές αζω-ενώσεις στις οποίες λείπει μια υδροξυομάδα του υποκατάστατη δεν δίνουν αντίδραση φθορισμού με το αργίλιο (III).

Η βέλτιστη περιοχή pH για την αντίδραση φθορισμού του AVN και του αργιλίου(III) ήταν μεταξύ 4.0 και 5.0. Μελετήθηκαν τόσο όξινα όσο και αλκαλικά διαλύματα και βρέθηκε ότι κάτω από τιμή pH 3.0 και πάνω από τιμή pH 6.0 δεν συμβαίνει αντίδραση φθορισμού μεταξύ του αργιλίου(III) και του AVN. Για το λόγο αυτό, χρησιμοποιήθηκε ένα ρυθμιστικό διάλυμα οξικού pH 5.0 για την αποφυγή ανεπιθύμητων αποκλίσεων των μετρήσεων, όπως επίσης και για το λόγο ότι το πλατώ του φθορισμού δεν καλύπτει μεγάλο εύρος pH.

Όπως συμβαίνει σε πολλές περιπτώσεις, η θερμοκρασία καθορίζει τον ρυθμό με τον οποίο προχωρά η αντίδραση. Ο λόγος που η αντίδραση αυτή προχωρά αργά πιθανόν οφείλεται στο γεγονός ότι το AVN είναι ένα «ευέλικτο» μόριο και μπορεί να πάρει πολλές διαμορφώσεις. Έτσι σύμφωνα με την πειραματική διαδικασία που ακολουθήσαμε, τα δείγματα θερμάνθηκαν στους 60°C για 30 λεπτά και στη συνέχεια οι μετρήσεις έγιναν σε θερμοκρασία δωματίου. Η σταθερότητα του συμπλόκου αργιλίου (III)-AVN μελετήθηκε επίσης και βρέθηκε ότι μετά την διαδικασία θέρμανσης και ψύξης παρέμενε σταθερό για τουλάχιστον 80 λεπτά.

Σύμφωνα με πειραματικά δεδομένα τόσο η συγκέντρωση του AVN όσο και του αργιλίου(III) επηρεάζει τον χρόνο ολοκλήρωσης της αντίδρασης. Για το λόγο αυτό καθορίσθηκε χρόνος ίσος περίπου με τον χρόνο ολοκλήρωσης της αντίδρασης, με χρήση 10πλάσιας ποσότητας AVN σε σχέση με το αργίλιο(III), για να επιτύχουμε ποσοτική ανάλυση και άλλες μετρήσεις.

Ο χρόνος ολοκλήρωσης της αντίδρασης όπως επίσης και η μοριακή αναλογία χρησιμοποιήθηκε επιτυχώς για τον καθορισμό διαφορετικών ειδών μεταξύ του αργιλίου(III) και του AVN. Πειραματικά δεδομένα αποδεικνύουν την ύπαρξη επτά συμπλόκων μεταξύ του

μετάλλου (M) και του υποκατάστατη (L) σε αναλογία: ML, ML_2, ML_3, ML_4, ML_5, ML_6 και ML_7.

Ξένα ιόντα που απαντούνε σε αρκετά δείγματα, παρεμποδίζουν τον προσδιορισμό του αργιλίου(III) και εμφανίζονται σφάλματα τα οποία οφείλονται α) σε αντικατάσταση του συζευγμένου του αργιλίου(III), β) σε απόσβεση φθορισμού του AVN εξαιτίας της συμπλέξεις του υποκατάστατη με τα ιόντα και γ) σε απορρόφηση της ακτινοβολίας φθορισμού από τα σύμπλοκα του AVN με τα ιόντα αυτά. Για το λόγο αυτό επιλέχθηκε ένα σύστημα επικάλυψης, αποτελούμενο από 1,10-φαινανθρολίνη, χλωριδίου του υδροξυλαμμωνίου και θειικό βηρύλλιο, το οποίο και χρησιμοποιήθηκε για την αποφυγή των παρεμποδίσεων.

Διαλύματα παρακαταθήκης και εργασίας του αργιλίου(III) παρασκευάστηκαν σε 0.1 N νιτρικό οξύ προς αποφυγή υδρόλυσης και σχηματισμού πιθανών συμπλοκών μετάλου-χλωριδίων. Έλεγχος με επαναλαμβανόμενες φθορισμομετρικές μετρήσεις προτύπων και καμπύλες βαθμονόμησης, οι οποίες ήταν σταθερές για μια εβδομάδα, έγιναν με χρήση του ίδιου διαλύματος εργασίας.

Αποτιμώντας τα υπέρ και τα κατά της πειραματικής διαδικασίας, καταλληλότερος εξοπλισμός θα ήταν απαραίτητος για βελτιστοποίηση του εύρους της καμπύλης βαθμονόμησης και των βασικών στατιστικών παραμέτρων όπως τυπικής απόκλισης και ευαισθησίας, τα οποία τελικά καθορίζουν την ανιχνευσιμότητα και το όριο ποσοτικοποίησης της μεθόδου.

Με την χρήση καμπύλης βαθμονόμησης, της μεθόδου γνωστής προσθήκης και εφαρμογής της μεθόδου των ελάχιστων τετραγώνων, οι διακυμάνσεις του φθορισμού σε σχέση με τη συγκέντρωση του αργιλίου(III) εφαρμόστηκαν στον προσδιορισμό μετάλλων σε δείγματα αναφοράς, και αποτελούν την πρωτοτυπία της παρούσης διατριβής.

Το εύρος διακύμανσης της καμπύλης αναφοράς υπολογίστηκε με πρότυπα διαλύματα αργιλίου(III) συγκέντρωσης από 10^{-9} μέχρι 10^{-6} M. Ενώ το όριο ανίχνευσης και ποσοτικοποίησης είναι 2.28×10^{-10} και 7.6×10^{-10} αντίστοιχα, τα οποία υπολογιστήκαν από την τυπική απόκλιση του τυφλού δείγματος.

Abbreviation:

Stdev – standard deviation

RStdev – relative standard deviation

5-Br-SASH – 5-bromo-salicylaldehyde salicylhydrazone

8-HQ – 8-hydroxylquinoline

8-Q – 8-quinolinol

A.C.OP – alternating current oscillopolarography

AAGR – 2,4,2'-trihydroxyazobenzene-5'-sulfonic acid

AAS – atomic-absorption spectrometry

AdCSV- adsorptive cathodic stripping voltammetry

AdPV – adsorptive pulse voltametry

AdSV – adsorptive stripping voltammetry

Alizarin red PS – 1,2,4-trihydroxy 9,10-anthraquinone-3-sulfonic acid

ARS – alizarine red S, 1,2-dihydroxyanthraquinone sulfonate

CE – capillary electrophoresis

CFA – continuous flow analysis

CKS – catalytic kinetic spectrophotometry

CNDA – 3-carboxy-2-naphthylamine-N,N-diacetic acid

CRM – certified reference material

CSF - cerebrospinal fluid

CTAB – hexadecyltrimethylammonium bromide

CTMAB – cetyltrimethylammonium bromide (cationic surfactant)

DA – 3,4-dihydroxyphenylethylamine

DASA – 1,2-dihydroxyanthraquinone-3-sulfonic acid

DFO – desferrioxamine

DHP – 2,3-dihydroxypyridine

DPAdSV - differential pulse adsorptive stripping voltammetry

DPV – differential pulse voltammetry

DRAB – 2, 2'-dihydroxyazobenzene

DRS – diffuse reflectance spectrophotometry

DSAHP – N,N'-disalicylidene-1,3-diamino-2-hydroxypropane

E – extraction

EBBR – 1-(2-hydroxy-a-naphthylazo)-2-naphthol-4-sulphonic acid

EBT – 1-(1-hydroxy-2-naphthylazo)-2-naphthol-6-nitro-4-sulphonic acid

ECR – eriochrome cyanine R

EDTA – etylenediaminetetraacetic acid

EIA – electroinjection analysis

ET-AAS – electrothermal atomic-absorption spectrometry

ETA-LEAF – electrothermal atomization-laser excited atomic fluorescence

ETPTP -7-ethylthio-4-oxa-3-phenyl-2-thioxa-1,2-dihydropyrimido-[4,5-d]pyrimidine

ETV-ICP-AES – electrothermal vaporization inductively-coupled plasma-atomic emission-spectrometry

F - fluorescence

FAAS –flame atomic-absorption spectrometry analysis

FBA – flow-batch analysis

FIA – flow injection analysis

FIAS – flow-injection atomic spectrometry

FIF – flow-injection-spectrofluorimetry

FIs – flow-injection-spectrophotometry

Fosetyl – tris(ethyl) phosphonate

GFAAS – graphite furnace atomic-absorption spectrometry

Hdmp – 1,2-dimety-3-hydroxypyrid-4-one

Hma – 3-hydroxy-2-methyl-4H-pyran-4-one

HNB – hydroxynaphtol blue

HPF/HHPN – high-performance flow/hydraulic high-pressure nebulization system

HPIC - high-performance ion chromatography

HPLC- high-performance liquid chromatography

HQS – 8-hydroxyquinoline-5-sulfonic acid

IC – ion chromatography

ICPAES – inductively-coupled plasma-atomic emission spectrometry

ICPOES – inductively-coupled plasma optical – emission spectrometry

IEC – ion exchange chromatography

INAA – instrumental neutron activation analysis

IndirectV – indirect voltammetry

IP-RP-HPLC – ion-pair reversed-phase high-performance liquid chromatography

IP-RPP - ion-pair reversed-phase partition

ISE – ion-selective electrod

KD- kinetic differentiation mode

KS – kinetic spectrophotometry

LC – liquid chromatography

L-dopa – 3,4-dihydroxyphenylalanine

LIF – laser-induced fluorescence

Lumogallion– 5-chloro-2-hydroxy-3-(2,4-dihydroxy phenylazo) benzenesulfonic acid

MCPF - m-carboxyphenylfluorone

MOAP – microwave activated oxygen plasma

Morin – 3.5.7.2'-4' pentahydroxy flavone

MSFIA - multisyringe flow injection analysis

OP - oscillopolarography

P - potentiometry

PCV - pyrocatechol violet

PMBP – 1-phenyl-3-methyl-4-benzoyl-5-pyrazolone

PR-HPLC – reversed-phase high-performance liquid chromatography

PTFE – polytetrafluoroethylene

RAA – reactor activation-analysis

RBC – red blood cell

rFIA – reverse flow-injection analysis

RP – reversed phase

RPLC – reversed-phase liquid chromatography

SAHP – salicylaldehyde picolinoylhydrazone

SCX – strong cation exchange

SE – solvent extraction

SIA – sequential injection analysis

SO(2)CAS – sulfonylcalix[4]arenetetrasulfonate

SPADNS – 4,5 dihydroxyl-3-(p-sulphophenylazo)-2,7-naphthalene-disulphonic acid trisodium salt

SPE – solid phase extraction

SS – sorption-spectroscopy

STP-GFAAS **– stabilized temperature platform graphite furnace atomic-absorption spectrometry**

THGA furnace **– transversely heated graphite atomizer furnace**

TX-100 – Triton X-100

UV – spectrophotometry

V **– voltammetry**

CONFERENCES

1."Errors in spectrophotometry", Mavroudis Deemertzis, Alexandru Vasile Calin, Cristina Ioana Vijdeluc, Iannis Fiamengos, Constantine D. Stalikas, Dimitra Kovala-Demertzi. The 5th International Conference, Instrumental Methods of Analysis Modern Trends and Applications, Greece, Patras, 30 september – 4 octomber 2007.

2."Sensitive spectrophotometric determination of copper with Di-2-pyridylketone", Alexandru Vasile Calin, Cristina Ioana Vijdeluc, Iannis Fiamengos, Constantine D. Stalikas, Dimitra Kovala-Demertzi, Mavroudis Deemertzis. 9 th Eurasia Conference on Chemical Sciences, Turkey, Antalya September 2006

3."The thermal effects of platinum (II) and palladium (II) complexes with 2-acetyl pyridine and pyridine-2-carbaldehyde N(4)-ethyl-thiosemicarbazones in membrane bilayers", E. Siapi, T. Mavromoustakos, D. Kovala-Demertzi, C. Vijdeluc, M. A. Demertzis. Inorganic reaction Mechanisms Meeting, Greece, Athens, January 2004.

4."Spectrofluorimetric Determination of Aluminum Traces Based on the Reaction with Acid Alizarin Violet N", Cristina Ioana Vijdeluc, Constantine D. Stalikas, Dimitra Kovala-Demertzi , Mavroudis Deemertzis.The 3th International Conference, Instrumental Methods of Analysis Modern Trends and Applications, Greece Thessaloniki September, 2003

5."Spectrofluorimetric determination of Aluminum Traces Based on the Reaction with Acid Alizarin Violet N", Cristina Ioana Vijdeluc, Constantine D. Stalikas, Dimitra Kovala-Demertzi , Mavroudis Deemertzis. The 3th Aegean Analytical Chemistry Days. Greece, Polihnitos Lesvos September-Octomber 2002.

6."Spectrofluorimetric Determination of Aluminum Traces Based on the Reaction with Acid Alizarin Violet N", Cristina Ioana Vijdeluc, Constantine D. Stalikas, Dimitra Kovala-Demertzi , Mavroudis Deemertzis. The 5th Conference of the Chemistry Department., Basic and Applied Chemical Research, Greece, Ioannina Octomber 2002.

PUBLICATIONS

1."UV-VIS spectral information of Platinum (II) and Palladium (II) complexes with pyridine-2-carboxaldehyde-thiosemicarbazone and their correlation with antineoplastic and cytogenetic effects, Costel Sarbu, Cristina Vijdeluc, Mavroudis A. Demertzis, Dimitra Kovala-Demertzi. Rev.Chim.(Bucuresti) 55 (7): 478-482 2004

2."The thermal effects of platinum (II) and palladium (II) complexes with 2-acetyl pyridine and pyridine-2-carbaldehyde N(4)-ethyl-thiosemicarbazones in membrane bilayers", E. Siapi, T. Mavromoustakos, D. Kovala-Demertzi, C. Vijdeluc, M. A. Demertzis.Thermochimica Acta: 53-58 2004